2012

Microrna s in Breast Cancer Metastasis: Molecular Regulation of Endothelial Recruitment by Cancer Cells & Regulation of Metastasis Suppressor Microrna s

Kim J. Png

MICRORNAS IN BREAST CANCER METASTASIS:

MOLECULAR REGULATION OF ENDOTHELIAL RECRUITMENT BY CANCER CELLS & REGULATION OF METASTASIS SUPPRESSOR MICRORNAS

A Thesis Presented to the Faculty of
The Rockefeller University
in Partial Fulfillment of the Requirements for
the degree of Doctor of Philosophy

by

Kim J. Png

June 2012

MICRORNAS IN BREAST CANCER METASTASIS:
MOLECULAR REGULATION OF ENDOTHELIAL RECRUITMENT BY CANCER CELLS & REGULATION OF METASTASIS SUPPRESSOR MICRORNAS

Kim J. Png, Ph.D.

The Rockefeller University 2012

Metastasis is a highly complex, multi stage process that is clinically daunting, causing the majority of deaths from solid malignancies. A previous study identified three microRNAs that robustly suppresses breast cancer metastasis to lung and bone – miR-126, miR-206 and miR-335. While miR-335 suppressed metastasis through inhibition of cell-autonomous metastatic phenotypes of cell migration and invasion, the role of miR-126 in metastasis remained unknown. Here, endogenous miR-126 is shown to regulate the non-cell autonomous phenotype of endothelial recruitment to metastatic breast cancer cells. Through coordinate targeting of IGFBP2, PITPNC1 and MERTK, miR-126 inhibits endothelial recruitment, which is required for metastatic angiogenesis and metastatic colonization. IGFBP2 secreted by metastatic cells promotes endothelial recruitment through binding of IGF-1 in the extracellular space, activating IGF type-I receptor on endothelial cells. In contrast, MERTK receptor cleaved from metastatic cells acts as a decoy receptor for GAS6, sequestering GAS6 away from endothelial MERTK receptor, which normally signals to inhibit endothelial recruitment. Co-injection of endothelial cells with breast cancer cells non-cell autonomously rescues their miR-126-induced defect in metastasis, revealing a role for cancer cell-endothelial interactions in metastatic initiation. These findings reveal endothelial recruitment and endothelial interactions in the tumour microenvironment to be integral features of metastatic breast cancer.

All three previously discovered breast cancer metastasis suppressor microRNAs display de-regulated expression in cancer through unknown mechanisms. These findings reveal that the human miR-335 locus undergoes both genetic deletion and epigenetic promoter hypermethylation in metastatic derivatives obtained from independent patients' tumours. Additionally, matched primary tumour-metastases pairs revealed the silencing of miR-335 expression to occur at least partially through genetic deletion. Genetic deletion of miR-335 also correlates with ovarian cancer recurrence, suggesting that miR-335 may play a regulatory role in ovarian cancer. The miR-126 locus, however, is not subjected to either genetic deletion or epigenetic promoter hypermethylation. Early evidence suggests that miR-126 expression is inhibited through a processing defect in the biogenesis of mature miR-126 from pre-miR-126. These findings reveal individual metastasis suppressor microRNAs to be regulated by divergent mechanisms – generic (genetic or epigenetic) and microRNA-specific (processing) regulatory mechanisms.

Dedicated to Michael, Janet & Gavin,

For being the most loving and caring family

ACKNOWLEDGMENTS:

I would like to express my gratitude to my advisor, Sohail Tavazoie, for his patience, enthusiasm and support throughout my time in his lab. He has been a great mentor, teaching me how to be a better scientist, both in terms of intellectual curiosity and analytical capability. More importantly, he has imparted many life skills that I will remember for the rest of my professional career. I have also been inspired by the amazing research environment he has created through his balanced style of leadership, which allowed for scientific independence while also providing guidance when it was needed.

I also wish to thank all the members of the Tavazoie lab, both past and present, for an intellectually stimulating, helpful, friendly and truly supportive environment. I have been blown away by the intelligence of each and every individual and never had to look beyond the lab to gain inspiration in times of doubt. In particular, I am extremely grateful to Nils Halberg. He has been the most wonderful person to work with and has fulfilled many roles throughout my graduate career – a mentor, a collaborator, a supporter, and most importantly, a friend. I am also grateful to Mitsu Yoshida, for meticulously helping me with experiments and constantly helping to refine my project. I am also thankful to Jiamin Loo, a fellow starting member of the Tavazoie lab. He has been one of the most helpful people I have personally known and I truly enjoyed bouncing ideas back and forth across our bay(s) through the last few years. Many thanks also to Claudio Alarcon, Hien Tran, Hani Goodarzi, Hyeseung Lee, Lisa Fish, Jason Ross, Nora Pencheva, Paul Furlow, Xander Ngyuen, Caitlin Sengelaub, Fung Ying Man, Doowon Huh, Colin Buss and Alexis Scherl.

I would like to express my deepest gratitude to my thesis committee members, Tarun Kapoor and Barry Coller, for their time, encouragement and scientific advice over the years. I am also extremely thankful to Siavash Kurdistani for being my outside committee member. I would also like to extend my gratitude to the Rockefeller University Dean's office for being so helpful throughout my time here.

My deepest thanks go to my friends who have been an invaluable source of support during my graduate studies. I would like to thank my friends in New York, who have helped me form a home away from home and enabled me to live a balanced lifestyle while still focusing on my project. I would also like to thank my fellow A*STAR scholars distributed around the world, who have been a great source of support, both for obtaining literature and encouragement through the tough periods. Many thanks to Ying Min Wang, Mingzi Zhang, Fong Tian Wong, Asha Shekaran, Shawn Tan and Brian Liau.

Most importantly, I would like to thank my family for their unconditional love and support throughout my entire life and especially during my graduate studies – my father, Michael, for being my emotional anchor and voice of reason, my mother, Janet, for being my source of strength and inspiration, and my brother, Gavin, for always knowing how to make me smile. No words can ever express the joy and gratitude I have for being blessed with being a part of this family.

TABLE OF CONTENTS

LIST OF FIGURES

LIST OF TABLES

CHAPTER 1:
Introduction

Breast Cancer

Breast cancer is a disease whereby a neoplasm develops from cells in breast tissue. Breast cancer is the second most common type of cancer among women in United States, with approximately 12% of women developing invasive breast cancer over the course of their lives. In 2011, an estimated 230,000 women were diagnosed with invasive breast cancer and 57,000 women were diagnosed with non-invasive (*in situ*) breast cancer. Breast cancer is also responsible for the second highest cancer death rate for women in United States. In 2011, an estimated 39,000 women will die from breast cancer. Importantly, men also develop breast cancer, with approximately 2000 male cases being diagnosed in 2011.[1]

There are several histologic subtypes of breast cancers: ductal carcinoma, medullary carcinoma, lobular carcinoma, tubular carcinoma, mucinous carcinoma and inflammatory breast cancer. Infiltrating Ductal Carcinoma (IDC) is the most frequent type of breast cancer and represents 78% of all diagnosed breast malignancies. At an early stage when neoplastic cells are still confined to the ductal system, Ductal Carcinoma In-Situ (DCIS) is the diagnosis. The diagnosis of DCIS portends a highly favourable prognosis.[2]

As insights into the molecular and cellular basis of breast cancer have increased over the years, molecular subtyping of breast cancer has become useful in the choice of treatment and development of new therapies. There are four common molecular subtypes for breast cancer–Luminal A, Luminal B, Triple negative and HER2-positive (HER2+). Most breast cancers are luminal subtypes, which are comprised of cells that resemble the luminal cells that line mammary ducts. Luminal A is the most common of all subtypes and tends to be Estrogen receptor-positive (ER+) and/or Progesterone receptor-positive (PR+) and HER2-negative (HER2-). These tumours tend to have relatively high survival rates and low recurrence rates. Luminal B tumours are also Estrogen receptor-positive (ER+) and/or Progesterone receptor-positive (PR+) and show high proliferation rate as determined by Ki67 staining. Additionally, luminal B tumours tend to and have mutations in p53, a key tumour suppressor gene. Luminal B tumours display higher metastasis rates than luminal A tumours and are generally larger in size at diagnosis. Triple negative breast cancers do not over-express ER, PR or HER2, and are typically comprise of cells that are similar to the basal cells that line mammary ducts. The triple negative subtype represents 14-20% of breast cancers and is often aggressive, displaying worse prognosis than the luminal subtypes. Triple negative breast cancers recur more frequently than other subtypes and recurrence tends to involve the spread of cancer to other organs. HER2 breast cancers are positive for HER2 (HER2+) but negative for both ER and PR (ER-/PR-). Approximately 7-12% of breast cancers are HER2+ and these tumours tend to have poor prognosis with early and frequent recurrence. These tumours also tend to possess p53 mutations.[3]

Upon diagnosis, breast cancer is typically staged to guide appropriate treatment plans. Stage 0 (Carcinoma *in situ*) marks the pre-malignant stage, whereby atypical cells are confined within the ducts or lobules and have not spread into the surrounding breast tissue. Stage I breast cancer is early stage invasive breast cancer, where the tumour is less than 2 cm in diameter and is confined to breast tissue. Stage II breast cancer has spread to the axillary lymph nodes or has grown larger than 5 cm. Stage III breast cancer has spread to axillary lymph nodes, causing them to adhere to each other or to other nearby structures. Additionally, the cancer may have spread to the chest wall, the skin of the breast or to lymph nodes near the breastbone. Stage IV breast cancer marks spread to other organs of the body, such as to distal lymph nodes, lungs, bones, liver, brain or skin, a process termed distal metastasis.[4] Importantly, the five-year survival rate decreases dramatically from 93% to 15% as the stage of breast cancer presented at diagnosis increases from stage 0 to stage IV.[5]

Metastasis

Metastasis refers to the phenomenon whereby cancer cells spread from the original organ site to distal organs. Although many advances and developments have been made recently in surgical techniques, radiotherapy and targeted therapy, the majority of deaths from solid neoplasms are attributable to distal metastasis, rather than the primary tumours from which these malignancies originate.[6-9] Metastasis is a complex, multi-step process that starts with cancer cells exiting the primary tumour site and ends with the colonization of a distal organ site.[10-12] Primary tumours are typically biologically heterogeneous and contain genotypically and phenotypically diverse subpopulations of tumour cells.[13] Metastases are derived from a selected subpopulation of the primary tumour cells that gain the ability to undergo all the steps necessary for successful metastasis. In order to enhance current clinical approaches towards eradication of metastasis, it is crucial to identify the subset of cells that have the capacity to successfully metastasize.

The process of cancer metastasis begins when tumour cells detach from neighbouring cells and the extracellular matrix and invade into the surrounding tissue. The proteolysis of the interacting proteins between the tumour cell and the basement membrane interface signifies the transition from a benign carcinoma *in situ* (e.g. DCIS) to a malignant invasive tumour. The tumours cells that have detached from the primary tumour then migrate towards a vascular supply and intravasate across the endothelial cell layer into the systemic circulation. Following this, tumour cells typically circulate as small aggregates in circulation, where they must survive hemodynamic forces and cell death signals. Tumour cells then arrest in distal

microvascular beds by passive mechanical or active mechanisms, before extravasating out into the distal organ. Specifically, tumour cells can migrate across intercellular junctions between neighbouring endothelial cells (paracellular) or migrate through the cytoplasm of a single endothelial cell (transcellular). To promote extravasation, tumour cells may also produce factors that stimulate endothelial cell retraction or proliferate in the vessel lumen until the vessel ruptures, allowing cancer cells to enter the organ tissue. Upon extravasation into the target organ, tumour cells must proliferate and interact with other cell types in the microenvironment, eventually colonizing the distal site in the form of a metastatic nodule.[14]

The mechanistic dissection of the various steps involved in metastasis requires an animal model that can recapitulate the features of human metastasis. Although several transgenic mouse models of solid tumours metastasis are available, dissemination of tumour cells in these models are typically incompletely penetrant and do not adequately parallel the preferred routes of spread in humans. These models often implicate mouse genes as mediators of metastasis, which may not be an accurate representation of the genes involved in clinical progression of human cancer. To overcome these limitations, the Tavazoie laboratory has utilized an *in vivo* selection model of the later stages of human breast cancer metastasis in immunodeficient mice.[15,16] This *in vivo* selection model was originally developed by Isaiah Fidler and colleagues to study metastasis by mouse cells.[17] In these models, a heterogeneous population of human breast cancer cells is injected into the circulation of a mouse and allowed to metastasize to specific organ sites. The metastases derived from these mice are then dissociated and re-injected into another mouse, a process which is repeated to allow for *in vivo* selection of a subset of cells that have the ability to

efficiently metastasize to a specific target organ. Comparisons can then be made between the resulting highly metastatic subpopulation of cancer cells and its poorly metastatic parental population, allowing for the identification of gene expression changes that are responsible for a metastatic phenotype.[15,16,18] This *in vivo* selection model allows one to overcome the limitations of transgenic models as metastasis is observed in the same target organs as humans (lungs and bones for breast cancer) and is highly penetrant, while also allowing for the identification of candidate human genes that are involved since the cells are originally obtained from a human patient.

Metastasis is a highly inefficient process–less than 0.01% of circulating tumour cells are able to successfully form a secondary tumour.[19] Specifically, the initiation of cell growth in secondary organs that leads to colonization is the most limiting step that must be overcome for the successful completion of metastasis.[20] Some tumour cells go into senescence upon entry into the secondary organs, while others are unable to trigger the angiogenic switch necessary for tumour growth.[21,22] To overcome these barriers to colonization, tumour cells undergo a complex series of signalling events and interactions with the surrounding stroma, allowing them to successfully proliferate to form the expanding tumour.

Some cancer types tend to metastasize to specific organs, independent of the number of tumour cells delivered to an organ. This has been observed in both clinical studies of cancer patients and mouse models of cancer, leading to Paget's "seed and soil" hypothesis[23], which suggests that metastasis is not random and that some tumour cells ("seed") have preferences

for the microenvironment of specific organs ("soil"). For example, breast cancer typically metastasizes to the lungs, bones and liver. Consequently, a metastatic nodule is only established if a "seed" is implanted in "soil" that is suitable for it–that is, if the microenvironment of the target site meets the requirements of the disseminated cancer cell. This "seed and soil" hypothesis highlights the importance of cancer cell-microenvironment interactions in the process of metastasis and also highlights the potential of factors that facilitate cross-talk between cancer cells and stroma cells as candidates for therapeutic intervention of metastasis.[24]

Although many discoveries have been made regarding the various molecular and cellular determinants that regulate the phenomenon of metastasis, targeted therapy developed for the treatment of late stage cancers have been largely unsuccessful. Specifically, targeted efforts directed towards targeting the tumour microenvironment have been largely focused on inhibition of angiogenesis that support tumour growth through the inhibition of VEGF[25-27], a proangiogenic cytokine that is overexpressed in the majority of human tumours. However, VEGF inhibition failed to prolong the survival of late stage patients by an appreciable amount of time[28]. Thus, continued investigations of mechanisms that mediate tumour-microenvironment interactions are needed to lead to the identification of new targets for therapeutic intervention of metastasis.

MicroRNAs

MicroRNAs (miRNAs) are small non-coding RNAs (ncRNAs) that are ~22 nucleotides (nt) in length and regulate gene expression at the post-transcriptional level through base pairing to their target mRNAs.[29,30] The first miRNA was described in *C. elegans* when screens for mutants that affect the timing of the switch of cell fate in development resulted in the identification of two genes, *lin-4* and *let-7*, which surprisingly encode small ncRNAs instead of proteins.[31] Since then, over 15,000 miRNAs have been identified in a wide variety of species including animals, plants and viruses. There are hundreds of unique miRNAs in a given species and each miRNA is predicted to regulate a variety of target genes. Computational studies have predicted that human miRNAs can regulate up to 60% of all human protein coding genes.[32] MicroRNAs have also been linked to many cellular processes including differentiation, growth and cell death.[33] Additionally, perturbations of miRNA expression have been established in numerous diseases such as cancer.[34,35]

The biogenesis of a miRNA requires a series of stepwise processing events starting from its primary transcript to its final mature 22 nt form. The canonical maturation pathway begins with transcription of the miRNA gene, typically by RNA polymerase II, to generate the primary miRNA (pri-miRNA) transcript. The pri-miRNA contains a hairpin RNA structure that is recognized by the nuclear RNAse-III enzyme, Drosha, and its co-factor DGCR8. These proteins work together in a complex known as the Microprocessor, which is responsible for the cleavage of the pri-miRNA into the pre-miRNA, a shorter hairpin molecule that is between 60-100 nt in length. The pre-miRNA is then the exported from the

nucleus into the cytoplasm by Exportin-5 in a RanGTP-dependent process. In the cytoplasm, the pre-miRNA is further cleaved by the RNAse III endonuclease Dicer, generating an RNA duplex that is the length of the final mature miRNA. The two strands of the miRNA are then separated and the 'guide' strand is loaded onto an Argonaute-containing RNA-induced silencing complex (RISC), which then mediates binding of the mature miRNA to the target mRNA through sequence complementarity. The other strand is known as the 'passenger' strand, which can either be discarded or loaded onto another RISC complex.[36,37] Upon binding to its target mRNA, repression of the expression of the target gene can occur either through mRNA degradation by the cleavage activity of Argonaute (Ago) proteins within the RISC complex or through translation inhibition when the RISC complex sterically hinders ribosome progress.[38,39]

The region representing nucleotides 2-8 at the 5' end of the mature miRNA is known as the seed sequence and miRNAs are thought to bind to mRNAs at sequences complementary to this region. However, it is possible to find targets that are not complementary to the seed sequence, suggesting that partial complementarity can be thermodynamically stable.[40-42] Additionally, the interaction between the miRNA and its target can be modulated and facilitated by other factors, such as RNA binding proteins, secondary structures in target RNAs and the co-localisation of miRNAs and target mRNAs in specific subcellular compartments.[43]

MiRNAs typically bind to their target mRNAs in the 3'UTR region, which is involved in the regulation of translation, mRNA stability and localization.[30,43] Thus, the binding of miRNAs to the 3'UTR region can potentially affect all of these processes. There is also increasing evidence that miRNAs can also suppress the expression of their target genes by binding to the coding regions of these genes.[44-46] Additionally, a single mRNA can be regulated by several miRNAs, suggesting that miRNAs can function as complex networks to regulate the expression of a single gene.

Many malignant tumours and cancer cell lines have been found to display widespread deregulation of miRNA expression relative to normal tissues. MicroRNAs have since been determined to have the ability to act as oncogenes or tumour suppressors. For example, the miR-17-92 cluster is frequently amplified in B cell lymphoma[47] and its expression is required for the generation c-Myc-induced lymphoma, thus acting as an oncomiR.[48] Conversely, microRNAs can also act as tumour suppressors–the let-7 family of miRNAs inhibits the expression of Ras, which promotes tumorigenesis by increasing proliferation.[49,50] Thus, through the regulation of downstream genes that act as either oncogenes or tumour suppressors, miRNAs act as important mediators of cancer progression.

Metastasis Suppressor MicroRNAs

In contrast to tumour initiation, which can result from the cooperation of a few oncogenes, metastasis requires the concerted action of numerous genes due to the various phenotypes required of disseminated cells, which includes but is not limited to the ability to migrate, invade, intravasate, resist anoikis, extravasate, proliferate and colonize a new environment. Current approaches that pharmacologically inhibit single targets are not therapeutically efficacious, suggesting that effective treatment for the prevention of metastasis will likely require the inhibition of multiple genes. There are several possible upstream regulatory mechanisms that could control the expression of multiple genes–epigenetic changes, gene amplification/deletion, activation of signalling pathways and non-coding RNAs. In particular, miRNAs can inhibit the expression of several genes through the suppression of translation or destabilization of target transcripts. Thus, miRNAs are attractive candidates as key regulators of metastasis.

Using a systemic and functional approach, in conjunction with a mouse model system that recapitulates human breast cancer metastasis, Tavazoie *et al*. identified three miRNAs (miR-126, miR-335 and miR-206) that strongly suppress metastasis of human breast cancer cells to the lungs and bones of mice.[51] The expression levels of these metastasis suppressor miRNAs were silenced in highly metastatic human cell lines and metastatic primary breast cancer cells obtained from patients. Additionally, clinical data has revealed that patients whose primary tumours display silencing of these miRNAs are more likely to develop metastatic relapse relative to patients whose primary tumours retain expression of these miRNAs.

In the study by Tavazoie *et al*., miR-335 and miR-206 were found to suppress metastasis through the inhibition of cell migration and invasion. Specifically, miR-335 inhibited these mechanisms, in part, through the inhibition of the transcription factor SOX4 and extracellular matrix protein Tenascin C (TNC). However, the mechanism underlying the inhibition of metastasis by miR-126 remained unknown. Thus, the role of miR-126 in metastatic progression and its downstream targets that mediate its effects are outstanding questions. Additionally, given the dramatic effects of these metastasis suppressor miRNAs on metastasis, understanding of the upstream mechanisms that underlie their inactivation is needed. These upstream mechanisms could shed light on the regulation of miRNAs in human cancer, potentially allowing us to understand how the expression of these metastasis suppressor miRNAs could be restored. Through further studies into both the downstream and upstream mechanisms involved in metastasis suppressor miRNA pathways, additional targets for the therapeutic inhibition of metastasis could also be identified.

CHAPTER 2:
Materials and Methods

Cell Culture

The MDA-MB-231 breast cancer cell line and its metastatic derivatives, as well as 293T cells, were cultured with Dulbecco's modified Eagles' medium (DMEM) supplemented with 10% Fetal Bovine Serum (FBS). The CN34 primary malignant pleural effusion line and its metastatic derivatives were cultured with M199 media supplemented with 2.5% FBS, 10μg/mL insulin, 0.5μg/mL hydrocortisone, 20ng/mL EGF, 100ng/mL and cholera toxin. H29 cells were cultured with DMEM media supplemented with 10% FBS, 20ng/mL doxycycline, 2μg/mL puromycin and 0.3mg/mL G418 and HUVEC cells were cultured with EGM-2 media (CC-3162, Lonza, Basel, Switzerland).

Animal Studies

All animal work was conducted in accordance with protocols approved by the Institutional Animal Care and Use Committee at The Rockefeller University. For the mammary tumour growth assay, breast cancer cells were resuspended in 50μl of a 1:1 ratio of matrigel and PBS and injected directly into mammary fat pads of 6-8 week old age-matched female NOD/SCID mice.[11] For lung metastasis assays, breast cancer cells were resuspended in 200μl of PBS and injected into the tail veins of 6 week old age-matched female NOD/SCID mice.[51] For the CN34 lung metastasis assay, 6 week old age-matched female NOD/SCID gamma mice were used instead. For the systemic metastasis assays, breast cancer cells were resuspended in 50μl of PBS and injected intracardiacally into 8 week old age-matched female Athymic mice.[15,52] For liver metastasis assays, breast cancer cells were resuspended in 50μl

of a 1:1 ratio of matrigel and PBS and injected into the spleens of 6 week old age-matched female NOD/SCID mice. After injection into the spleen, a splenectomy is then performed to prevent the growth of a tumour in the spleen. Specifically, for the cancer cell/HUVEC co-injection liver metastasis colonization assay, 500K HUVECs and 500K LM2/miR-126 overexpressing cells were mixed in a 1:1 ratio in PBS before injection.

Inducible miR-126 expression was obtained by cloning pre-miR-126 into the tet-ON containing pTripz vector (Thermo Scientific, Huntsville, AL). At day 3, 2mg/ml doxycycline (Sigma Aldrich) was added to the drinking water containing 5% sucrose. Control mice were given drinking water with 5% sucrose.

Generation of lentivirus, retrovirus, knockdown and overexpressing cells

For generation of lentivirus, $1x10^6$ 293T cells were seeded onto a 10cm plate and incubated for 24h. 12μg of vector K (Gag/Pol), 6μg of vector A (Env) and 12μg of the appropriate shRNA plasmid were then co-transfected into the 293T cells using 40μL of TransIT®-293 transfection reagent (MIR 2700, Mirus Bio LLC, Madison, WI). After 16h, the media was replaced with fresh antibiotic-free DMEM supplemented with 10% FBS. After another 24h, the virus was harvested by spinning for 5 min at 1,500g before being filtered through a 0.45μm filter. For generation of retrovirus, H29 cells were seeded onto a 10cm plate and allowed to grow to 90% confluence. 10μg of the appropriate plasmid was then transfected into H29 cells using 60μl of lipofectamine™ 2000 transfection reagent (11668-019, Invitrogen by Life technologies, Carlsbad, CA). After 16h, the media was replaced with fresh antibiotic-free DMEM supplemented with 10% FBS. After another 48h, the virus was

harvested by spinning for 5 min at 1,500g and filtered through a 0.45μm filter. 2mL of the appropriate virus was used to transduce 50K cancer cells in the presence of 10μg/mL of polybrene (TR-1003-G, Millipore, Billerica, MA). After 24h, the media was changed to DMEM supplemented with 10% FBS and 2μg/mL puromycin (lentivirus) or 10μg/mL blasticidin (retrovirus) for selection. After another 72h or 7 days for puromycin or blasticidin selection respectively, the cells were washed and allowed to grow in D10F and tested for knock down of the gene of interest by qPCR. Primers used to clone miR-126 targets into the pBabe vector for over-expression studies are shown in Table 1. shRNA sequences used to silence miR-126 targets are shown in Table 2.

Table 1: Cloning primers for over-expression of miR-126 targets

Gene	Primers
IGFBP2	F: CCGGCCGGATCCATGCTGCCGAGAGTGGGCTG R: CCGGCCTACGTACTACTGCATCCGCTGGGTGT
MERTK	Custom Made Synthesis
PITPNC1	F: CCGGCCGGATCCATGCTGCTGAAAGAGTACCG R: CCGGCCTACGTATTACTCAGATTTGGGCCGAC

Table 2: shRNA sequences for knockdown of miR-126 targets

Gene	Sequence
IGFBP2_sh1	CCGGCCAGTTCTGACACACGTATTTCTCGAGAAATACGTGTGTCAGAACT GGTTTTT
IGFBP2_sh2	CCGGCAGGTTGCAGACAATGGCGATCTCGAGATCGCCATTGTCTGCAACC TGTTTTT
MERTK_sh1	CCGGGCTTCTGGTCTTGATGTATTTCTCGAGAAATACATCAAGACCAGAA GCTTTTT
MERTK_sh2	CCGGCCTGCATACTTACTTACTTTACTCGAGTAAAGTAAGTAAGTATGCA GGTTTTT
PITPNC1_sh1	CCGGCGGGTGTATCTCAACAGCAAACTCGAGTTTGCTGTTGAGATACACC CGTTTTTG
PITPNC1_sh2	CCGGCAATGGATGAAGTCCGAGAATCTCGAGATTCTCGGACTTCATCCAT TGTTTTTG
shSHMT2	CCGGCCGGAGAGTTGTGGACTTTATCTCGAGATAAAGTCCACAACTCTCC GGTTTTTG
shcontrol	CCGGCAACAAGATGAAGAGCACCAACTCGAGTTGGTGCTCTTCATCTTGT TGTTTTT

LNA/siRNA mediated miRNA knockdown

LNA (Exiqon) or siRNA were transfected into cells using lipofectamine^{TM} for 16 hours. Cells were used for HUVEC recruitment assays or lung metastasis assays 96 hours post transfection. siRNA sequences that were used are shown in Table 3

Table 3: siRNA sequences for knockdown of miR-126 targets

Gene	Sequence
For knock down in MDAm126KD cells:	
IGFBP2	CCAGUUCUGACACACGUAUUUUU
MERTK	CCUGCAUACUUACUUACUUUAUU
PITPNC1	CGGGUGUAUCUCAACAGCAAAUU
For knock down in HUVEC cells:	
MERTK 1	AAUACUGAAAAGGUGGGGCTT
MERTK 2	AUUCCUUCAUGCAGACCGCTT
AXL	AAUGCUGCAAUUCCUGAACTT

Endothelial Recruitment

25K cancer cells were seeded into 24-well plates approximately 24h before the start of the recruitment assay. HUVEC cells were serum starved in EGM-2 media supplemented with 0.2% FBS for 24 hours. The HUVEC cells were then labelled with CellTracker Red CMTPX dye (C34552, Invitrogen) for 45min and rescued in EGM-2 media supplemented with 2% FBS for 30min. Meanwhile, cancer cells were washed with PBS and 1mL 0.2% FBS EGM-2 media was added to each well. Each well was then fitted with a 3.0μm HTS Fluroblock Insert (351151, BD Falcon, San Jose, CA). For antibody experiments, the appropriate concentration of each antibody was then added to each well: 50ng/mL anti-IGFBP2 (AF674, R&D Systems, Minneapolis, MN), 20μg/mL anti-IGF-1 (AF-291-NA, R&D Systems), 40μg/mL anti-IGF-2 (MAB292, R&D Systems), 20μg/mL anti-IGF1R

(MAB391, R&D Systems), 5μg/mL anti-IGF2R (AF2447, R&D Systems), 10μg/mL anti-MERTK (AF891, R&D Systems), 20μg/mL anti-Axl (AF154, R&D Systems) and anti-IgG (AB-108-C, R&D Systems). For endothelial recruitment assays that require pre-incubation, either HUVEC cells or cancer cells were incubated with appropriate antibody or recombinant protein for 1h and washed once with PBS. The HUVEC cells were then serum starved for 1h before resuspending 100K HUVECs per mL of 0.2% FBS EGM-2. 0.5mL of the resuspension was then added into each Fluoroblock insert and the recruitment assay was allowed to proceed for 16h. After completion of the assay, Fluoroblock inserts were fixed with 4% paraformaldehyde for 15min and mounted onto slides with VectaShield mounting media (H-1000, Vector Laboratories, Burlingame, CA). 3 images of each insert were taken and the images were analysed using ImageJ (NIH).

Scratch Assay

HUVEC cells were grown to 100% confluency in 60mm dishes. 24h prior to the start of the scratch assay, HUVEC cells were serum starved in EGM-2 media supplemented with 0.2% FBS while cancer cells were seeded on plastic coverslips (Nalgene NUNC International). The HUVEC cells were then labelled with CellTracker Red CMTPX dye (Invitrogen) for 45min and rescued in EGM-2 media supplemented with 2% FBS for 30min. Coverslips with cancer cells were washed with PBS and then transferred onto 60mm dishes containing a HUVEC monolayer. A scratch across the HUVEC monolayer was then made using a 200μl pipet tip. 3 images of each dish were taken after 36 hours and the images were analysed using ImageJ (NIH) to quantify the area covered by HUVEC cells.

Chemotaxis Assay

250μl of Matrigel (BD Biosciences, #356231) containing the given amounts of bovine serum albumin (A2153, Sigma Aldrich), rhIGFBP2 (674-B2, R&D Systems), rhGas6 (885-GS, R&D Systems), anti-IGF1R (MAB391, R&D Systems) and MerFc (891-MR-100, R&D Systems) were allowed to solidify at the bottom of a 24 well plate for 30min before 250 μl HUVEC media containing 0.2% FBS were added. A 3.0μm HTS Fluroblock Insert (351151, BD Falcon) was then placed in each well. HUVEC cells were labelled with CellTracker Red CMTPX dye (C34552, Invitrogen) before resuspending 300K HUVECs per mL of 0.2% FBS EGM-2. 0.5mL of the resuspension was then added into each Fluoroblock insert and the assay allowed to proceed for 20h. The inserts were then fixed for 15 min in 4% paraformaldehyde and mounted onto slides with VectaShield mounting media (H-1000, Vector Laboratories). 5 fields of the basal side of each insert were then imaged and the images were analysed using ImageJ (NIH).

Migration Assay

HUVEC cells were grown to 90% confluence and stimulated by the given concentrations of bovine serum albumin (BSA, Sigma Aldrich, #A2153), rhIGFBP2 (674-B2, R&D Systems) and anti-IGF1R (MAB391, R&D Systems) in HUVEC media containing 0.2% FBS for 40 min at 37°C. The cells were then trypsinized and 50K cells were added into HTS Fluroblock Inserts (351151, BD Falcon). After 24 hours in 37°C with 5% CO_2, the inserts were removed, the membrane excised and fixed in 4% paraformaldehyde. HUVEC cells that had migrated to the basal side of the membrane were visualized with DAPI and counted in 5 fields per membrane using Image J (NIH).

Endothelial Adhesion

HUVEC cells were seeded on a 6cm plate and allowed to grow to confluence. Cancer cells were serum starved in DMEM media supplemented with 0.2% FBS for 30min, labelled with CellTracker Green CMFDA dye (C7025, Invitrogen) for 45min and incubated in DMEM media supplemented with 10% FBS for 30min. Cancer cells were then trypsinized and resuspended to 10K cells per mL of 10% FBS/DMEM. 5mL of the resuspension was then added to each plate of HUVECs and the plate was incubated at 37°C for 10min. The plates were then washed gently with PBS and fixed with 4% Paraformaldehyde for 15min. Each plate was then covered with 1mL of PBS and 6 images were taken from each plate. The number of cancer cells adherent to the HUVEC cells were then quantified using ImageJ (NIH).

Endothelial Proliferation

$1x10^6$ cancer cells were seeded to a 10cm plate and allowed to grow for 24h. The cancer cells were then washed gently with PBS and EGM-2 media supplemented with 2% FBS was added to each plate. The conditioned EGM-2 media was collected after 24h. 25K HUVEC cells were seeded in triplicate in a 6 well plate and allowed to grow for 16h. The HUVEC cells were then washed gently with PBS and 3mL conditioned EGM-2 media was added to each well. After 48h, the conditioned media was replaced with another 3mL of conditioned media. After another 48h, the cells were trypsinized and counted using a haemocytometer.

Tube formation Assay

Tube formation assay was performed according to manufacturer's protocol (354149, BD BioCoat™ Angiogenesis System–Endothelial Cell Tube Formation). Briefly, HUVEC cells were serum starved in EGM-2 media supplemented with 0.2% FBS for 24 hours. The HUVEC cells were then labelled with CellTracker Red CMTPX dye (C34552, Invitrogen) for 45min and subsequently treated in EGM-2 media supplemented with 2% FBS for 30min. Meanwhile, the tube formation assay plate, which was in 96-well format, was incubated at 37°C for 30min. The cancer cells and HUVEC cells were trypsinized and resuspended at 400K/mL and 800K/mL respectively in EGM-2 media supplemented with 2% FBS. The cancer cell and HUVEC cell suspensions were then mixed at a 1:1 ratio and 50μl of each mixture was seeded into each well of the tube formation assay plate. The assay plate was incubated at 37°C for 16h. Images of each well were taken and the images were processed using MetaMorph analysis software (Molecular Devices, Inc.) to obtain the number of branch points per image.

Analysis of miRNA and mRNA expression

Total RNA was extracted from the various cell lines using the MiRvana kit (AM1560, Applied Biosystems, Austin, TX). The Taqman microRNA assay (4427975-0002228, Applied Biosystems) was used to quantify expression levels of pri-miRNA and mature miRNA. For quantification of mRNA, 1μg of total RNA was reverse transcribed using the cDNA First-Strand Synthesis Kit (18080-051, Invitrogen). Approximately 50ng of the resulting cDNA was then mixed with SYBR green PCR Master MIX (4309155, Applied Biosystems) and appropriate primers (Table 4). Quantitative mRNA expression data was

obtained using an ABI Prism 7900HT Real-Time PCR System (Applied Biosystems). Smad4 was used as an endogenous control for normalization. Expression analysis of human breast cancers at various disease stages was performed using the TissueScan qPCR Array Breast Cancer Panels 2 and 3 (BCRT102 & BCRT103, Origene, Rockville, MD).

Table 4: qPCR primers for Gene Expression

Gene	Forward	Reverse
AXL	CGTAACCTCCACCTGGTCTC	TCCCATCGTCTGACAGCA
ABCB9	GACCTTCACCTACCGCACTC	CACAGGAGCTCTTCCCACTG
BEX2	GCCCCGAAAGTAGGAAGC	CTCCATTACTCCTGGGCCTAT
BGLAP	GGCGCTACCTGTATCAATGG	TCAGCCAACTCGTCACAGTC
CA12	CCAAGGCTACAATCTGTCTGC	GGGCAGGTTCAGCTTCACT
GDF15	CCGGATACTCACGCCAGA	AGAGATACGCAGGTGCAGGT
GEM	GACAGCATGGACAGCGACT	AACCATCAGGGTTCGTTCAT
IGF1R	AAAAACCTTCGCCTCATCCT	TGGTTGTCGAGGACGTAGAA
IGFBP2	CCAAGAAGCTGCGACCAC	GGGATGTGCAGGGAGTAGAG
ITGB4	TCAGCCTCTCTGGGACCTT	TATCCACACGGACACACTCC
EGFL7	TACACTCTGTGTGCCCAAGG	CAGCCTCTGCACTTCTTCCT
KIAA0746	GTTGTCTGTGCAGATGTACGC	TAGCAGGGCCAGGTTAAAAA
KLF4	GCCGCTCCATTACCAAGA	TCTTCCCCTCTTTGGCTTG
MARS	AACAACCTGGGCAACTTCAT	ACCATCTCAGGCACATAGCC
MERTK	GGAGACAGGACCAAAGC	GGGCAATATCCACCATGAAC
MEST	AGGGATCCGCAACAATGAC	TGGGGATAGTTACAGAGGCAAG
PADI4	AAGTGCAAGCTGACCATCTG	GCCGATCTCCATTTCATCC
PHGDH	TGGTGGAAAAGCAGAACCTT	AACAATAAGGCCTTCACAGTCC
PITPNC1	GCGCTACTACAAAGAATCTGAGG	GAGCACATGATAGGCTGATGAC
PSAT1	TCTTGTGCGGGAATTGCTA	AAGGGGACAGCACTGAACTG
PYGB	TCCAGGGTCCTGTATCCAAA	CCACGAAGTACTCCTGCTTCA
RGC32	TGCTGATCTTGACAAAACTTTAGC	GCAGGTCCTCGGAACTTTCT
SHMT2	GAGGGAGAAGGACAGGCAGT	CTCGGCTGCAGAAGTTCTCT
SMAD4	TGGCCCAGGATCAGTAGGT	CATCAACACCAATTCCAGCA
THBD	AATTGGGAGCTTGGGAATG	TGAGGACCTGATTAAGGCTAGG
TNFSF4	GTATCCTCGAATTCAAAGTATCAAAGT	CTGAGTTGTTCTGCACCTTCA
VIPR1	CTGTCCCCTCATCTTCAAGC	CAGCTGCGGCTTACATTG

miR-126 Target Prediction

Potential miR-126 targets were identified by using 3 sets of microarray profiles: LM2 control cells relative to LM2 cells over-expressing miR-126 (GSE No. 23905) and 2 replicate arrays of MDA and LM2 cells (GSE No. 23904 and Minn et. al[16]). Using these arrays we used the following criteria to identify possible miR-126 targets genes: 1) Genes down-regulated more than 1.6 fold upon miR-126 overexpression in LM2 cells and 2) Genes up-regulated by more than 1.4 fold in one of the two LM2 versus MDA arrays. All potential targets were subsequently verified by qPCR.

Metastasis free survival analysis

Upon identifying the 8 miR-126 regulated genes through an integrative analysis, we sought to determine whether the expression of these genes in aggregate correlates with human clinical metastasis. Published microarray data of series from UCSF[53], NKI[54], and MSKCC[16] were used to obtain probe-level expression values. For genes that were represented by multiple probes, probes that displayed sufficient signal intensity as well as the highest coefficient of variation (most informative) in an independent dataset were used. Each breast cancer was classified as miR-126 signature positive if the sum of the Z-scores for the expression values of the 8 genes was greater than the mean of the population. Kaplan-Meier metastasis-free survival curves were generated using Graphpad Prism 5 software (GraphPad Software Inc., LA Jolla, CA). Statistical significance for differences between survival curves of patients was determined using the Mantel-Cox log-rank test using Graphpad Prism 5 software.

Luciferase Reporter Assay

The full-length 3'UTR's and CDS's of ABCB9, IGFBP2, ITGB4, MERTK, PITPNC1, PSAT1, SHMT2 and VIPR1 were cloned into the psiCheck2 dual luciferase reporter vector (C8021, Promega, Madison, WI). MDA-MB-231 cells expressing either a control hairpin or a hairpin targeting miR-126 were transfected with the respective specific reporter construct. 30 hours after transfection, the cells were lysed and the ratio of renilla to firefly luciferase expression was determined using the dual luciferase assay (E1910, Promega). Cloning primer sequences are shown in Table 5.

Potential miR-126 sites in genes were identified by alignment to the complementary miR-126 sequence 5-TTACTCACGGTACGA-3, and mutagenesis was performed using the QuickChange Multi Site-Directed Mutagenesis Kit (200514, Agilent Technologies, Santa Clara, CA). Based on the UCSC genome browser the 3'UTR of MERTK was mutated at position 5 (GTT to CAC), the 3'UTR of IGFBP2 was mutated at position 246 (GGT to CAC), the CDS of PITPNC1 was mutated at position 709 (TAC to GTA) from the start codon and the CDS of SHMT2 was mutated at position 1126 (GGT to CAC). Mutagenesis primers are in shown in Table 6.

Table 5: Cloning Primers for 3'UTR and CDS of candidate miR-126 targets

Gene	Primers
ABCB9 3'UTR	F: CCGGCCCTCGAGTGGGGGGCCCCTGCTTCTCC R: CCGGCCGCGGCCGCTTAGGGGTAAGAGGTAGTAC
ABCB9 CDS	F: CCGGCCCTCGAGATGCGGCTGTGGAAGGCGGT R: CCGGCCGCGGCCGCTCAGGCCTTGTGACTGCCGT
IGFBP2 3'UTR	F: CCGGCCCTCGAGACCGCAGCCAGCCGGTGCCT R: CCGGCCGCGGCCGCTTACTTTTCCTTCCTTTAAT
IGFBP2 CDS	F: CCGGCCCTCGAG ATGCTGCCGAGAGTGGGCTG R: CCGGCCGCGGCCGCCTACTGCATCCGCTGGGTGT
ITGB4 3'UTR	F: CCGGCCCTCGAGCCGCACCCTGCCCCACCCCC R: CCGGCCGCGGCCGCTAGCAGTAGcCAAAACCATTT
ITGB4 CDS	F: CCGGCCCTCGAGATGGCAGGGCCACGCCCCAG R: CCGGCCGCGGCCGCTCAAGTTTGGAAGAACTGTT
MERTK 3'UTR	F: CCGGCCCTCGAGGGAGAGGTGCGGGGAGACAT R: CCGGCCGCGGCCGCCTTCCTTATTCATATTTTAT
MERTK CDS	F: CCGGCCCTCGAGATGGGGCCGGCCCCGCTGCC R: CCGGCCGCGGCCGCTCACATCAGGACTTCTGAGC
PITPNC1 3'UTR	F: CCGGCCCTCGAG CAATGGATGAAGTCCGAGAA R: CCGGCCGCGGCCGCTTAAAAGACAGAAACAAGTA
PITPNC1 CDS	F: CCGGCCCTCGAG ATGCTGCTGAAAGAGTACCG R: CCGGCCGCGGCCGCTCATGTACTTGTTTGGGCAT
PSAT1 3'UTR	F: CCGGCCCTCGAGACACATCCTAACCAGGATAT R: CCGGCCGCGGCCGCTTAGATGTTTTAGGACTTTA
PSAT1 CDS	F: CCGGCCCTCGAGATGGACGCCCCCAGGCAGGT R: CCGGCCGCGGCCGCTCATAGCTGATGCATCTCCA
SHMT2 3'UTR	F: CCGGCCCTCGAGAGGCACCTGGGAAATGAGGC R: CCGGCCGCGGCCGCCAAAATACAATTTCATTTAA
SHMT2 CDS	F: CCGGCCCTCGAGATGCTGTACTTCTCTTTGTT R: CCGGCCGCGGCCGCTCAATGCTCATC
VIPR CDS	F: CCGGCCCTCGAGATGCGCCCGCCAAGTCCGCT R: CCGGCCGTTTAAACTCAGACCAGGGAGACTTCGG
VIPR1 3'UTR	F: CCGGCCCTCGAGCCACCAGGATCCCAGGGGCC R: CCGGCCGCGGCCGCTCCAAGCCAACATTTATTGT

Table 6: Mutagenesis Primers for miR-126 targets

Gene	Primers
IGFBP2 3'UTR	F:AAGGGGGTTGTGGTCGGGGAGCTGGCACACAGGTTTGGGGAGGGGGAAGAGAA R: TTCTCTTCCCCCTCCCCAAACCTGTGTGCCAGCTCCCCGACCACAACCCCCTT
MERTK 3'UTR	F: ATTCTAGGCGATCGCTCGAGGGAGACACGCGGGGAGACATTCCAAAAATCAAG R: CTTGATTTTTGGAATGTCTCCCCGCGTGTCTCCCTCGAGCGATCGCCTAGAAT
PITPNC1 CDS	F: TATGACAATGGATGATGTTCGGGAAGTAGAGAAAAACATGCATGAACAAACCA R: TGGTTTGTTCATGCATGTTTTTCTCTACTTCCCGAACATCATCCATTGTCATA
SHMT2 CDS	F: GCGAGGCTACTCACTGGTATCAGGTCACACTGACAACCACCTGGTGCTGGTGG R: CCACCAGCACCAGGTGGTTGTCAGTGTGACCTGATACCAGTGAGTAGCCTCGC

Cancer cell proliferation

2.5 X 10^4 LM2 cells expressing a control hairpin or short hairpins targeting IGFBP2, PITPNC1 or MERTK were seeded in triplicate in 6 well plates and viable cells were counted at 5 days after seeding.

Histology

Lungs were prepared by perfusion fixation with 4% paraformaldehyde infused through the vascular system and through the trachea. After excision, the lungs were placed in 4% paraformaldehyde overnight and embedded in paraffin. 5 minutes prior to fixation, 100 mg biotinylated lectin (B-1175, Vector Laboratories) was injected into the circulation via the tail vein. 5μm thick paraffin sections were stained with primary antibodies against MECA-32 (Developmental Studies Hybridoma Bank, The University of Iowa, IA), Vimentin (VP-V684, Vector Laboratories) and with FITC-labelled Avidin (B-1175, Vector Laboratories) for the detection of injected biotinylated lectin. Primary antibodies were detected using various Alexa Flour dye-conjugated secondary antibodies. Fluorescence was obtained using a Zeiss laser scanning confocal microscope (LSM 510).

To determine the vascularisation of metastatic nodules, the MECA-32 and lectin signals were quantified using ImageJ while the metastatic nodules' extents were determined through co-staining with human vimentin. The collective area covered by vessels was determined by subtracting background (rolling ball radius of 1 pixel) and by using a pre-determined threshold as cut-off. Vessel density is given as the percentage of area covered by the blood vessels compared to the total area of the metastatic nodule. A metastatic nodule was defined

by an area positive for vimentin staining with a total area above 2000 μm^2. The Kolmogorov-Smirnov test was used to determine the significance of difference in the blood vessel density for both MECA-32 and lectin staining using the publicly available software at http://www.physics.csbsju.edu/stats/KS-test.html

Mammary fat pad tumours were excised and submerged into 4% paraformaldehyde for 24 hours. The fixed tissue was embedded in paraffin and sectioned in 5 μm thick slices. Immunodetection were performed using antibodies directed towards MECA-32 (Developmental Studies Hybridoma Bank), Mac-2 (CL8942AP, Cederlane, Burlington) and CD45 (550539, BD Biosciences). Detection of primary antibodies was performed using various biotinylated secondary antibodies (Vector Laboratories). The signal was subsequently amplified using the ABC kit (Vector Laboratories), and detected using DAB (3,3′-diaminodbenzidine). Before mounting the slides were counterstained with hematoxilin.

Dextran permeability was determined as described in Arnold et al., 2010[55] with slight modifications. Briefly, an intravenous bolus of 10mg/ml rhodamine B labelled with low molecular weight Dextran (1 x 10^4 kDa: D1824, Invitrogen) in sterile PBS was infused. 15 min after, the mice were anaesthetized and the lungs were perfused with OCT, removed and frozen on dry ice. 10 μm section was cut and the dextran permeability inside metastatic nodules, as determined by vimentin staining, was measured by fluorescence microscopy. Using ImageJ (NIH), a preset threshold was used to determine the levels of dextran permeability. The results are presented as the mean percentage of the thresholded area inside the metastatic nodule.

Tracking of HUVEC cells in the liver metastasis assay was performed by labelling 500K HUVECs with CellTracker Red CMTPX dye (Invitrogen) and co-injecting them with 500K LM2/miR-126 overexpressing cells into the portal circulation. 4 days later, the livers were removed, frozen in OCT and cut into 10 μm sections. Cancer cells were stained using antibodies against human vimentin (Vector Laboratories) and the mouse endothelial cells were stained using antibodies against mouse CD31 (Biolegend).

Flow Cytometry

Primary mammary fat pad tumours were excised and dissociated into single cells as previously described. Briefly, tumours were minced and placed in culture medium containing a 1:1 mixture of DMEM/F12 media with 0.125% collagenase III and 0.1% hyaluronidase. Samples were incubated at 37°C for 3h, with gentle shaking. After collagenase treatment, cells were centrifuged, resuspended in 0.25% trypsin and incubated for another 30min at 37°C. Cells were then resuspended in PBS. To analyse the endothelial cell population of the tumour, FITC-CD45 (eBioscience), PE/Cy7-CD31 (Biolegend) and PerCP/Cy5.5 were used. Dead cells were excluded using LIVE/DEAD aqua dead cell stain (Invitrogen). Endothelial cells were analysed using LSRII and FloJo.

ELISA

IGBFP2, MERTK and VEGF levels in conditioned media were quantified using the IGFBP2 ELISA kit (RayBiotech), Total Mer DuoSet (R&D Systems), and the VEGF ELISA kit (R&D Systems).

Western Blotting

Cellular lysates from MDA-MB-231 cells were prepared by lysing cells in 1 ml ice-cold RIPA buffer containing protease inhibitors (Roche, Mannheim, Germany). Conditioned media were prepared by incubating MDA-MB-231 cells in serum free media for 24 hours. The media was then concentrated twenty times by spin filtering. 40μg protein was subsequently separated on a 4-12% SDS-PAGE, and transferred to a PVDF membrane. The following antibodies were used for protein detection: mouse anti-MERTK (CVO-311, Caveo Therapeutics), goat anti-IGFBP2 (R&D Systems), rabbit anti-human PITPNC1 (custom made against human amino acids 308-325 in the long isoform of human PITPNC1), rabbit anti-phosphoIGF1Rβ-Y1131 (Cell Signaling), rabbit antiIGF1Rβ (Cell Signaling), and rabbit anti-GAPDH (Sigma-Aldrich).

***In vivo* Endothelial Recruitment (Matrigel Plug) Assay**

Recombinant IGFBP2 (1μg/ml), MerFc (10μg/ml) or BSA (11ug/ml) were mixed with Matrigel (BD Bioscience). 100 μl was injected into the mammary fat pads of NOD-SCID mice and allowed to solidify. 48 hours later, the plugs were removed, fixed in 4% paraformaldehyde overnight and embedded in paraffin. 5 μm thick sections were stained with an antibody targeting MECA32. Mammary fat pads contain containing large comparable-sized matrigel plugs that were typically centralised in the fat pad were analysed. The majority of the control and experimental plugs were obtained from the same mouse, controlling for inter-animal variability. Six representative images of each plug were obtained at 20X magnification and the number of endothelial cells per field were counted.

Analysis of Genomic Copy Number

Total genomic DNA was extracted and purified from cell populations using the DNeasy kit (Qiagen). For DNA content normalization, GAPDH was used as endogenous control. Primers used in the qPCR for genomic copy number is shown in Table 7.

Table 7: qPCR primers for Genomic Copy Number

Gene	Forward	Reverse
miR-335_a	CTATTGGAAGTCCTGCGTGTATC	CCATCATTAAGGAGCAACAAGAG
miR-335_b	AGGCACTGAGTTATGTTTTCAGC	CAATCTGTTTCTCAGTTTCTTCACC
miR-126_a	CATGTCCTGGGGTTACTGCT	CTAGCACTGCATTCATCCACAT
miR-126_b	ATATCAGCCAAGAAGGCAGAAGT	ACTCACCGTACGAGTTTGAAGTG
let7	CTCCTTCCCCTGAAATCTGTTT	AGGATCCAGTGTGAAAGAGACAC
GAPDH	AGCCACATCGCTCAGACAC	GCCCAATACGACCAAATCC

Array CGH

Array-CGH was performed on various breast cancer cell lines using the Agilent Human Genome CGH Microarray 44K Kit. 500ng of genomic DNA was hybridized to each array with female human genomic DNA (Promega) as control. Hybridization signals were normalized and analyzed by Agilent CGH Analytics Software.

Methylation Specific PCR (MSP) and Pyrosequencing

Genomic DNA was treated with bisulfite prior to MSP and pyrosequencing analysis using the EZ-DNA methylation-Gold kit (Zymo Research) as per manufacturer's recommendations. MSP was performed on 5ng of bisulfite treated DNA using the primers shown in Table 8. Pyrosequencing analysis was performed as previously described[56] using the primers shown in Table 9.

Table 8: Primers for Methylation Specific PCR

Gene	Forward	Reverse
miR-335		
Island 1 Methylated	GTAGTTTTTTTAGTGTTCGTGGGTC	CAAACCTCCCTTCGACTACG
Island 1 Unmethylated	AGTTTTTTTAGTGTTTGTGGGTTGT	CTACAAACCTCCCTTCAACTACAC
Island 2 Methylated	TTTTGTATTGTGATTTTATTTTACGT	AACAAATTTCCTTTACAACAACG
Island 2 Unmethylated	TTTGTATTGTGATTTTATTTTATGT	AAACAAATTTCCTTTACAACAACAC
Island 3 Methylated	GTTCGTGTTTTTGGTGGTTATC	TTCGAAACGTAAATACTAAACCGTA
Island 3 Unmethylated	TTCAAAACATAAATACTAAACCATA	TGTGTTTTTGGTGGTTATTGG
miR-126		
Methylated	TAGTTTTTTGTTTGTTCGACGATAC	AAAAAACGACTTTTTATACTCCGTC
Unmethylated	GTTTTTTGTTTGTTTGATGATATGT	AAAAAACAACTTTTTATACTCCATC

Table 9: Pyrosequencing Primers for miR-335 promoter

Island	Primers
1	F1: 5'-biotin/TTATTAGTTTGGTGGTGGGTTTAATAG-3' R1: 5'-CCTAAATACCCCAACTCTTTCCTTAAA-3' S1: 5'-AAAACAACAAAACTCTAAAATA-3'
2	F1: 5'-TAGGGGAGGGTTTTTGTAGTAGAA-3' R1: 5'-biotin/AACCACAAAAATAAAATACCCCTCTA-3' S1: 5'-AGGGTTTTTGTAGTAGAATTT-3'
3	F1: 5'-AGAAAGGAGTTATTGTTAGAGGGGTA-3' R1: 5'-biotin/CCAAAAAAAATACCCAAATATACTAATTAC-3' S1: 5'-TAGAGAGGTTGGGAGG-3'

Representational Oligonucleotide Microarray Analysis (ROMA) of breast cancer tumours

Deletions of the miR-335 locus were identified using ROMA analysis of human breast cancers. These clinical samples were previously obtained at MSKCC through an IRB approved protocol.[57] Deletions were classified as focal if one of their arms localized within 2 Megabases of the miR-335 locus and gross if they did not fulfill this criteria.

Northern Blotting

Total RNA was extracted from the various cell lines using the MiRvana kit. 50μg RNA was subsequently separated on a 15% denaturing gel and transferred to a Hybond C+ membrane. The membrane was cross-linked with 1-methlylimidazole and 1-ethyl-3-(3-dimethylaminopropyl) carbodiimide (EDC) at 60°C for 2h, before hybridization overnight at 37°C with DIG-labelled probes. Using reagents from the DIG Northern Start Kit (Roche), the membrane was then blocked at r.t. for 3h and incubated with anti-DIG Ab at a dilution of 1:15,000 at r.t. for 30min. CDP-Star was then applied to the membrane before it exposure to films for signal detection.

CHAPTER 3:
MiR-126 mediates endothelial recruitment, metastatic angiogenesis and metastatic initiation by breast cancer cells

Introduction

A previous study that embarked on a systematic search for regulators of metastasis identified a set of microRNAs that robustly suppresses breast cancer metastasis to both lungs and bones.[51] While two of these miRNAs, miR-335 and miR-206, suppressed metastasis by inhibiting cell migration, miR-126 inhibited metastasis through a different mechanism. MiR-126 over-expression caused only a modest reduction in primary tumour growth, which is in stark contrast to its dramatic metastasis suppression effects. Thus, its role in metastasis remains unresolved. Low miR-126 expression levels in primary tumours strongly predicts future metastatic relapse in breast cancer patients, supporting an important role for this miRNA in human breast cancer metastasis.

Subsequent to its identification as a metastasis suppressor miRNA, miR-126 silencing has also been noted in a wide variety of other epithelial malignancies such as cervical[58], gastric[59], colon[60], prostate[61], liver[62] and lung[63] cancers. Besides that, silencing of miR-126 has also been described in cancers arising in diverse species including the mouse[64], and the Tasmanian devil[65]. These findings suggest that this miRNA plays a key suppressive role in cancer progression and that unlike most miRNAs, which display varied expression patterns in distinct cancer types, miR-126 may regulate a general process subserving cancer progression.

In separate studies, miR-126, which is developmentally expressed in endothelial cells, was genetically deleted or knocked down in mice and zebrafish respectively. MiR-126 inhibition during embryonic development led to partial embryonic lethality, loss of vascular integrity, and haemorrhage[66]. In particular, endothelial-expressed miR-126 was found to be required for normal developmental angiogenesis and vascular integrity in mouse and zebrafish[67,68] systems, specifically through targeting of SPRED1 and PIK3R2[66,68]. Since then, miR-126 has been implicated in breast cancer tumorigenesis through regulation of PIK3R2, which is an upstream regulator of the VEGF/PI3K/AKT signalling pathway. Thus, it would be interesting to determine whether miR-126 inhibits breast cancer metastasis through regulation of genes and mechanisms similar to those that it regulates in endothelial cells or if it suppresses metastasis through other unique mechanisms.

Therefore, miR-126 has been implicated in cancer in numerous cancer types and in diverse species. Importantly, miR-126 is clinically relevant to the progression of human breast cancer–the expression levels of miR-126 serve as a strong predictive indicator for metastasis-free survival. However, little is known about the molecular and cellular determinants that underlie the ability of this miRNA to suppress cancer progression. We thus decided to investigate the role of miR-126 in metastasis and elucidate the mechanisms that enable it to suppress breast cancer progression effectively.

Results

Endogenous miR-126 inhibits Metastasis

Dissecting the mechanism by which a robust metastasis suppressor such as miR-126 regulates metastatic colonization is challenging, given that its over-expression in multiple metastatic human cell lines led to nearly complete eradication of metastases, precluding the *in vivo* comparison of metastatic nodules formed by miR-126 over-expressing and control breast cancer cells.[51] To circumvent this problem, metastatic progression was analysed in the setting of miR-126 silencing. This allowed for the comparison of *in vivo* metastatic events between miR-126 knockdown (KD) and control breast cancer cells and to elucidate the effects of endogenous miR-126 on metastasis, while also determining if the previously reported suppression of metastatic colonization by over-expression of miR-126 were due to artefacts of over-expression studies. Stable miR-126 and control knockdown cells were first generated by transducing poorly metastatic parental MDA-231 breast cancer cells with the lentiviral-based miRZip anti-sense hairpin microRNA inhibition system (Figure 1).

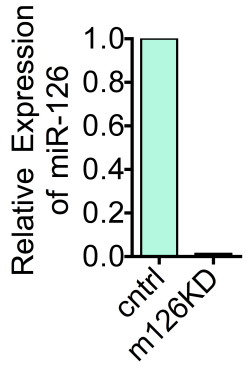

Figure 1| miR-Zip miRNA antisense shRNA system stably inhibits miR-126 expression in MDA cells. MDA cells were transduced with lentivirus expressing either a miR-Zip construct that targets miR-126 or a scrambled version. The expression levels of mature miR-126 were then tested using qPCR.

The miR-126KD and control MDA-231 cells were injected into immunodeficient NOD-SCID mice via the tail vein and evaluated for lung colonization capacity. Colonization by breast cancer cells was monitored through quantitative bioluminescence imaging. MiR-126 silencing in parental MDA-231 breast cancer cells increased lung metastatic colonization significantly as assessed by bioluminescence imaging (Figure 2). Immunohistological staining for human vimentin in the lungs obtained from these mice confirmed that miR-126 inhibition dramatically increased metastatic colonization based on gross histology (Figure 2). These findings are consistent with previous experiments whereby miR-126 over-expression strongly abolished metastasis.

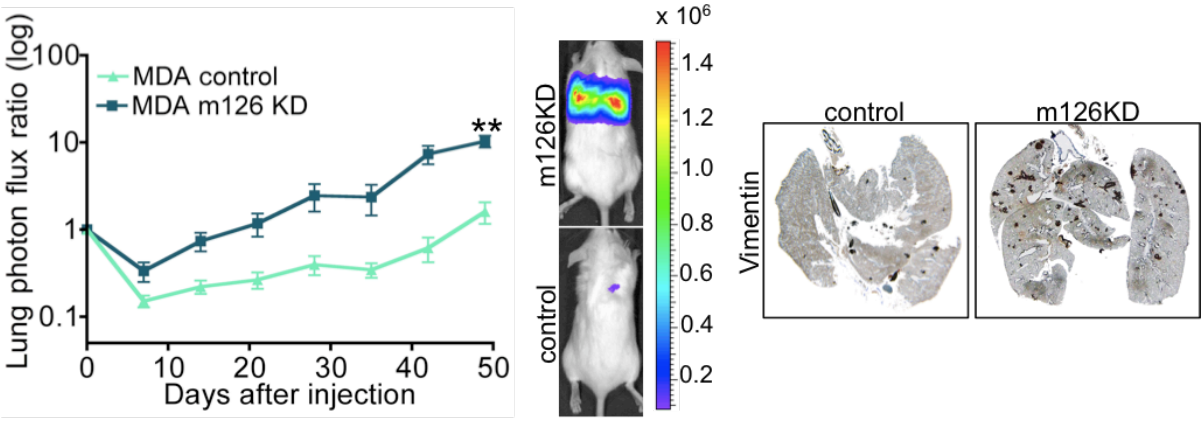

Figure 2| Endogenous miR-126 suppresses lung metastatic colonization. Bioluminescence imaging of lung metastasis by poorly metastatic breast cancer cells upon miR-126 inhibition. 4 X 10^4 MDA-MB-231 cells expressing a short hairpin (miR-Zip) targeting miR-126 or the control hairpin were injected intravenously into immunodeficient NOD-SCID mice. Representative mice shown correspond to the MDA-MB-231/miR-126KD set (top) and MDA-MB-231/scrambled set (bottom) at day 49. Lung colonization was quantified through bioluminescence imaging. n=5; error bars represent s.e.m.; p-value based on a one-sided student's t-test at day 49. Lungs were extracted at day 49 and immunohistochemically stained for human vimentin (right). **P<0.001.

The MDA/miR-126KD and MDA/control cell lines were then tested for their ability to undergo systemic metastasis via intracardiac injection into immunodeficient Nude mice. Inhibition of miR-126 in MDA-231 breast cancer cells significantly increased systemic metastasis to several organs such as the bone and brain (Figure 3). These cell lines were also subjected to a liver colonization assay by injecting them into the hepatic portal veins of NOD-SCID mice via the spleen. Silencing of miR-126 in MDA-231 breast cancer cells increased liver metastasis significantly, as assessed by both bioluminescence imaging and examination of gross histology (Figure 4). These results showing that miR-126 knockdown increases metastasis in several different colonization assays indicate that the metastasis suppression effects of endogenous miR-126 are not organ specific.

MiR-126 was also stably knocked down in the poorly metastatic CN34 breast cancer cell line, an independent primary malignant population obtained from the pleural fluid of a patient with metastatic breast cancer. The CN34/miR-126KD and CN34/control cell lines were then subjected to the lung and systemic metastasis assay. Inhibition of endogenous miR-126 in the CN34 cell line enhanced both lung and systemic metastasis (Figure 5), showing that the suppressive effects of miR-126 on metastasis were not cell line-specific.

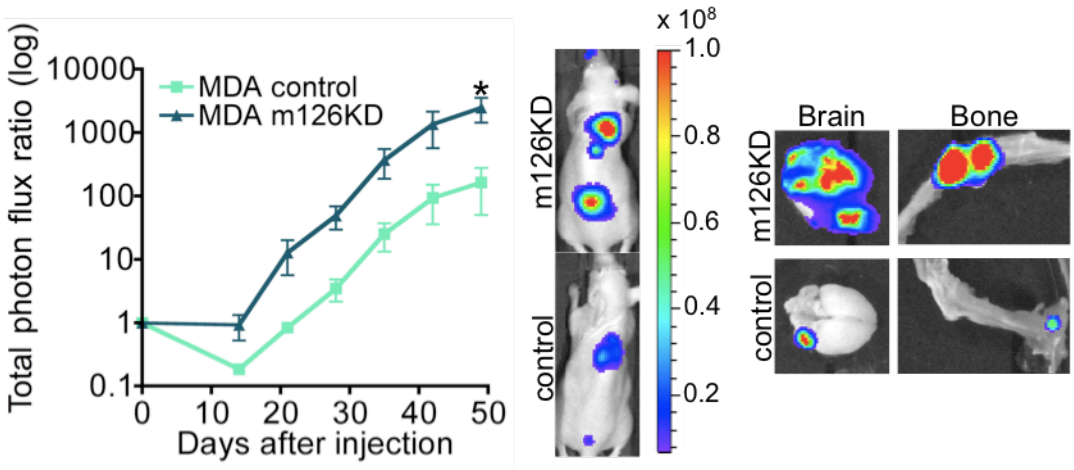

Figure 3| Endogenous miR-126 suppresses systemic metastasis. Bioluminescence imaging of systemic metastasis by poorly metastatic breast cancer cells with inhibited miR-126 expression. 4 X 10^4 MDA-MB-231 cells expressing a short hairpin targeting miR-126 or the control hairpin were injected via intracardiac route into athymic nude mice. Representative mice shown correspond to the MDA-MB-231/miR-126KD set (top) and MDA-MB-231/scrambled set (bottom) at day 34. Whole body colonization was measured by bioluminescence and quantified. n=4; error bars represent s.e.m.; p-value based on a one-sided student's t-test at day 34. Representative images of bone and brain metastatic nodules are shown (right). *P<0.05.

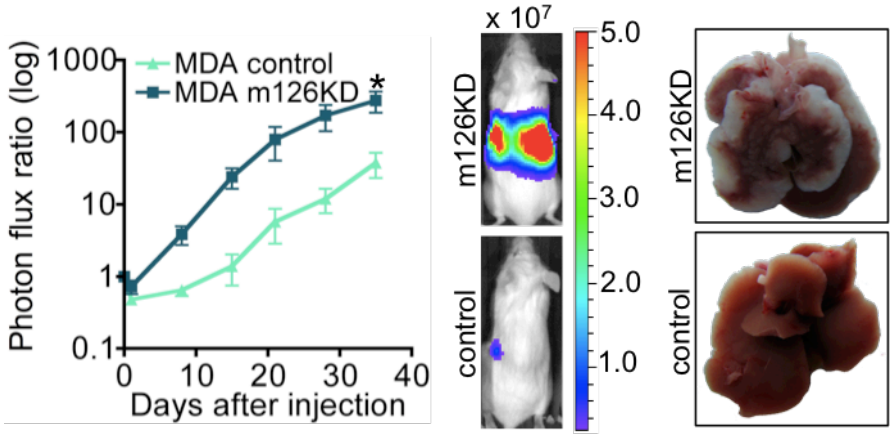

Figure 4| Endogenous miR-126 suppresses metastatic liver colonization. Bioluminescence imaging of liver metastasis by poorly metastatic breast cancer cells with suppression miR-126 expression. 5 X 10^5 MDA-MB-231 cells expressing a short hairpin targeting miR-126 or the control hairpin were injected via the spleen into NOD-SCID mice. Representative mice shown correspond to the MDA-MB-231/miR-126KD set (top) and MDA-MB-231/scrambled set (bottom) at day 35. Liver colonization was measured by bioluminescence and quantified. n=6; error bars represent s.e.m.; p-value based on a one-sided student's t-test. Representative images of the livers extracted at day 35 are shown (right). *P<0.05.

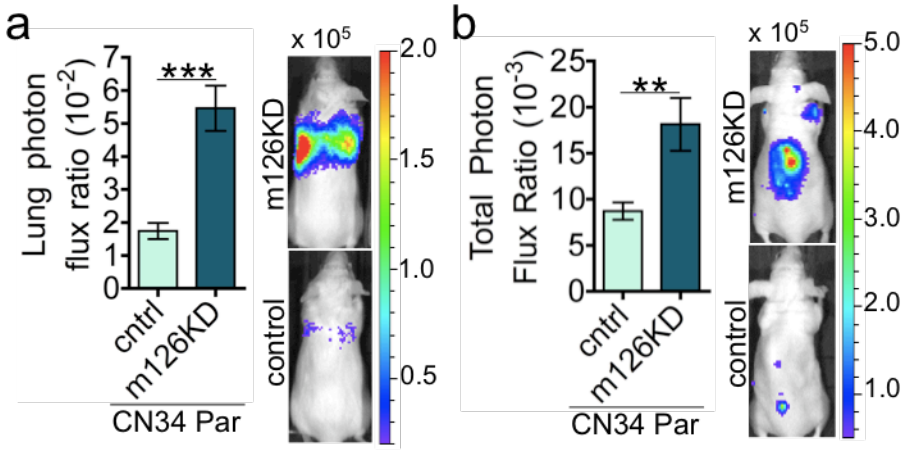

Figure 5| Endogenous miR-126 suppresses lung and systemic metastasis in a primary malignant population. a, Bioluminescence quantification of lung metastasis by 5 X 10^5 poorly metastatic CN34 breast cancer cells expressing a hairpin targeting miR-126 (CN34/miR-126KD) or a control hairpin (CN34/control); n=7. **b,** Bioluminescence quantification of systemic metastasis by 1 X 10^6 CN34/miR-126KD and CN34/control cells; n=6. Error bars represent s.e.m.; all p-values based on one-sided student's t-tests. **P<0.001; ***P<0.0001.

miR-126 inhibits Metastatic Initiation and Colonization

I next wondered to what extent was the dramatic increase in metastatic colonization observed with miR-126 inhibition due to the suppression of tumour growth by miR-126. Previous studies showed overexpression of miR-126 in cancer cells to significantly decrease *in vitro* proliferation. However, inhibition of endogenous miR-126 did not significantly increase *in vitro* proliferation, and it resulted in only a modest increase in primary tumour growth (Figure 6). This increase in mammary tumour volume (~39.4%) is an order of magnitude smaller than the effect of miR-126 silencing on metastasis, indicating that metastasis suppression by miR-126 is not simply due to its ability to repress tumour growth.

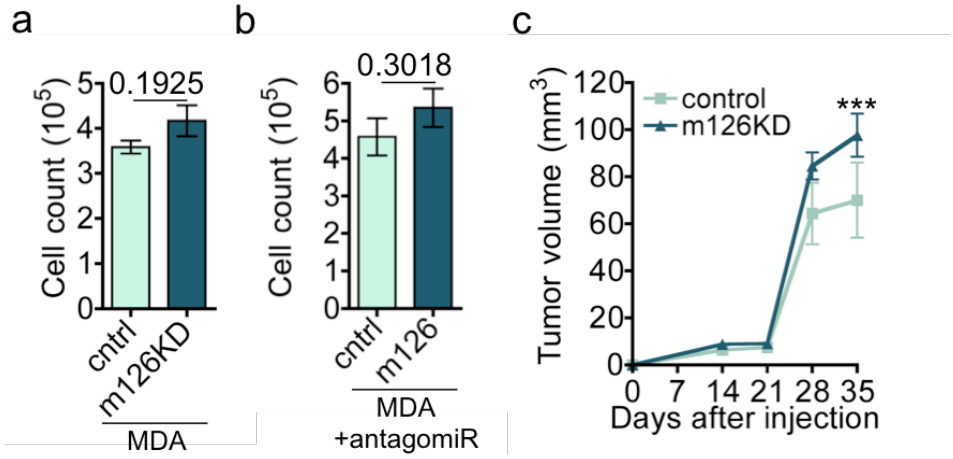

Figure 6| Endogenous miR-126 has modest effects on breast cancer cell proliferation and primary tumour growth. **a,** 5 X 10^4 MDA cells expressing a short hairpin targeting miR-126 or the control hairpin were seeded into a 6-well plate in triplicate. After 120h, the cells were trypsinized and counted. n=3; error bars indicate s.e.m.; p-values based on a one-sided student's t-test. **b,** 5 X 10^4 .5 X10^4 MDA cells treated with control and miR-126 targeting LNA oligos were subjected to an *in vitro* proliferation assay. n=3; error bars indicate s.e.m.; p-values based on a one-sided student's t-test. **c,** 5 X 10^5 MDA cells expressing a short hairpin targeting miR-126 or the control hairpin were injected into the mammary fat pads of immunodeficient mice. Tumour volumes were measured over time. n=15; error bars indicate s.e.m.; p-values based on a one-sided student's t-test at day 35. ***P<0.0001.

To better understand the role of miR-126 in metastatic colonization, we quantified the numbers and sizes of all metastases through image analysis of lungs from mice injected with MDA/miR-126KD or MDA/control cells. Quantification of the nodules within the lungs revealed a significant increase in the number of metastatic nodules in lungs of mice injected with miR-126KD cells (13.6 ± 3.2) as compared to those injected with control cells (4.9 ± 1.8) (Figure 7a). This increase in number of nodules is independent of nodule size, and it is importantly more pronounced at smaller nodule sizes. This is consistent with primarily an increase in the initiation of metastases rather than an increase in the growth of established metastases. Similarly, silencing of miR-126 significantly increased the number of metastatic foci in other organs in the systemic metastasis assay (Figure 7b), revealing miR-126 to regulate the generic phenomenon of metastatic initiation.

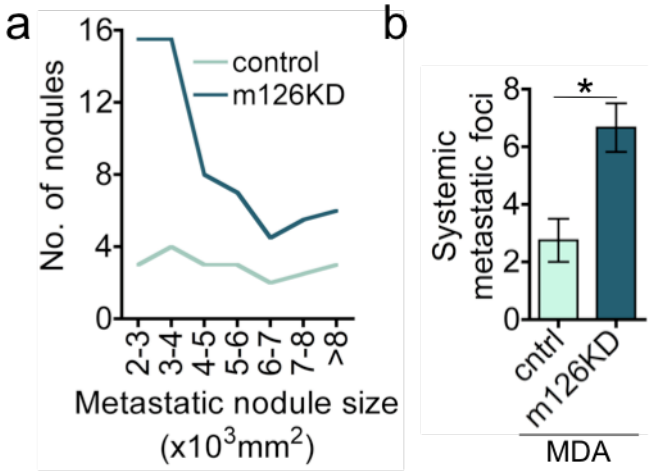

Figure 7| Endogenous miR-126 suppresses the initiation rate of metastatic events. a, Sizes and numbers of metastatic nodules in lungs extracted from Figure 2 were measured using ImageJ. **b**, Total number of metastatic foci in mice from Figure 3 were counted from the bioluminescence images. *P<0.05.

If miR-126 silencing provides a metastatic initiation advantage to cancer cells as they initiate metastases in the metastatic niche, its induction in the initial phase of metastasis formation should reduce the number of metastatic nodules. To test this, miR-126 expression was conditionally restored in highly metastatic LM2 cells (originally derived from the poorly metastatic MDA-231 population), which display silencing of miR-126, after extravasation into the lungs (Day 3), enabling us to also study the effects of miR-126 in the absence of any potential complicating effects of this miRNA on extravasation. Consistent with previous results, restoration of miR-126 expression in highly metastatic breast cancer cells at this early phase of metastasis initiation significantly reduced the number of metastatic nodules observed at day 49 (Figure 8). These findings show that miR-126 silencing enhances the efficiency of metastasis formation, leading to a larger number of metastases, thus revealing endogenous miR-126 to be a suppressor of metastatic initiation and metastatic colonization.

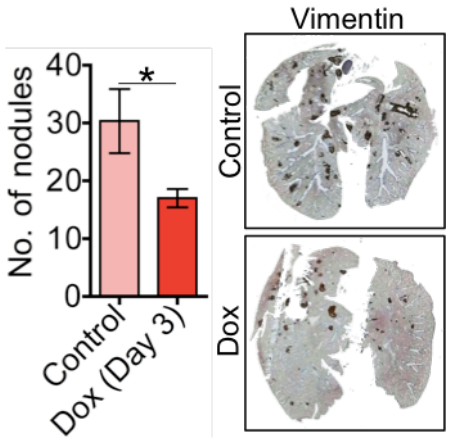

Figure 8| Conditional expression of miR-126 suppresses metastatic colonization. 4 X 10^4 Lm2 cells expressing a doxycycline inducible pre-miR-126 cassette were injected via the tail vein into NOD-SCID mice at day 0. At day 3, doxycycline (2 mg/ml) and sucrose (5%) were added to the drinking water in one group of mice and only 5% sucrose in the other. At day 48, the lungs were removed and immunohistochemically stained for human vimentin (right). Total number of nodules in each lung is shown to the left. *P<0.05.

miR-126 suppresses Metastatic Angiogenesis

Our findings suggest that miR-126 silencing may provide metastatic cells and incipient metastases an advantage during metastatic colonization. While considering the basis of the selective advantage provided by miR-126 silencing, I observed that the metastatic nodules in lungs of mice injected with MDA/miR-126KD cells displayed higher vessel densities upon microscopic visualization of lung H&E tissue sections. To quantify this, co-immunostaining was performed on lungs from these mice for human vimentin, which labels breast cancer cells, and the mouse endothelial marker MECA-32. This allowed for the quantification of endothelial density within metastatic nodules in lungs of mice injected with either miR-126KD or control breast cancer cells. Image analysis and quantification revealed metastases derived from miR-126KD cells to have a significantly higher endothelial density (Figure 9, 35% increase).

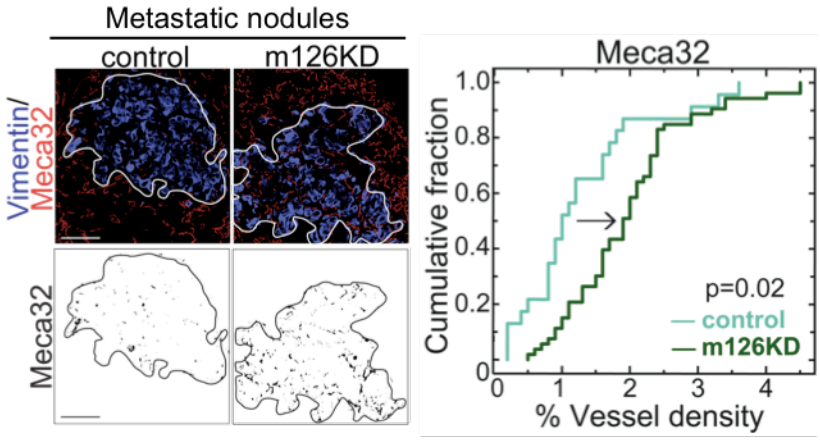

Figure 9| miR-126 suppresses endothelial content in lung metastases. Lung sections from Figure 2 were histologically double-stained for human vimentin and MECA-32. The border of each nodule was demarcated based on vimentin staining and lectin/MECA-32 staining within circumscribed region (lower panels). The distribution of percent endothelial density (area positive for lMECA-32 staining per area) is shown in a cumulative fraction plot; n=8 (18 and 68 nodules in control and miR-126 KD groups, respectively). p-value based on the Kolmogorov-Smirnov test.

To determine if enhanced endothelial density in miR-126KD metastases represent a corresponding increase in functional vessels, sugar-binding lectin was injected into the circulation of mice prior to lung extractions. Subsequently, the lung sections were co-stained for vimentin and lectin. Lectin histochemistry revealed that metastases derived from MDA/miR-126KD cells contained increased density of functional blood vessels relative to those derived from MDA/control (Figure 10, 33% increase).

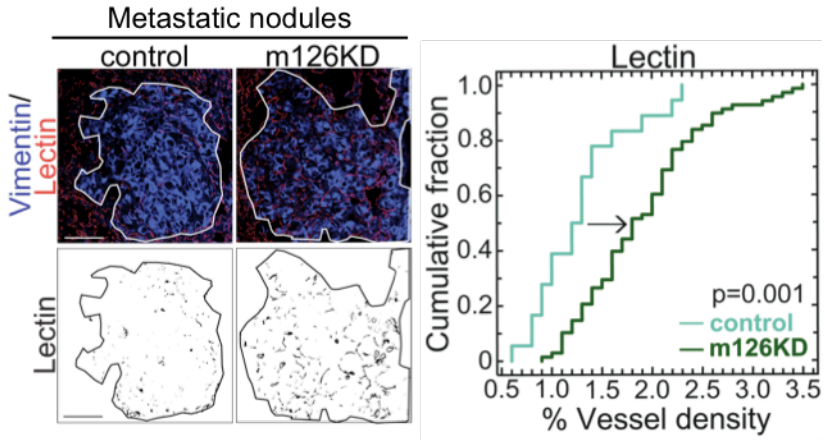

Figure 10| miR-126 inhibits formation of functional vessels in lung metastases. Lung sections from Figure 2 were histologically double-stained for human vimentin and intravenously injected lectin. The border of each nodule was demarcated based on vimentin staining and lectin staining within circumscribed region (lower panels). The distribution of percent vessel density (area positive for lectin staining per area) is shown in a cumulative fraction plot; n=8 (18 and 68 nodules in control and miR-126 KD groups, respectively). p-value based on the Kolmogorov-Smirnov test.

Finally, I determined whether miR-126 regulated hemodynamic perfusion to the metastatic nodules by injecting low molecular weight dextran (1 x 10^4kDa) into the tail vein of mice prior to sacrifice. Subsequent visualization of the dextran and image analysis of lungs determined that metastases derived from MDA/miR-126KD cells have significantly increased perfusion as compared to those from control cells (Figure 11). Together, these independent and complementary methods reveal miR-126 to suppress metastatic endothelial density, functional metastatic angiogenesis and perfusion–providing metastases with a selective advantage through increased endothelial interactions and angiogenesis.

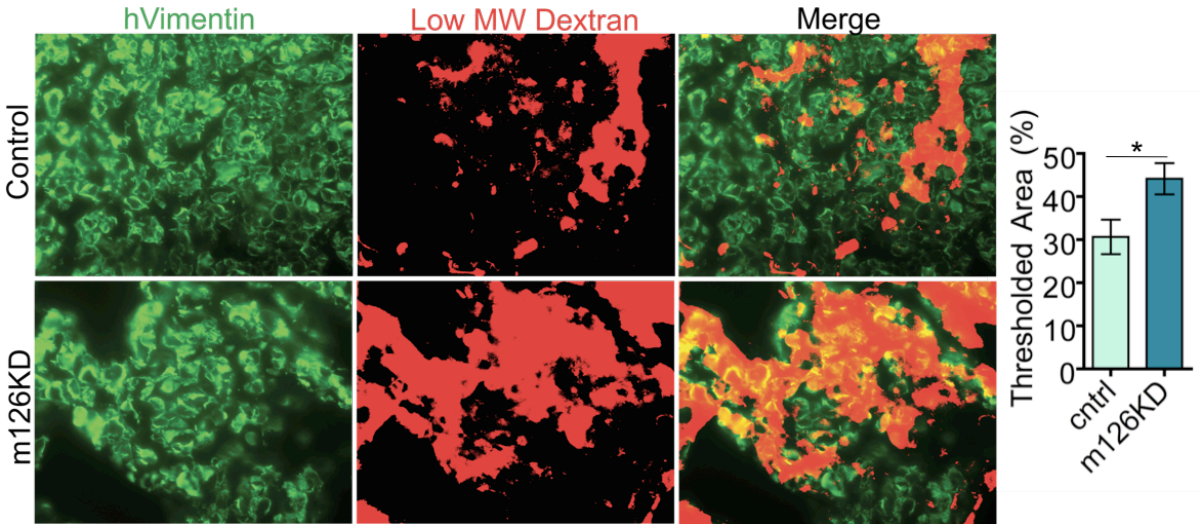

Figure 11| miR-126 regulates perfusion in lung metastases. Lung sections from Figure 2 were histologically double-stained for human vimentin and FITC labelled low-molecular weight dextran (10,000 MW), which was injected intravenously prior to sacrifice. The dextran molecules were allowed to circulate for 15 min before mice were euthanized and the lungs excised. Frozen sections were prepared and stained for human Vimentin in order to localize metastatic nodules, while the FITC signal inside the nodules was quantified with a constant threshold using ImageJ. n=5; error bars represent s.e.m., p-values obtained using a one-sided student's t-test. *P<0.05.

miR-126 suppresses Endothelial Recruitment by Breast cancer cells

To elucidate the cellular basis for the observed effects of endogenous miR-126 on metastatic angiogenesis, the ability of miR-126 to regulate various *in vitro* cancer-endothelial interactions that have previously been shown to be involved in the regulation of cancer angiogenesis–endothelial adhesion, endothelial proliferation and tube formation–was analysed. Restoring miR-126 expression to LM2 cells did not suppress adhesion of metastatic cells to endothelial cells (Figure 12a), proliferation of endothelial cells (Figure 12b), or tube formation as assessed by automated quantification of branch points (Figure 12c). Consistent with this, inhibition of miR-126 in MDA-231 cells did not enhance any of these angiogenic phenotypes (Figure 12).

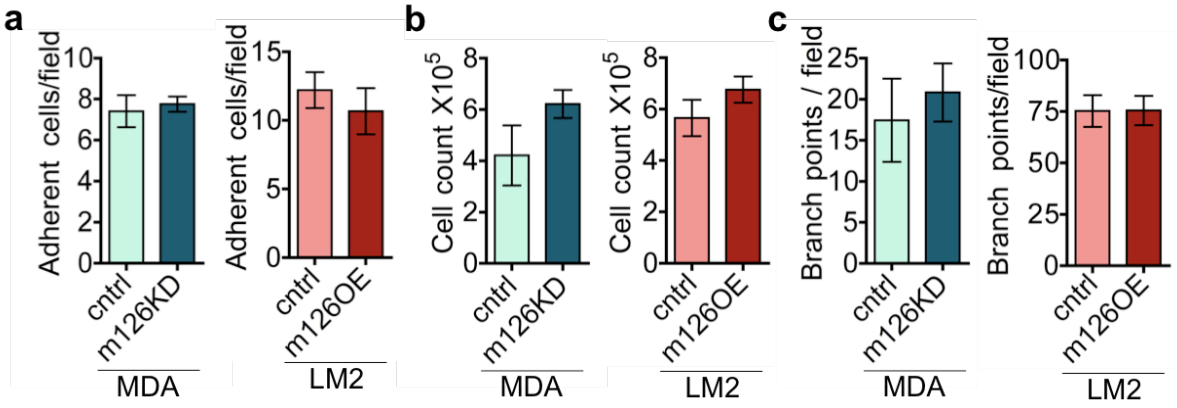

Figure 12| miR-126 does not suppress endothelial adhesion, proliferation or tube formation. a, 5 X 10^4 MDA cells expressing a hairpin targeting miR-126 or control hairpin or LM2 cells over-expressing miR-126 or a control hairpin were seeded onto a HUVEC monolayer. Images of cells that had adhered to a HUVEC monolayer was quantified. n=4; error bars represent s.e.m. **b,** Conditioned media from 5 X 10^5 MDA/miR-126KD, MDA/control, LM2/m126OE or LM2/control cells was obtained by incubating cells in EGM-2 media for 24h. 2.5 X 10^4 HUVEC cells were grown in the conditioned media and viable cells counted 5 days after seeding. n=3; error bars represent s.e.m. **c,** 2 X 10^4 HUVEC cells were mixed with 1 X 10^4 MDA/miR-126KD, MDA/control, LM2/m126OE or LM2/control cells and tube formation was assayed. n=3; error bars represent s.e.m.

I next speculated that miR-126 might regulate the recruitment of endothelial cells to metastatic cells. Metastatic LM2 cells placed in the bottom of a Boyden chamber strongly recruited human umbilical venous endothelial cells (HUVECs) through a porous trans-well insert and displayed a significantly enhanced ability to recruit endothelia compared to their poorly metastatic parental line. Endothelial recruitment by metastatic cells was strongly suppressed (47% reduction) by miR-126 over-expression. Conversely, knockdown of miR-126 in the poorly metastatic MDA-231 parental population significantly increased (146% increase) endothelial recruitment (Figure 13).

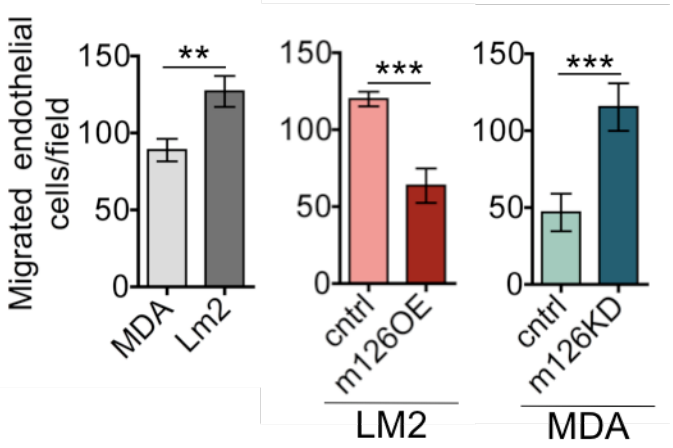

Figure 13| miR-126 inhibits endothelial recruitment by breast cancer cells. 2.5 X 10^4 MDA cells, LM2 cells, LM2 cells expressing miR-126 or the control hairpin, as well as MDA-MB-231 cells expressing a short hairpin targeting miR-126 or the control hairpin were seeded in quadruplicate. Trans-well migration of 5 X 10^4 HUVEC cells towards the cancer cells was then assessed by counting the number of cells that had migrated to the basal side of the trans-well inserts in images obtained using ImageJ. n=4; error bars represent s.e.m., p-values were obtained using student's t-test. **P<0.001; ***P<0.0001.

To confirm if this recruitment effect was independent of axis of movement, a scratch assay was modified with coverslips seeded with cancer cells placed on one side of a scratch made on a HUVEC monolayer. Recruitment of endothelial cells was then monitored by following the coverage of the scratch by endothelial cells. Consistent with previous results, knockdown of miR-126 in poorly metastatic MDA-231 cells had a greater ability to attract endothelial cells, resulting in a greater coverage of the scratch area after a period of 36h (Figure 14).

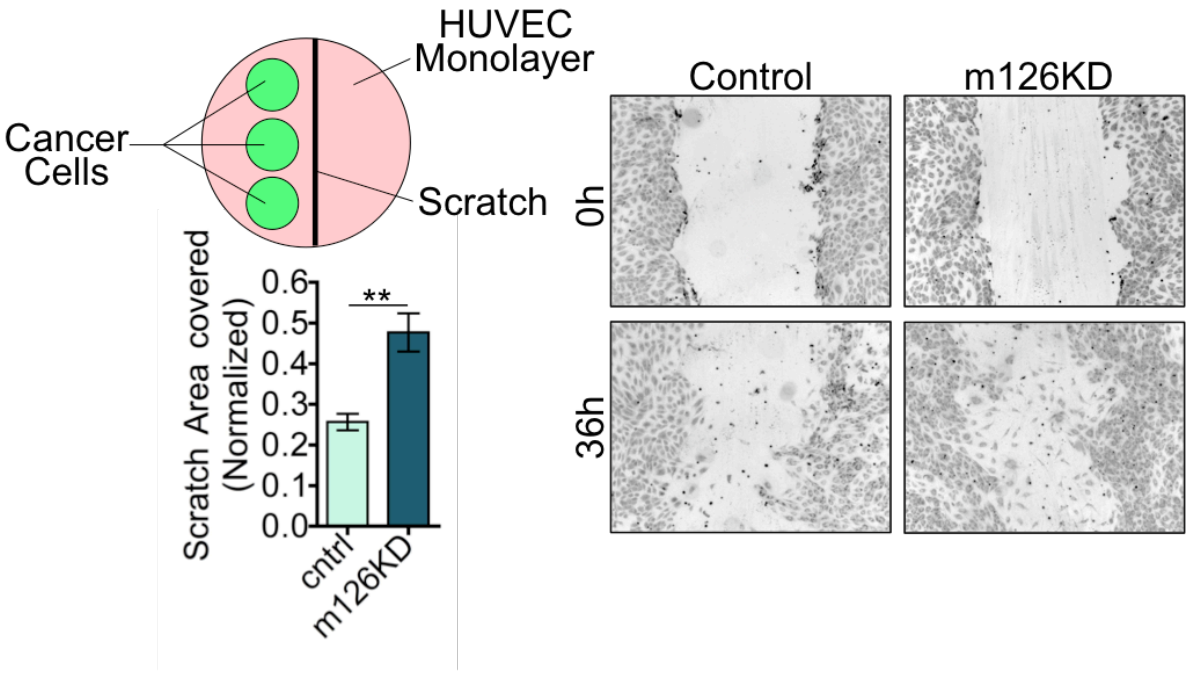

Figure 14| Endogenous miR-126 suppresses horizontal endothelial recruitment. HUVEC cells were grown to 100% confluency in 60mm dishes. 3 coverslips seeded with MDA cells expressing a hairpin targeting miR-126 or control hairpin were transferred onto the HUVEC monolayer and a scratch was made across the HUVEC monolayer using a 200µl pipet tip. 3 images were taken along each scratch and analysed for the area covered by HUVEC cells using ImageJ software. n=3; error bars represent s.e.m., p-values obtained using a one-sided student's t-test. **P<0.001.

The CN34LM1a line, a highly lung metastatic derivative that was previously obtained through *in vivo* selection of the CN34 Par line, also displayed significantly increased capability to recruit endothelial cells compared to its poorly metastatic parent line. Similarly, both gain- and loss-of-function experiments revealed miR-126 to significantly suppress endothelial recruitment by the CN34 population as well (Figure 15).

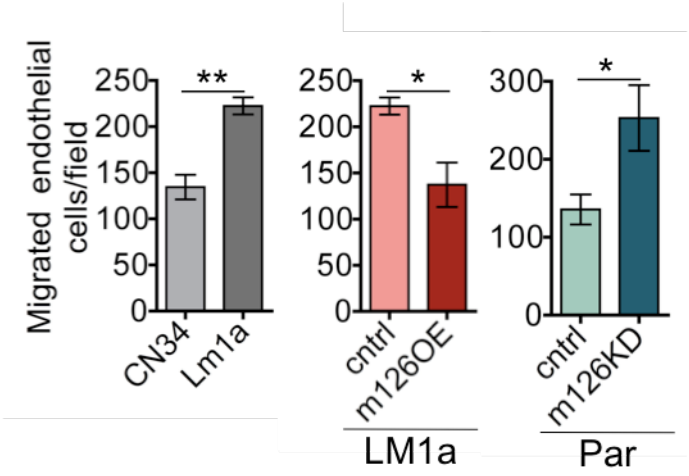

Figure 15| miR-126 inhibits endothelial recruitment in a primary malignant population. 2.5 X 10^4 CN34 Par cells, LM1a cells, LM1a cells expressing miR-126 or the control hairpin, as well as CN34 Par cells expressing a short hairpin targeting miR-126 or the control hairpin were seeded in quadruplicate. Trans-well migration of 5 X 10^4 HUVEC cells towards the cancer cells was then assessed by counting the number of cells that had migrated to the basal side of the trans-well inserts in images obtained using ImageJ. n=4; error bars represent s.e.m., p-values were obtained using student's t-test. *P<0.05; **P<0.001.

To determine if the miR-126 endothelial recruitment phenotype was restricted to triple negative breast cancer cells, the HER2-positive SkBr3 breast cancer cell line was transfected with either miR-126-targeting or control antagomiR and subjected to the endothelial recruitment assay. Silencing of miR-126 significantly enhanced endothelial recruitment by SkBr3 cells, suggesting that the miR-126 endothelial recruitment phenotype is independent

of breast cancer subtypes (Figure 16a). The endothelial recruitment assay was then repeated with human microvascular venous endothelial cells (HMVECs) derived from lung blood, which allowed us to more accurately model *in vivo* endothelial recruitment during lung colonization. Consistent with previous results, the highly metastatic LM2 cells had significantly enhanced ability to recruit endothelial cells as compared to their poor metastatic parental MDA cells, and this ability was highly dependent on miR-126 (Figure 16b). These findings reveal enhanced endothelial recruitment capacity to be a key feature of metastatic breast cancer populations and identify endogenous miR-126 as a major regulator of this process.

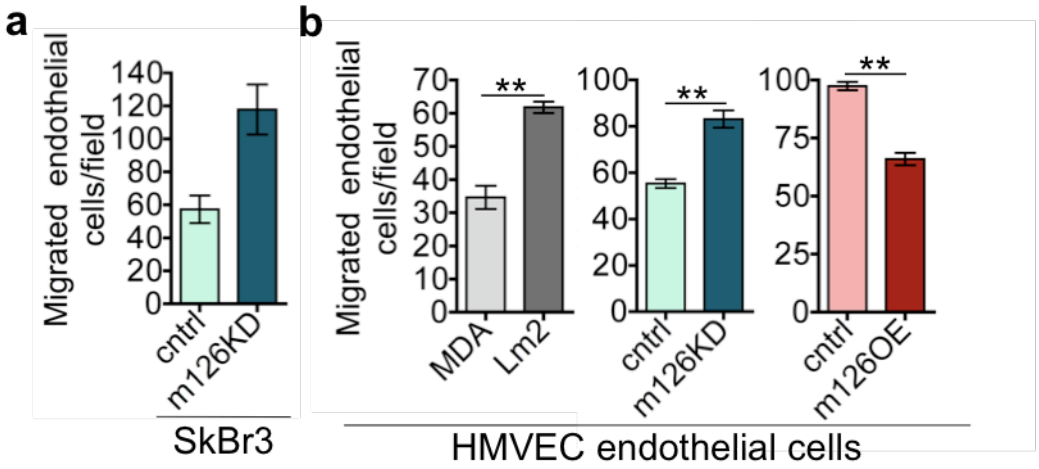

Figure 16| miR-126 inhibits endothelial recruitment by cancer cells in a cell line-independent manner. a, SkBr3 breast cancer cells transfected with control or miR-126-targeting LNAs were subjected to the HUVEC recruitment assay; n=5. **b,** MDA, LM2, LM2 cells expressing miR-126 or the control hairpin, as well as MDA cells expressing a short hairpin targeting miR-126 or the control hairpin, were subjected to endothelial recruitment assays using lung-derived HMVEC endothelial cells. n=6; error bars represent s.e.m., p-values obtained using a one-sided student's t-test. **P<0.001.

I next sought to determine if endogenous miR-126 can selectively regulate endothelial recruitment to breast cancer cells independent of their location. Breast cancer cells were implanted into the mammary fat pads of mice and the resulting tumour analysed for vessel density. Endothelial recruitment to highly metastatic LM2 cells in the mammary fat pad was inhibited by over-expression of miR-126 (Figure 17a), while miR-126 inhibition in poorly metastatic MDA cells significantly increased endothelial recruitment and functional vessel content of tumours growing in mammary fat pads as determined by MECA-32 and lectin staining respectively (Figure 17a-b). This recruitment effect was selective to endothelial cells, as miR-126 silencing did not increase leukocyte or macrophage densities in mammary tumours (Figure 17c-d). These findings reveal that miR-126 selectively regulates endothelial recruitment to breast cancer cells independent of their anatomic location and provide a non-cell autonomous mechanism for the enhanced primary tumour-size phenotype seen with miR-126 inhibition.

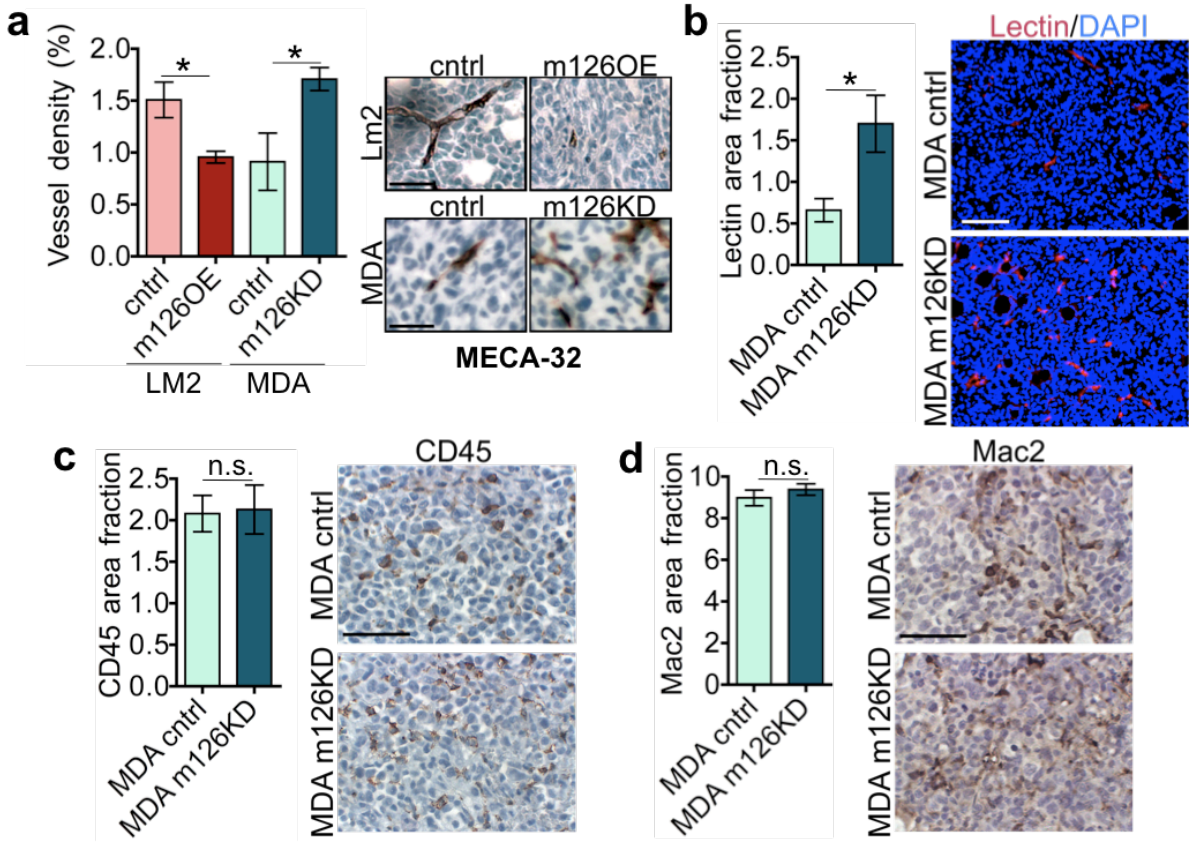

Figure 17| Endogenous miR-126 regulates angiogenesis, but not CD45 positive lymphocyte or Mac-2 positive macrophage recruitment. **a,** 5 X 10^5 MDA cells expressing control hairpin or hairpin targeting miR-126 or LM2 cells over-expressing miR-126 or a control hairpin were injected into mammary fat pads of NOD-SCID mice. Size-matched tumours were excised and stained for MECA-32. **b-d,** 5 X 10^5 MDA cells expressing control hairpin or hairpin targeting miR-126 were injected in mammary fat pads; 5 min prior to sacrifice, biotinlyated lectin was injected into the tail-vein. Size matched tumours were excised and functional blood vessels were detected through staining for the injected lectin (b), $CD45^+$ lymphocyte detected by anti-CD45 (c), and $Mac\text{-}2^+$ macrophages detected by anti-Mac-2 (d). *P<0.05.

Identification of MiR-126 gene signature that predicts Metastasis-free Survival

To identify the molecular targets of miR-126 that mediate endothelial recruitment and metastatic colonization, we employed an integrative systemic approach. MicroRNAs are known to mediate post-transcriptional silencing through both target mRNA degradation as well as transcript destabilization and translational inhibition. Mounting evidence suggests that the great majority of miRNA targets display reduced RNA message levels due to transcript destabilization.[69,70] This has allowed for the identification of numerous miRNA targets through unbiased, non-algorithmic, transcriptomic profiling methods, which display adequate sensitivity to detect subtle changes in transcript abundance.[71] To identify the biological mediators of miR-126, transcriptomic analysis was performed and the global transcript alterations among LM2 cells over-expressing miR-126, poorly metastatic MDA-231 cells and highly metastatic LM2 cells were compared.

Given the established role of miR-126 in suppressing metastasis, the biological effectors of miR-126 should display increased expression in highly metastatic cells relative to the poorly metastatic cells and also be suppressed upon over-expression of this miRNA in highly metastatic cells. Through this analysis, a set of 23 genes that are inhibited (>1.6-fold) upon miR-126 over-expression and upregulated (>1.4-fold) in highly metastatic LM2 cells relative to the parental MDA-231 cells (Figure 18, Table 10) was identified.

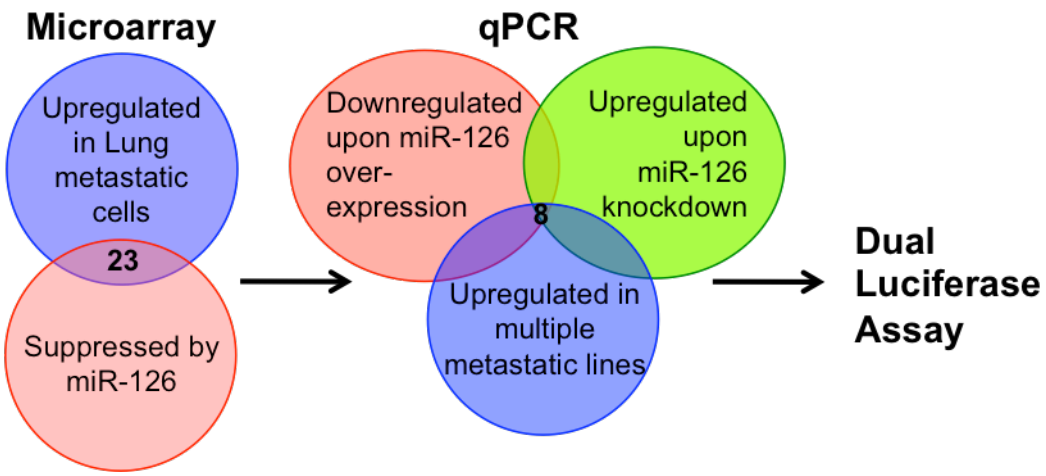

Figure 18| Schematic depicting integrative approach that led to identification of putative miR-126 target genes. Venn diagram showing the integrative experimental path that resulted in the identification of putative miR-126 target genes. Transcriptomic profiling of genes down-regulated by greater than 1.6 fold upon miR-126 over-expression were overlapped with genes upregulated by more than 1.4 fold in metastatic LM2 cells as compared to the parental MDA cells. This led to the identification of 23 potential miR-126 target genes. By qPCR, 8 of these 23 genes were modulated by miR-126 in both the MDA-231 breast cancer cell line and the primary CN34 cell line. These 8 genes were functionally tested for direct regulation by miR-126 through luciferase reporter assays.

Table 10: List of genes downregulated by miR-126 in LM2 cells

Gene Name	Fold	Gene Name	Fold	Gene Name	Fold	Gene Name	Fold
GDF15	-4.15	KIAA1267	-1.93	SDF2L1	-1.82	LPIN1	-1.72
RARA	-3.53	NT5C2	-1.93	RPH3AL	-1.82	GEM	-1.72
P8	-2.98	CTAGE5	-1.93	OGDH	-1.82	KIAA0746	-1.72
RPS6KA2	-2.54	CDA	-1.93	CDYL	-1.81	LOC115648	-1.72
C20orf100	-2.47	FLJ46385	-1.92	RHOQ	-1.81	TIA1	-1.72
C12orf39	-2.38	RALGPS2	-1.92	ITGB4	-1.81	FLJ10120	-1.71
HERPUD1	-2.37	BDNFOS	-1.91	PRKAR1A	-1.80	DUSP5	-1.71
CTH	-2.36	MBNL1	-1.91	CHAC1	-1.80	RNF12	-1.71
LOC23117	-2.35	MKX	-1.91	SCD	-1.80	KIAA0746	-1.71
LOC23117	-2.35	LPIN1	-1.90	PCK2	-1.80	PADI4	-1.71
ASNS	-2.35	DNAJB9	-1.90	CDC42BPB	-1.79	BEX2	-1.71
RGC32	-2.33	TncRNA	-1.90	DSCR1	-1.79	TAF13	-1.70
CTH	-2.33	BCL2L1	-1.90	TCF7L2	-1.79	KLF4	-1.70
NRP1	-2.28	DNAJB9	-1.90	TNRC6C	-1.79	DLG1	-1.70
RIT1	-2.26	ENTH	-1.89	TncRNA	-1.78	DDEFL1	-1.70
HMGA1	-2.24	S100A5	-1.89	CLDN23	-1.78	MID1IP1	-1.70
DDIT3	-2.20	CST4	-1.89	GPR153	-1.78	LOC124220	-1.70
MBNL1	-2.20	TRIB3	-1.89	KRTHA4	-1.78	C10orf58	-1.70
SUPT6H	-2.16	PHLDA1	-1.89	SCD	-1.78	CDKN1C	-1.70
LPIN1	-2.15	RGNEF	-1.89	VIPR1	-1.78	DTX3	-1.70
ZNF451	-2.12	GFPT1	-1.88	SLC1A4	-1.77	SETD5	-1.70
THBD	-2.10	TMTC2	-1.88	PNPLA3	-1.77	SLC7A11	-1.69
ITGB4	-2.10	TPARL	-1.87	PPP1R11	-1.77	WSB1	-1.69
BHLHB8	-2.09	INHBB	-1.87	CFLAR	-1.77	KIAA1618	-1.69
SLCO4C1	-2.09	FASN	-1.87	NSF	-1.77	PYGB	-1.69
AFF4	-2.07	CALB2	-1.86	ABHD4	-1.77	CSNK1A1	-1.69
ATP6V0D2	-2.05	IGFBP2	-1.86	SOCS2	-1.77	THBD	-1.68
KRT19	-2.05	SLC6A9	-1.86	TACSTD2	-1.76	CG012	-1.68
SMAD3	-2.04	PLAT	-1.86	SESN2	-1.76	DDX17	-1.68
ARHGAP5	-2.04	SIN3B	-1.86	CTNNB1	-1.76	BGLAP	-1.68
DNAJB9	-2.04	S100A6	-1.85	MAP1LC3B	-1.76	MAGI1	-1.68
ATF3	-2.03	WSB1	-1.85	LOC165186	-1.76	WARS	-1.68
LOC440092	-2.03	C20orf18	-1.85	FLJ20054	-1.75	LOC283050	-1.68
RIT1	-2.03	HMGCS1	-1.85	ZNF69	-1.74	AQP3	-1.68
ZNF499	-2.02	MBNL1	-1.85	TNFSF4	-1.74	LOC400581	-1.68
ATXN1	-2.02	MBNL1	-1.85	LOC441453	-1.74	CYLN2	-1.68
CST6	-2.01	WHSC1L1	-1.85	MARS	-1.74	CD97	-1.68
WBP2	-2.00	NCF2	-1.85	LOC647135	-1.74	CNTNAP3	-1.67
ZFAND3	-2.00	MERTK	-1.84	ACSL3	-1.74	PDE2A	-1.67
FLJ38717	-1.99	PFAAP5	-1.84	SCD	-1.74	AOF1	-1.67
LOC158160	-1.99	RTN4	-1.83	SERINC2	-1.73	IDS	-1.67
PITPNC1	-1.99	LARP6	-1.83	ZCCHC7	-1.73	SCD	-1.67
JMJD1C	-1.99	TRIB3	-1.83	ETNK1	-1.73	SHMT2	-1.67
PRO2852	-1.98	RAB37	-1.83	CHRM3	-1.73	RNF10	-1.67
AGR2	-1.97	LOC399959	-1.83	DCAMKL1	-1.73	CRLF3	-1.67
SLC7A5	-1.94	SYTL1	-1.82	C20orf119	-1.73	PSAT1	-1.67
NSF	-1.94	RHOQ	-1.81	CDKN1C	-1.73	FNBP1	-1.67
BCL2L1	-1.94	ITGB4	-1.81	CXorf33	-1.72	LOC554203	-1.66

Gene Name	Fold	Gene Name	Fold
CA12	-1.66	PITX1	-1.61
SF3B4	-1.66	P2RY2	-1.61
KHDRBS1	-1.66	HYOU1	-1.61
EGFR	-1.66	CSF2RA	-1.61
FRMD5	-1.65	SLC16A4	-1.61
ZNF252	-1.65	SQLE	-1.61
FNBP1	-1.65	EFHD2	-1.61
TNKS2	-1.65	ABCB9	-1.61
C9orf3	-1.65	C14orf118	-1.61
AOF1	-1.65	PIAS1	-1.61
PDP2	-1.65	PXN	-1.61
MLLT10	-1.65	C14orf118	-1.61
WIRE	-1.65	PIAS1	-1.61
ATXN1	-1.65	FLJ43663	-1.65
WARS	-1.65	SOS2	-1.61
RAB5B	-1.64	FLJ43663	-1.60
SQLE	-1.64	HCRP1	-1.60
SCNN1A	-1.64	LOC646916	-1.60
C14orf78	-1.64	NUP43	-1.60
SHMT2	-1.63	PEBP1	-1.60
PSCD3	-1.63	FLJ23556	-1.60
LOC643998	-1.63	NRP1	-1.60
PHGDH	-1.63	JUP	-1.60
HEXA	-1.63		
CDRT4	-1.63		
ACTN4	-1.63		
C6orf155	-1.63		
EXT1	-1.63		
JDP2	-1.63		
LSS	-1.63		
PITPNC1	-1.63		
C20orf18	-1.63		
CLDN7	-1.63		
NPC1	-1.62		
IDH1	-1.62		
THBD	-1.62		
GSTM4	-1.62		
ATP5C1	-1.62		
PMM1	-1.62		
C9orf5	-1.62		
COL8A2	-1.62		
CST1	-1.62		
MAGI1	-1.62		
G6PD	-1.62		
FOSL1	-1.61		
RASD1	-1.61		

Of these genes, 14 were validated to be significantly changed by quantitative real-time PCR (qPCR) of MDA-231 control and miR-126KD cells as well as LM2 control and miR-126 over-expressing cells. To further increase the confidence of this list, the expression of these genes in the metastatic derivatives of the independent CN34 line was tested and 8 of these genes were identified to display significantly increased expression in multiple metastatic CN34 derivatives relative to their parental line (Figure 19).

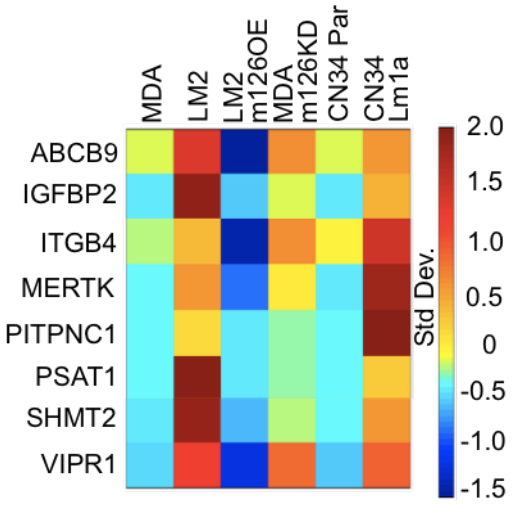

Figure 19| Expression levels of the 8 genes in the miR-126 gene signature. The miR-126 metastasis signature comprises 8 genes over-expressed in metastatic cells, down-regulated by miR-126OE, and up-regulated by miR-126KD. The heatmap represents variance-normalized expression levels based on microarray and qPCR analyses. Colourmap corresponds to standard deviations change from the mean.

To ascertain whether these 8 genes contribute to human metastasis, I determined whether their expression levels in primary human breast cancers correlate with distal metastasis-free survival. Interestingly, patients whose primary breast cancers displayed higher levels of these genes were significantly more likely to develop distal metastases and experienced shorter metastasis-free survival than those whose cancers had lower levels of these genes

(Figure 20). This association displayed significance in the UCSF (n=117; P < 0.0165), NKI (n=295; P < 0.0005), and the combined MSK/NKI/UCSF cohorts (n=494; P < 0.0004). The prognostic power of this signature was also subtype-independent (Figure 21). Thus, miR-126 suppresses the expression of a set of eight genes that are positively and strongly correlated with human metastatic relapse.

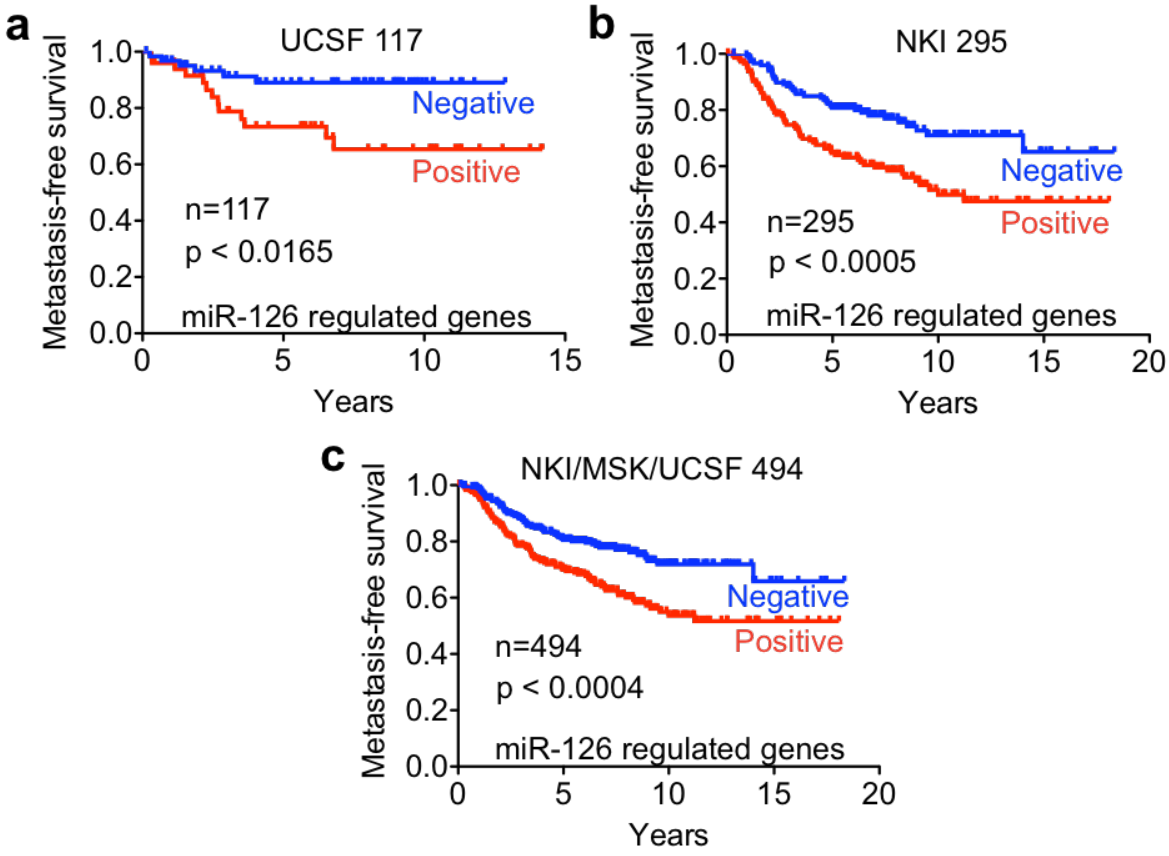

Figure 20| miR-126 gene signature predicts metastasis free survival. Kaplan-Meier curves for the (a) UCSF breast cancer cohort (117 tumours), (b) NKI cohort (295 tumours), and the (c) combined NKI/MSK/UCSF cohort (494 tumours) depicting metastasis-free-survival of those patients whose primary cancers over-expressed the miR-126 eight gene signature (positive) and those that did not (negative). An aggregate expression score (sum of the expression values of the 8 genes) greater or lower than the mean of the entire population is classified as miR-126 positive or negative, respectively. p-values based on the Mantel-Cox log-rank test.

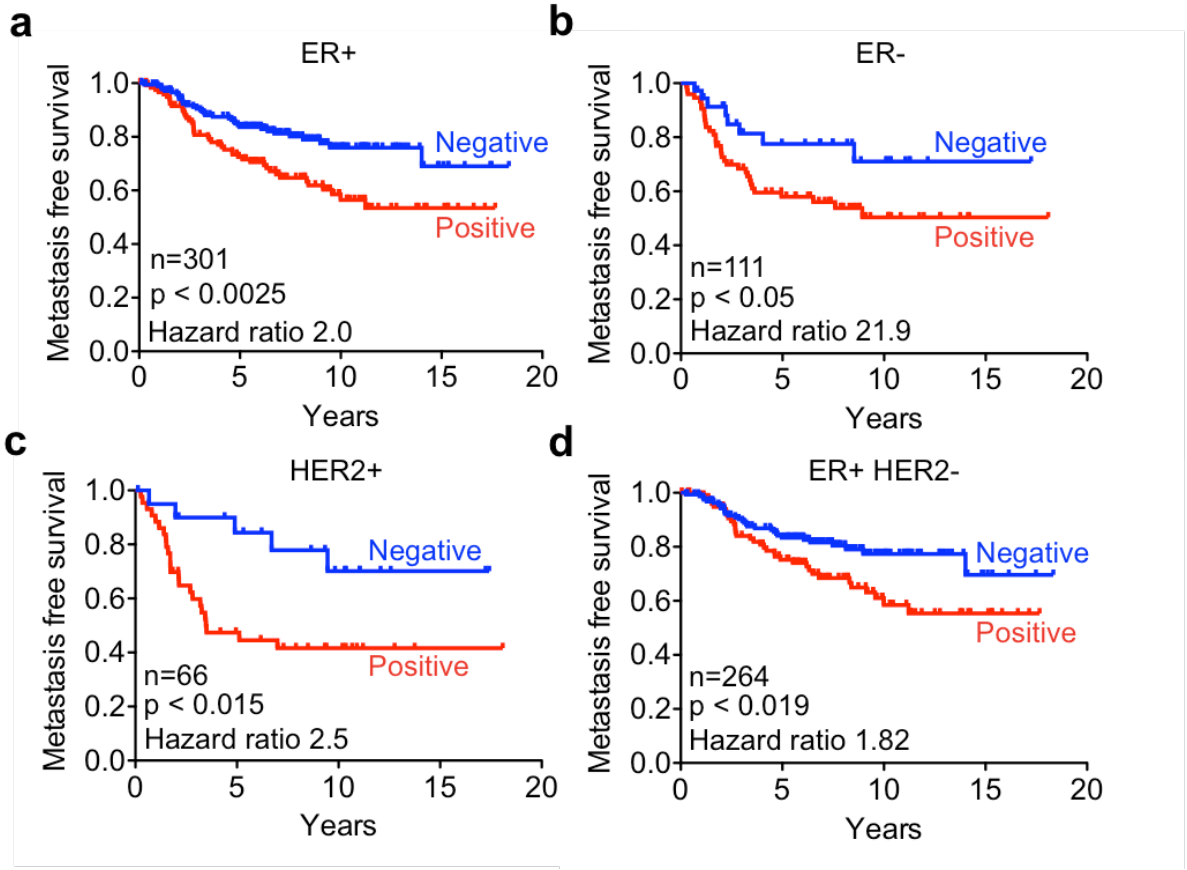

Figure 21| miR-126 gene signature predicts metastasis free survival in different subtypes of breast cancer. a-d, Kaplan-Meier curves for patients from the NKI and UCSF cohorts whose primary tumours were of subtype (a) ER+ (301 tumours), (b) ER- (111 tumours), (c) HER2+ subtype (66 tumours) and (d) ER+ HER2- subtype (264 tumours). Kaplan-Meier curves depict metastasis-free-survival of those patients whose primary cancers over-expressed the miR-126 eight gene signature (positive) and those that did not (negative). The expression values of these 8 genes were summed to obtain an aggregate expression score for each tumour. Aggregate expression scores that are greater than the mean of the entire population were classified as miR-126 positive while those lower than the mean were classified as miR-126 negative. p-values based on the Mantel-Cox log-rank test.

IGFBP2, MERTK and PITPNC1 promote Endothelial Recruitment

I next sought to identify the direct targets of miR-126 by cloning the 3'-untranslated regions (3'-UTR's) and coding sequences (CDS's) of all eight miR-126 regulated genes into the psiCHECK2 vector, generating luciferase fusion constructs. Luciferase reporter assays with the different constructs revealed miR-126 to regulate the expression of IGFBP2 and MERTK through interactions with their 3'UTR's and of PITPNC1 and SHMT2 through interactions with their coding regions as knockdown of endogenous miR-126 in MDA-231 cells enhanced expression of these specific luciferase fusion genes (Figure 22).

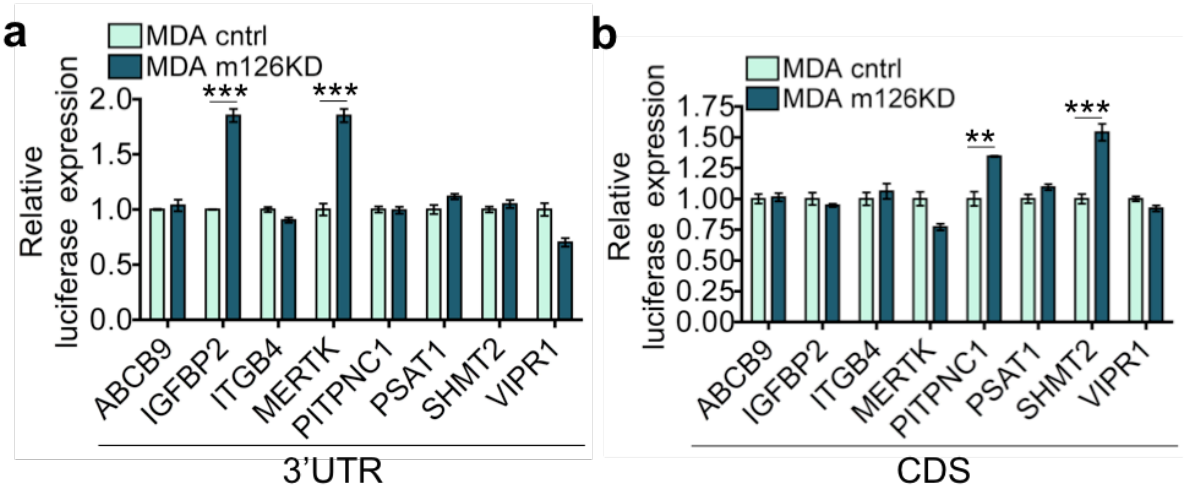

Figure 22| miR-126 regulates IGFBP2 and MERTK through 3' UTR interactions and PITPNC1 and SHMT2 through CDS interactions. Luciferase reporter assays of the miR-126 metastasis gene set in MDA-231 cells expressing a short hairpin targeting miR-126 as well as the control KD hairpin. Reporter constructs containing the luciferase gene upstream of the 3' UTR (a) or CDS (b) of ABCB9, IGFBP2, MERTK, PITPNC1, PSAT1, ITGB4, SHMT2 and VIPR1 were transfected into the various cell lines and luciferase activity was assayed at 30 hours post transfection. n=4; error bars represent s.e.m.; p-values were obtained using a one-sided student's t-test. **P<0.001; ***P<0.0001.

Mutation of sequences complementary to the miR-126 seed regions in either the 3'-UTR's of IGFBP2 and MERTK or CDS's of PITPNC1 and SHMT2 abolished miR-126 mediated regulation of luciferase expression (Figure 23). Thus, the IGF-binding protein 2 (IGFBP2), the receptor kinase MERTK, the phosphatidylinositol transfer protein PITPNC1 and the hydroxymethyltransferase enzyme SHMT2 comprise a set of direct targets of miR-126 in human breast cancer.

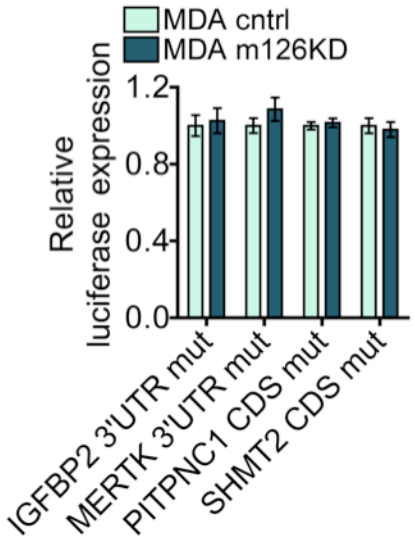

Figure 23| Mutation of miR-126 complementary regions inhibits miR-126 regulation of IGFBP2, MERTK, PITPNC1 and SHMT2. The miR-126 complementary regions of the 3'UTR/CDS constructs were mutated and the luciferase reporter assay was repeated with these constructs in MDA-MB-231 cells expressing a short hairpin targeting miR-126 or the control hairpin (right). n=4; error bars represent s.e.m.; p-values were obtained using student's t-test.

To determine if any of the direct targets of miR-126 regulate the recruitment of endothelial cells by cancer cells, each of the four genes–IGFBP2, MERTK, PITPNC1 and SHMT2–were knocked down using independent short hairpins in highly metastatic cells. Inhibition of IGFBP2, MERTK or PITPNC1 significantly suppressed the ability of metastatic LM2 and CN34-LM1A cells to recruit endothelial cells (Figure 24a-b), while SHMT2 knockdown had no effect on endothelial recruitment capacity. Consistent with this, over-expression of each of these 3 genes significantly enhanced endothelial recruitment significantly (Figure 24c). Importantly, knockdown of each of these genes did not result in a significant decrease in cell proliferation (Figure 24d).

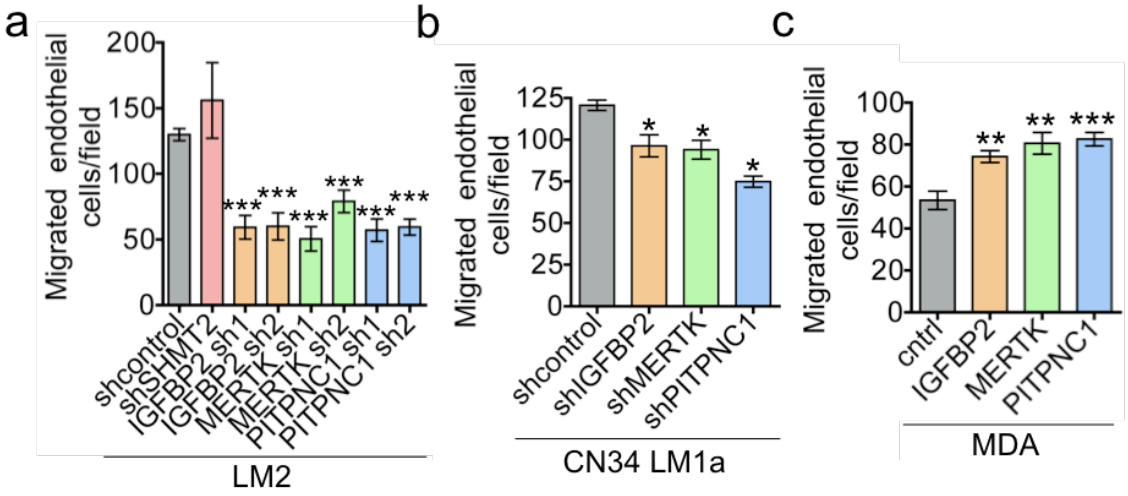

Figure 24| IGFBP2, MERTK and PITPNC1 promote endothelial recruitment by breast cancer cells. **a,** 2.5 X 10^4 LM2 cells expressing hairpins targeting IGFBP2, MERTK, PITPNC1, SHMT2 or the control hairpin were seeded in quadruplicate. Trans-well migration of 5 X 10^4 HUVEC cells towards the cancer cells were then assessed. Images of cells that migrated through the trans-well inserts were obtained and analysed using ImageJ software. n=4; error bars represent s.e.m., p-values obtained using a student's t-test. **b,** 2.5 X 10^4 CN34 Lm1a cells expressing short hairpins targeting IGFBP2, MERTK or PITPNC1 or the control hairpin were seeded in quadruplicate and subjected to the HUVEC recruitment assay. n=4; error bars represent s.e.m., p-values were obtained using a one-sided student's t-test. **c,** The coding regions of IGFBP2, MERTK and PITPNC1 were over-expressed in MDA cells and subjected to the HUVEC recruitment assay. n=7; error bars represent s.e.m., p-values obtained using a one-sided student's t-test. *P<0.05; **P<0.001; ***P<0.0001.

IGFBP2, MERTK and PITPNC1 promote Metastasis

Given the robust effects of each of these genes on endothelial recruitment, I wondered whether the expression levels of these genes individually correlate with metastatic propensity of human breast cancer. The expression levels of each of these genes was analysed in an independent set of 96 human breast cancers through qPCR. Patients with stage III and stage IV breast cancers display local metastatic dissemination and distal metastases respectively and collectively comprise those that develop distal relapse at much higher rates than stage I and II patients. Interestingly, expression levels of IGFBP2 ($P < 0.0003$), MERTK ($P < 0.002$) and PITPNC1 ($P < 0.004$) were individually significantly increased in primary cancers of stage III and IV patients relative to stage I and II patients (Figure 25).

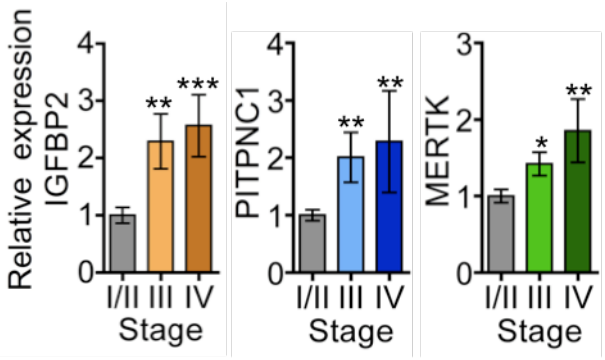

Figure 25| IGFBP2, MERTK and PITPNC1 is over-expressed in late stage breast cancer. The relative expression levels of IGFBP2, MERTK or PITPNC1 in human breast tumour samples from stage I/II (n=53) as compared to stage III (n=29) or stage IV (n=9) patients were quantified from the OriGene TissueScan Breast Cancer arrays using qPCR. Error bars represent s.e.m., p-values obtained using student's t-test. *P<0.05; **P<0.001; ***P<0.0001.

I next assessed if any of the miR-126 target genes were required for metastasis. Importantly, knockdown of IGFBP2 in highly metastatic LM2 cells using independent short hairpins significantly suppressed metastatic colonization to the lung (sh_1: 10-fold, sh_2: 6.2-fold; Figure 26a). Additionally, knockdown of MERTK and PITPNC1 in LM2 cells also strongly inhibited metastatic colonization to the lung (MERTKsh_1: 3.91-fold, MERTKsh_2: 3.08-fold; PITPNC1sh_1: 7.69-fold, PITPNC1sh_2: 4.55-fold; Figure 26b-c). Importantly, knockdown of IGFBP2, MERTK or PITPNC1 did not significantly affect proliferation (Figure 27).

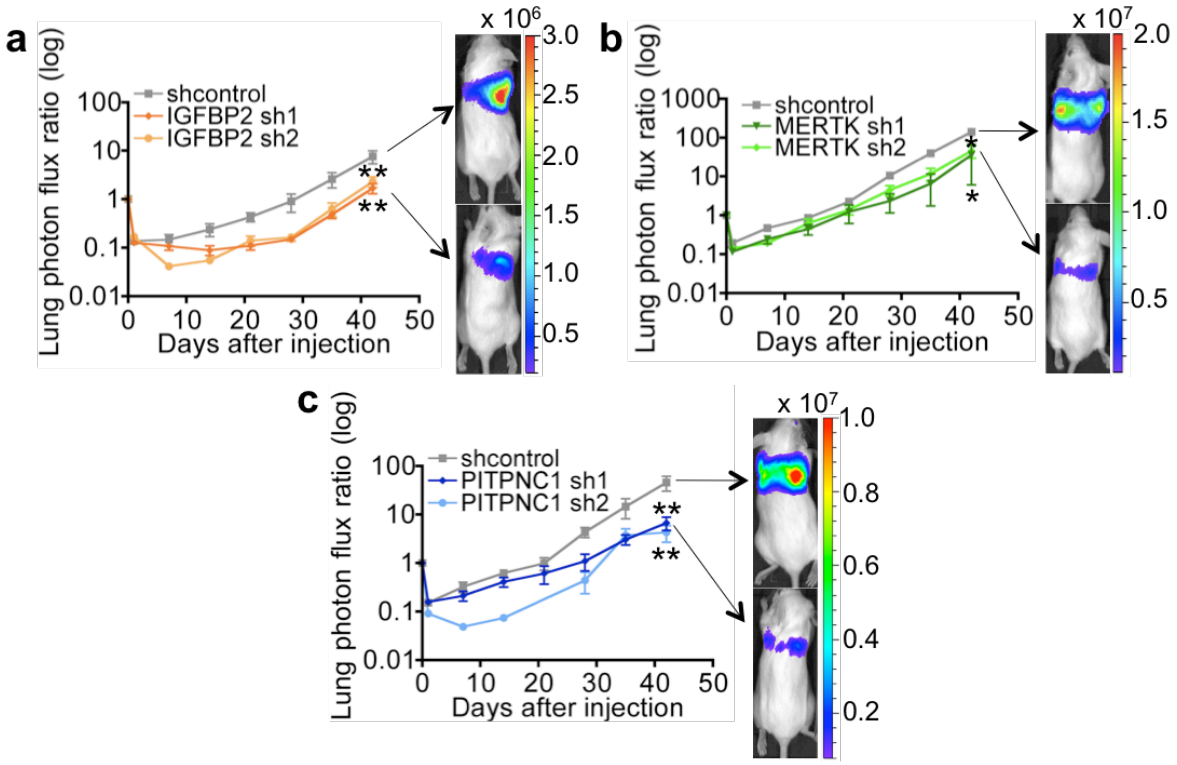

Figure 26| IGFBP2, MERTK and PITPNC1 promotes lung metastatic colonization. Bioluminescence imaging of lung metastasis by lung metastatic breast cancer cells with inhibited expression of the various miR-126 regulated genes. 4 X 104 LM2 cells expressing the control hairpin or independent short hairpins targeting IGFBP2 (a), MERTK (b) and PITPNC1 (c)were injected intravenously into immunodeficient NOD-SCID mice. Lung colonization was measured by bioluminescence imaging and quantified. n=5; error bars represent s.e.m.; p-value based on a one-sided student's t-test. *P<0.05; **P<0.001.

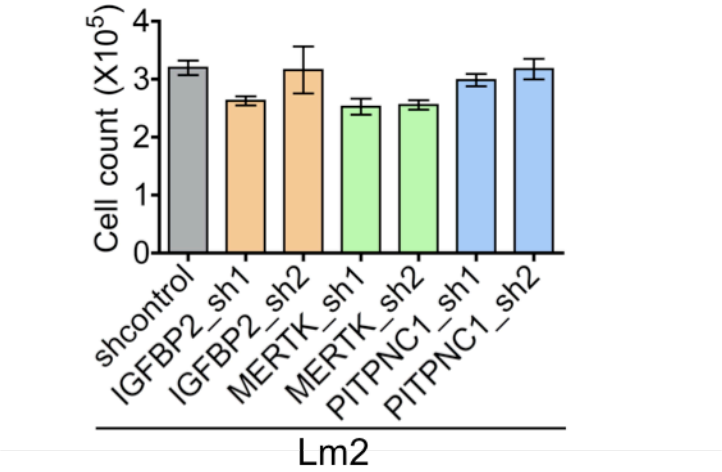

Figure 27| IGFBP2, MERTK and PITPNC1 do not significantly affect proliferation of breast cancer cells. 2.5 X 10^4 LM2 cells expressing a control hairpin or short hairpins targeting IGFBP2, PITPNC1 or MERTK were seeded in triplicate and viable cells were counted at 5 days after seeding. n=3; error bars represent s.e.m.

Given the roles of IGFBP2, MERTK and PITPNC1 in *in vitro* endothelial recruitment and metastatic colonization, I wondered if these genes regulate *in vivo* endothelial recruitment. MECA-32 staining of lungs from mice injected with LM2 control and knockdown cells was performed to quantify *in vivo* endothelial recruitment as measured by metastatic vessel density. Inhibition of IGFBP2, MERTK and PITPNC1 using independent hairpins significantly reduced metastatic endothelial density ($P < 0.0001$ and $P = 0.002$ for shIGFBP2, $P < 0.0001$ and $P = 0.005$ for shMERTK, and $P = 0.01$ and $P = 0.02$ for shPITPNC1; Figure 27a). Additionally, lectin perfusion and subsequent histochemical analysis revealed a significant reduction in functional vessel content as well (Figure 27b). Thus, the miR-126 target genes IGFBP2, MERTK and PITPNC1 are individually required for metastatic endothelial recruitment *in vivo*.

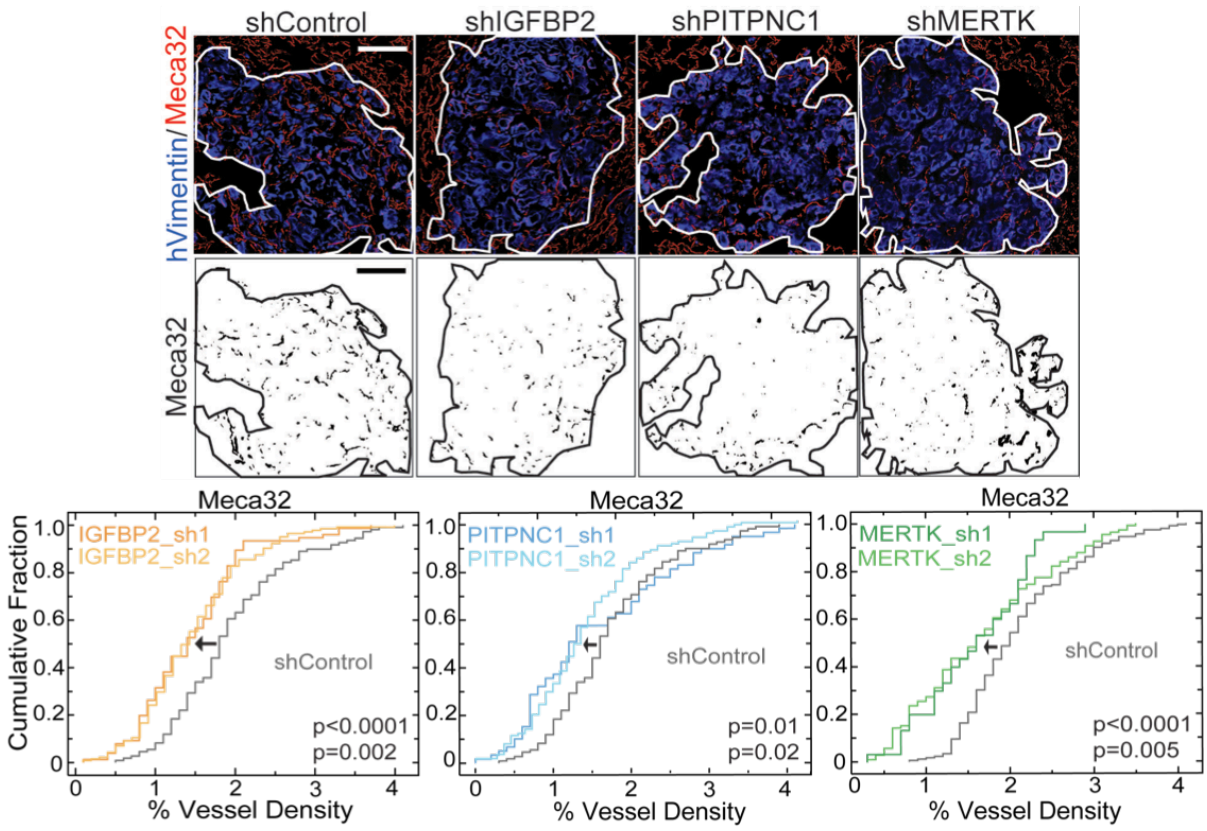

Figure 28| IGFBP2, MERTK and PITPNC1 enhances endothelial content in lung metastases. Lung sections were double stained for vimentin and MECA-32. The border of each nodule was drawn based on human-vimentin staining and MECA-32 staining inside the metastatic nodule highlighted in black (lower panels). The area positive for MECA-32 staining within each nodule was then determined by using ImageJ and presented as the area covered by MECA-32 staining per area of the given nodule (% vessel density). The distribution of % vessel density between the injected LM2 cells expressing hairpins targeting IGFBP2, MERTK, PITPNC1 or a control hairpin are shown in a cumulative fraction plot. n=4, p-value based on the Kolmogorov-Smirnov Test.

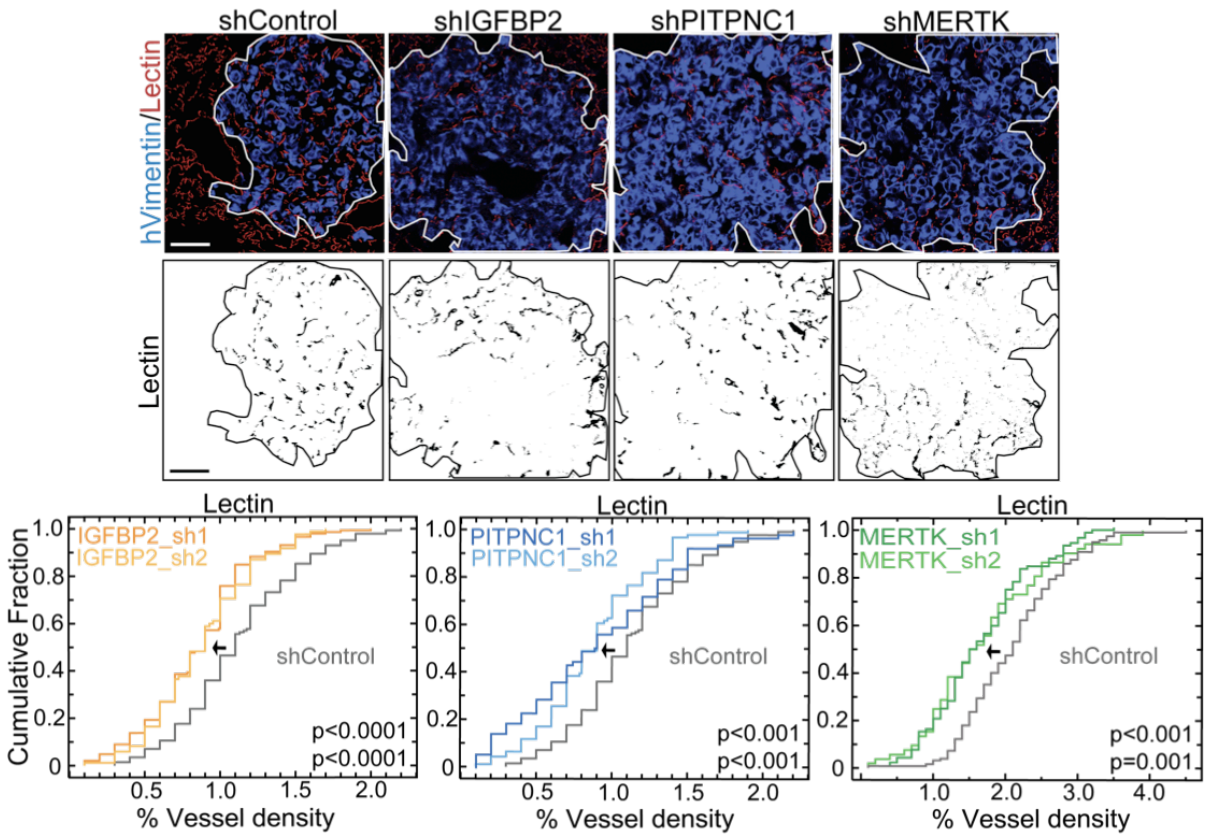

Figure 29| IGFBP2, PITPNC1 and MERTK promote metastatic angiogenesis. Lung sections from figure 3e were immunohistochemically double-stained for human vimentin and intravenously injected lectin. Nodule borders were demarcated based on vimentin staining and lectin staining inside metastatic nodules. ImageJ was used to determine the area positive for lectin staining within each nodule. % vessel density represents the area covered by lectin staining per area of a given nodule. The distribution of % vessel density of the injected LM2 cells expressing the control hairpin or short hairpins targeting IGFBP2, PITPNC1 or MERTK are shown in a cumulative fraction plot. n=5. p-value based on the Kolmogorov-Smirnov test.

Epistasis experiments revealed that knockdown of IGFBP2, MERTK or PITPNC1 in the setting of miR-126 knockdown significantly suppressed *in vitro* endothelial recruitment (Figure 30a) as well as metastatic colonization (Figure 31). Conversely, IGFBP2, MERTK or PITPNC1 over-expression in poorly metastatic LM2 cells over-expressing miR-126 rescued the ability of the cancer cells to recruit endothelial cells (Figure 30b). These findings reveal that the IGFBP2, MERTK and PITPNC1 epistatically interact with miR-126 in breast cancer cells, and are each individually required for *in vivo* endothelial recruitment, metastatic angiogenesis, and metastatic colonization. Importantly, the expression of each gene individually correlates with human metastatic breast cancer progression.

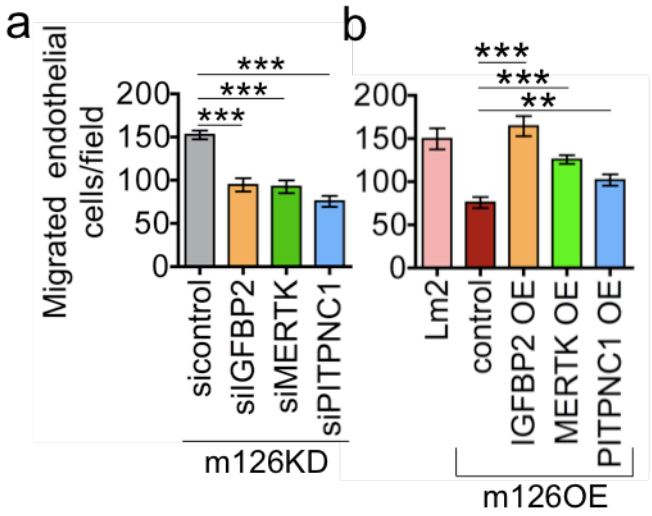

Figure 30| miR-126 regulates endothelial recruitment through IGFBP2, MERTK and PITPNC1. **a,** MDA/miR126 KD cells were transfected with siRNAs targeting IGFBP2, MERTK and PITPNC1 or control siRNA and subjected to HUVEC recruitment assays; n=9. **b,** Coding regions of IGFBP2, MERTK and PITPNC1 were over-expressed in LM2/miR-126 overexpressing cells that were subjected to HUVEC recruitment assays; n=6. Error bars represent s.e.m., p-values obtained using one-sided student's t-test.

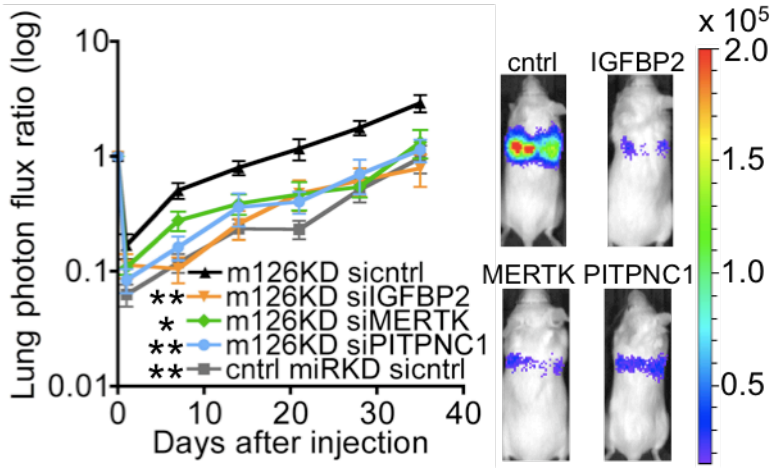

Figure 31| miR-126 regulates metastasis through IGFBP2, MERTK and PITPNC1. Bioluminescence imaging of lung metastasis by MDA/miR-126 KD cells transfected with siRNAs targeting IGFBP2, MERTK and PITPNC1 or control siRNA; n=5. Error bars represent s.e.m., p-values obtained using one-sided student's t-test.

Co-injection of Endothelial cells and Cancer cells promotes Metastasis

Finally, I hypothesized that if the inhibitory effect of miR-126 on metastasis is indeed dependent on its non-cell autonomous effects on the suppression of endothelial recruitment, it should be rescued upon the addition of endothelial cells. To study this, metastatic LM2 cells, as well as LM2 cells over-expressing miR-126 were injected into the portal circulation. Consistent with previous results, miR-126 over-expression strongly suppressed hepatic metastatic colonization. Interestingly, co-injection of LM2 cells over-expressing miR-126 with endothelial cells completely rescued the suppression of metastasis by miR-126 over-expression in LM2 cells (Figure 32). These dramatic results reveal endothelial recruitment to be the key metastatic phenotype regulated by miR-126 and implicate a role for cancer-endothelial interactions in metastatic initiation leading to colonization.

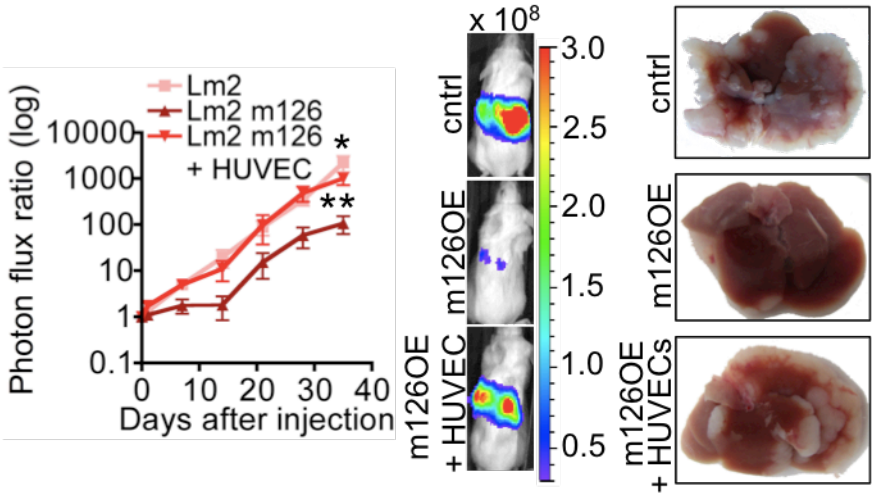

Figure 32| Co-injection of HUVECs rescues miR-126 suppression of metastasis. Bioluminescence imaging of liver metastasis by LM2/control, LM2/miR-126OE as well as LM2/miR-126OE cells co-injected with HUVEC cells. Representative mice and images of the livers extracted at day 35 are shown. n=4; error bars represent s.e.m.; p-value based on a one-sided student's t-test. *P<0.05; **P<0.001.

Discussion

These findings show that a miRNA expressed in cancer cells can non-cell-autonomously regulate the complex process of metastatic endothelial recruitment and consequently vascular perfusion through the coordinate regulation of IGFBP2, MERTK and PITPNC1–a novel set of angiogenesis and metastasis genes. Additionally, they reveal endothelial recruitment capacity as the key metastatic phenotype regulated by miR-126 and reveal a major role for cancer-endothelial interactions in metastatic initiation, leading to metastatic colonization. Metastatic cells display silencing of this miRNA and the resulting increased expression of these metastatic angiogenesis genes endow highly metastatic breast cancer cells with enhanced endothelial recruitment capacity relative to poorly metastatic cells, allowing cancer cells to more readily establish endothelial and blood vessel interactions. The recruited endothelial cells likely provide incipient metastases a key signal that promotes metastatic progression, suggesting a non-canonical role for endothelial cells in enhancement of metastatic initiation efficiency during cancer progression. This is consistent with emerging evidence for perfusion-independent activities of endothelial cells in other systems.[72] Further studies will have to be undertaken to understand the nature of this interaction between cancer cells and endothelial cells, which is highly fascinating as it suggests that tumour cells may hijack a normal developmental process to further their progression.

Furthermore, these findings reveal miR-126 to act in a cell-type specific fashion to suppress pathologic angiogenesis. In breast cancer, miR-126 expression inhibits pathologic endothelial recruitment to metastases, while in development, miR-126 expression promotes and maintains vessel integrity. Endothelial miR-126 was shown to regulate developmental

angiogenesis through targeting of SPRED-1 and PIK3R2[66,68], genes that were not regulated by miR-126 in breast cancer cells (Table 11). Conversely, miR-126 inhibition in endothelial cells does not enhance endothelial recruitment by endothelial cells as it does in breast cancer cells (Figure 33). Consistent with this, miR-126 inhibition in endothelial cells did not affect the expression of IGFBP2, MERTK and PITPNC1 but did indeed increase expression of established endothelial miR-126 targets SPRED1 and PIK3R2 (Figure 34). Future research will need to be performed to reveal how miRNAs, such as miR-126, targets different mRNAs in different cell types. Thus, miR-126 is revealed to act in a cell-type specific manner. Interestingly, the same miRNA can act in different cell types via distinct molecular mechanisms to promote physiologic developmental angiogenesis or suppress aberrant pathologic cancer angiogenesis.

Table 11: Average fold change of previously identified miR-126 targets

Gene Name	LM2	LM2 m126OE	Fold
SPRED1	979	851	-1.1029
PIK3R2	2188	1513	-1.2634

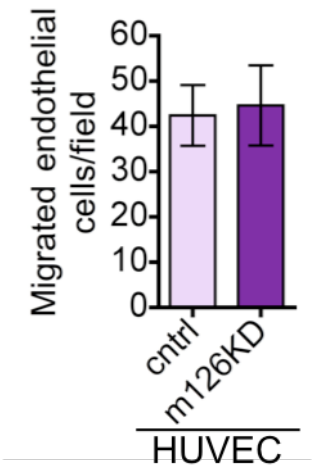

Figure 33| Endothelial-expressed miR-126 does not inhibit recruitment of other endothelial cells. An antagomiR targeting miR-126 or a control antagomiR were transfected into HUVEC cells before being subjected to the HUVEC recruitment assay. Images of the basal side of the inserts were obtained and cells counted using ImageJ software. n=4; error bars represent s.e.m.

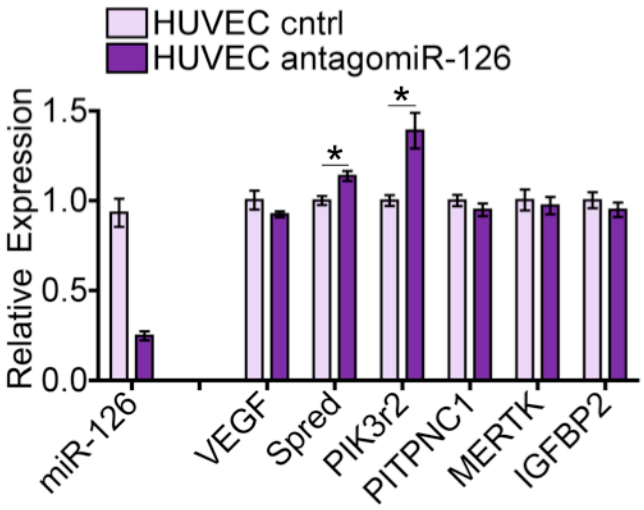

Figure 34| Endothelial-expressed miR-126 does not target IGFBP2, MERTK or PITPNC1. An antagomiR targeting miR-126 or a control antagomiR were transfected into HUVEC cells and the relative expression of potential targets in transfected cells were quantified using qPCR. Error bars represent s.e.m., p-values obtained using a one-sided student's t-test. *P<0.05.

Targeting the blood supply has long been thought to be an efficacious avenue to target tumours. In particular, VEGF was discovered as a promoter of tumourigenesis in primary tumours through its enhancement of angiogenesis.[73] Clinical trials have shown that VEGF inhibition, in combination with chemotherapy, can lengthen survival by 2-3 months in patients with stage IV colorectal or lung cancers.[25-27] Unfortunately, VEGF inhibition has not proven beneficial for metastasis prevention in either pre-clinical metastasis models[74,75] or the adjuvant setting[28]. Unknown factors that compensate for VEGF inhibition to promote metastatic angiogenesis have been proposed to be responsible for this outcome. As a result, a number of investigators have sought to identify factors that mediate metastatic angiogenesis. The systemic analysis and focus on metastasis and metastatic angiogenesis in my project has led to the identification of a number of molecules, including miR-126 and its downstream effectors–the secreted factor IGFBP2, the kinase MERTK, and the transferase PITPNC1–as novel targets for therapeutic inhibition with the potential for prevention of metastatic breast cancer in the adjuvant setting.

* *All experiments in this chapter were performed in collaboration with Nils Halberg, Ph.D.*

CHAPTER 4:
MiR-126 regulon mediates Endothelial Recruitment through divergent pathways

Introduction

In the previous chapter, miR-126 was shown to suppress the key metastasis phenotype of endothelial recruitment, which in turn inhibited metastatic initiation and metastatic colonization. Specifically, miR-126 regulates this phenotype through coordinate regulation of a novel set of metastatic angiogenesis genes–IGFBP2, MERTK and PITPNC. Interestingly, each of these genes was determined to be required for endothelial recruitment, metastatic angiogenesis, metastatic initiation and colonization. These genes represent novel targets for therapeutic inhibition with the potential for prevention of metastatic breast cancer. However, before pursuing these genes as therapeutic targets, it is imperative to understand the mechanism(s) underlying the capability of each of these genes to promote endothelial recruitment.

Insulin-like growth factor-binding protein 2 (IGFBP2) is a protein that belongs to a family of six highly conserved IGF-binding proteins (IGFBPs).[76-78] IGFBPs circulate or reside locally in the extracellular space and act as carrier proteins to regulate the bioavailability and half-life of the IGFs. They have been shown to either inhibit or stimulate the growth promoting effects of the IGFs through alteration of the interaction of IGFs with their cell surface receptors.[79,80] In addition, IGFBPs have also been shown to have IGF-independent effects on cell growth. IGFBP2 is the second most abundant circulating IGFBPs and has stronger binding affinity for IGF2 as compared to IGF1. Under normal physiological conditions,

IGFBP2 is expressed predominantly in highly proliferative fetal tissues that exhibit extensive cell movement, suggesting that IGFBP2 is an important protein involved in cell movement during development.[81] Furthermore, IGFBP2 has been shown to be over-expressed in glioblastoma multiforme (GBM), which in turn promotes GBM invasion through the activation of a network of cell adhesion and mobility genes.[82] Thus, IGFBP2 regulates cell migration in a variety of systems, placing it as a prime candidate for promoting migration of endothelial cells towards breast cancer cells.

Phosphatidylinositol transfer protein, cytoplasmic 1 (PITPNC1) is a member of the phosphatidylinositol transfer protein family (PITPs), which encode for lipid-binding proteins that transfer phosphatidylinositols (PIs) from one membrane compartment to another. PIs are phospholipids that play a role in signalling and the supply of PIs to membranes where they can be phosphorylated, a key event during cell signalling. Thus, PITPs act as important regulators of signalling by interfacing the spatial distribution of PI with its conversion into its various phosphorylated derivatives. Besides that, PITPs have also been implicated in vessel trafficking and protein secretion. Specifically, PITPNC1 belongs to the subgroup of Retinal degradation type B (RdgB) proteins, as the mutation of its homolog gene in *Drosophila* flies leads to the impairment of visual transduction due to degeneration of photoreceptors in the retina. However, unlike the other members of the RdgB family, PITPNC1 does not contain transmembrane motifs or the conserved carboxyl-terminal domain and very little is known about its actual function.[83]

Mer tyrosine kinase (MERTK) is a tyrosine kinase receptor that is part of the TAM family of receptors, which consists of three members–Tyro3, AXL and MERTK. Two related proteins, Gas6 (growth-arrest-specific 6) and the anticoagulant protein S, have been identified as ligands of TAM family receptors. Gas6, which acts as the major ligand for TAM receptors, has been shown to induce a variety of phenotypes through activation of the TAM receptors– cell survival, platelet-mediated thrombosis, phagocytosis of apoptotic cells and inhibition of VEGF-induced endothelial cell chemotaxis. MERTK is a type I transmembrane protein that encodes four extracellular domains (2 fibronectin type-III domains and 2 extracellular immunoglobulin-like domains) and a cytoplasmic tail that encodes a tyrosine kinase.[84] Recent studies show that a soluble form of MER is produced through proteolytic cleavage of its ectodomain, leaving behind a carboxyl-terminal portion that remains associated with the cell. Soluble MER then acts as a decoy, competitively inhibiting MERTK signalling during efferocytosis and platelet aggregation.[85,86]

Results

IGFBP2 promotes Endothelial Recruitment

Of the miR-126 targets, IGFBP2 is a secreted factor and thus poised to mediate intercellular communication between metastatic cancer cells and endothelial cells. I first sought to determine if metastatic cells secreted increased levels of IGFBP2. Analysis of conditioned media by ELISA revealed highly metastatic LM2 cells to secrete 2.1-fold higher levels of IGFBP2 than the poorly metastatic MDA-231 parental line, while miR-126 silencing in the MDA-231 line enhanced IGFBP2 secretion by 2.75-fold (Figure 35a). Importantly, miR-126 inhibition had no effect on the secretion of VEGF (Figure 35b), suggesting that the effect of miR-126 on secretion is specific to IGFBP2.

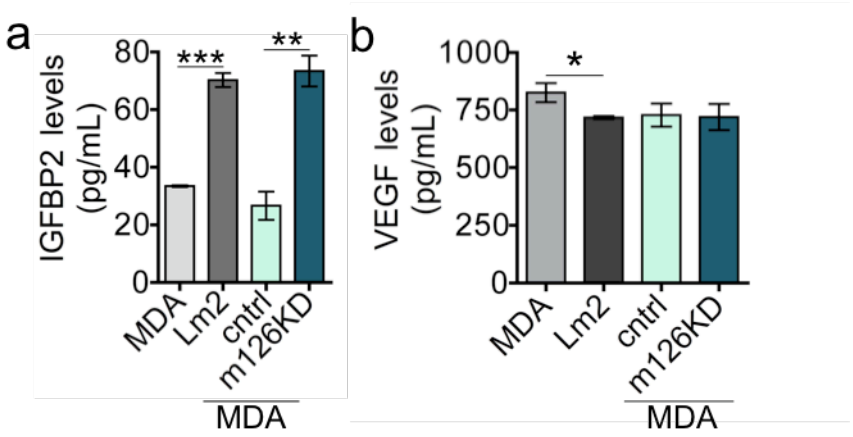

Figure 35| Endogenous miR-126 regulates IGFBP2 secretion by breast cancer cells. IGFBP2 (a) or VEGF (b) levels in conditioned media from MDA cells, LM2 cells and MDA cells expressing either a control hairpin or a hairpin targeting miR-126 were quantified by ELISA. n=4; error bars represent s.e.m., p-values obtained using a one-sided student's t-test. *P<0.05; **P<0.001; ***P<0.0001.

To determine if metastatic endothelial recruitment is mediated through secreted IGFBP2, IGFBP2 binding to IGFs was inhibited through incubation with a neutralizing antibody against IGFBP2. Antibody-mediated inhibition of IGFBP2 in a trans-well recruitment assay significantly inhibited metastatic cell endothelial recruitment to levels comparable to that obtained with miR-126 over-expression (Figure 36a). This effect was specific to the miR-126/IGFBP2 pathway, as inhibition of endothelial recruitment by IGFBP2 antibody was occluded upon miR-126 over-expression. Consistent with this, inhibition of IGFBP2 also eradicated the enhancement of endothelial recruitment seen with miR-126 knockdown (Figure 36a). Antibody-mediated inhibition of IGFBP2 also suppressed endothelial recruitment by the CN34-LM1a of the independent CN34 breast cancer line and also significantly suppressed miR-126-dependent endothelial recruitment (Figure 36b). Conversely, recombinant IGFBP2 rescued the endothelial recruitment defect of highly metastatic cells over-expressing miR-126 in a dose-dependent manner (Figure 37). These findings determine secreted IGFBP2 to act as an inter-cellular signal that mediates miR-126-dependent endothelial recruitment by metastatic cells.

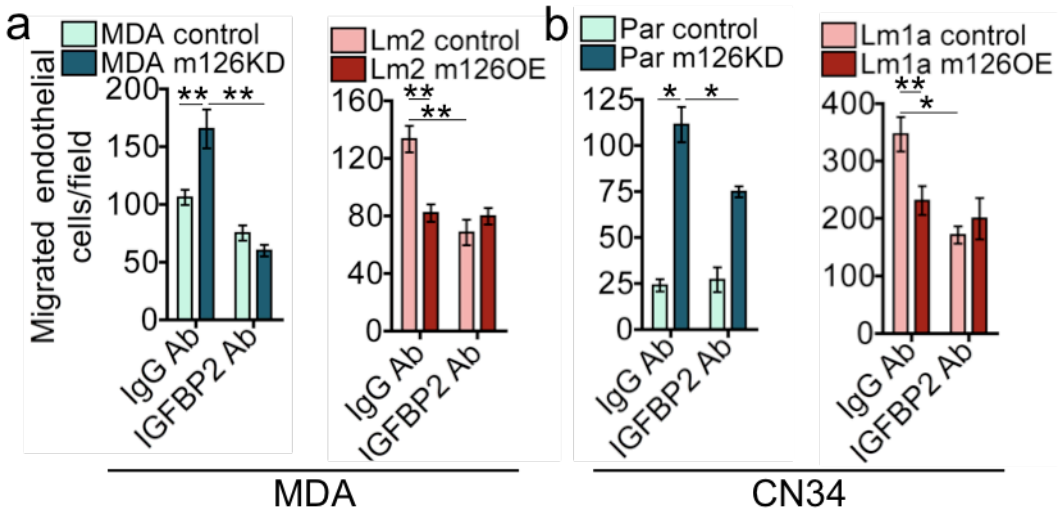

Figure 36| Antibody-mediated inhibition of IGFBP2 suppresses miR-126 dependent endothelial recruitment. a, 2.5 X 10^4 LM2 cells expressing miR-126 or control hairpin as well, as MDA cells expressing miR-126 or the control hairpin, were seeded in quadruplicate. Trans-well recruitment of 5 X 10^4 HUVEC cells in the presence of 50 ng/ml IGFBP2 Ab or 50 ng/ml control IgG Ab towards the cancer cells was then assessed. Images of the basal side of the trans-well inserts were obtained and the number of cells that had migrated was quantified using ImageJ. n=4; error bars represent s.e.m., p-values obtained using student's t-test. **b,** 2.5 X 10^4 CN34 Par cells expressing a short hairpin targeting miR-126 or the control hairpin, as well as CN34-Lm1a cells expressing miR-126 or the control hairpin, were subjected to the HUVEC recruitment assay in the presence of 50 ng/ml IGFBP2 Ab or 50 ng/ml control IgG Ab. n=4; error bars represent s.e.m., p-values obtained using student's t-test. *P<0.05; **P<0.001.

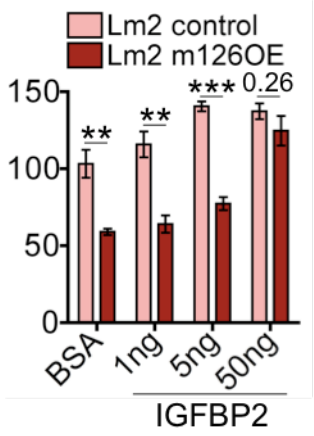

Figure 37| Recombinant IGFBP2 rescues miR-126 inhibition of endothelial recruitment. LM2/miR-126OE and LM2/control cells were subjected to HUVEC recruitment assay in the presence of 1, 5 or 50 ng/ml rhIGFBP2 or 50 ng/ml BSA; n=4; error bars represent s.e.m., p-values obtained using student's t-test. **P<0.001; ***P<0.0001.

IGFBP2 mediates Endothelial Recruitment through IGF1-dependent activation of IGF1R on endothelial cells

IGFBP2 is known to bind both IGF1 and IGF2 in the extracellular space and consequently, modulate their signalling activity. To determine whether any of the IGFs mediate miR-126-dependent endothelial recruitment, the trans-well recruitment assay was performed in the presence of blocking antibodies against IGF1, IGF2 or with immunoglobulin control. Inhibition of IGF1 with block antibody significantly inhibited endothelial recruitment resulting from miR-126 knockdown, while neutralizing antibody against IGF2 had no effect (Figure 38).

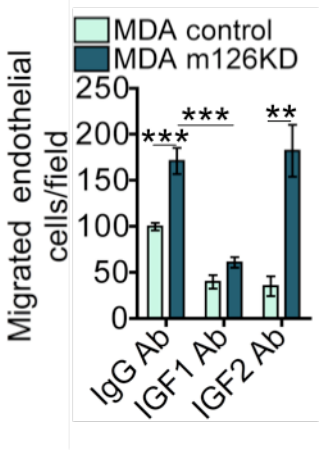

Figure 38| IGF1 mediates miR-126 suppression of endothelial recruitment. Trans-well recruitment of HUVEC cells incubated with 20 μg/ml IGF-1 blocking Ab, 40 μg/ml IGF-2 blocking Ab or control IgG towards MDA cells expressing a short hairpin targeting miR-126 or control hairpin was assayed. n=4; error bars represent s.e.m., p-values obtained using student's t-test. **P<0.001; ***P<0.0001.

Next, to determine which IGF receptors mediated miR-126-dependent endothelial recruitment by metastatic cells, the trans-well recruitment assay was performed with blocking antibodies against IGF type-1 receptor (IGF1R), IGF type-2 receptor (IGF2R) or with immunoglobulin control. Antibody-mediated inhibition of IGF1R, but not IGF2R, significantly suppressed miR-126-dependent endothelial recruitment (Figure 39a). I next sought to determine whether the activated IGF1R that was crucial for miR-126-dependent endothelial recruitment was residing on endothelial cells or on cancer cells. To this end, either cancer cells or endothelial cells were pre-incubated with the IGF1R-neutralizing antibody prior to the endothelial recruitment assay. Pre-incubation of endothelial cells with the blocking antibody suppressed miR-126-dependent endothelial recruitment, while pre-incubation of cancer cells did not (Figure 39b). Consistent with this, siRNA mediated knockdown of IGF1R in cancer cells did not have any significant effects on endothelial recruitment (Figure 40).

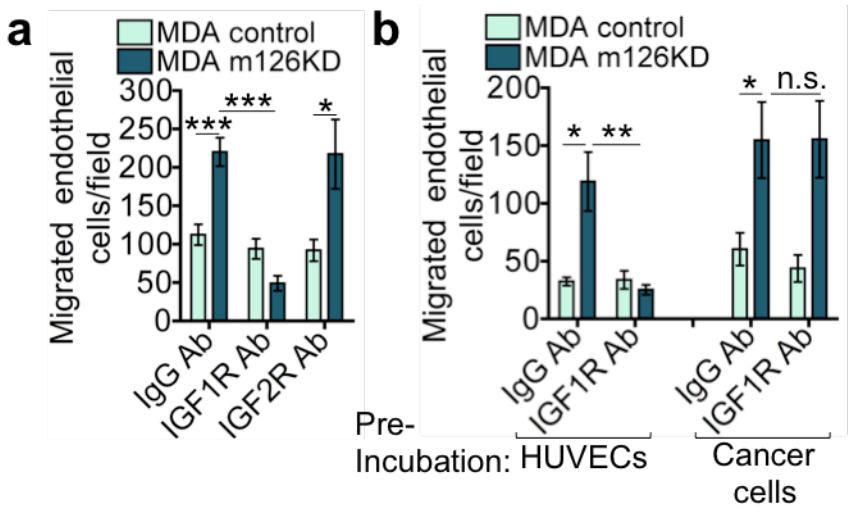

Figure 39| Endothelial IGF1R mediates miR-126 inhibition of endothelial recruitment. **a,** Trans-well recruitment of HUVEC cells incubated with 20 μg/ml IGF1R blocking Ab, 5 μg/ml IGF2R blocking Ab or control IgG towards MDA cells expressing a short hairpin targeting miR-126 or control hairpin was assayed. n=4; error bars represent s.e.m., p-values obtained using student's t-test. **b,** HUVEC and cancer cells were pre-treated with 20 μg/ml IGF1R blocking Ab or control IgG Ab for 1 hour before trans-well recruitment of 5 X 10^4 HUVEC cells towards 2.5 X 10^4 cancer cells was assessed. n=4; error bars represent s.e.m., p-values obtained using student's t-test. *P<0.05; **P<0.001; ***P<0.0001.

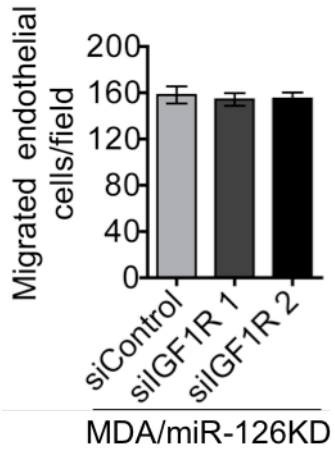

Figure 40| Cancer-express IGF1R does not regulate endothelial recruitment. 2.5 X 10^4 MDA/miR-126 KD cells transfected with a short hairpin targeting IGF1R or the control hairpin were seeded in quadruplicate. Trans-well migration of 5 X 10^4 HUVEC cells towards the cancer cells was then assessed. n=4; error bars represent s.e.m., p-values obtained using the one-sided student's t-test.

To ascertain that IGF1R is indeed activated on endothelial cells upon IGFBP2 signalling, HUVEC cells were incubated with either recombinant IGFBP2 or conditioned media from MDA/miR-126KD and MDA/control cells and activated of IGF1R was assessed by western blotting for phosphorylated IGF1R. Recombinant IGFBP2 alone was enough to induce phosphorylation of IGF1R on endothelial cells in a time-dependent manner (Figure 41a). Consistent with this, conditioned media from miR-126 knockdown cells had a greater ability to induce phosphorylation of IGF1R relative to control cells (Figure 41b). These findings reveal metastatic endothelial recruitment to result from the secretion of miR-126 target gene IGFBP2, which then binds IGF1 in the extracellular space and enhance IGF1-dependent activation of the IGF type 1 receptor on endothelial cells. Enhanced IGF1R activation on endothelial cells in turn stimulates endothelial migration towards metastatic breast cancer cells.

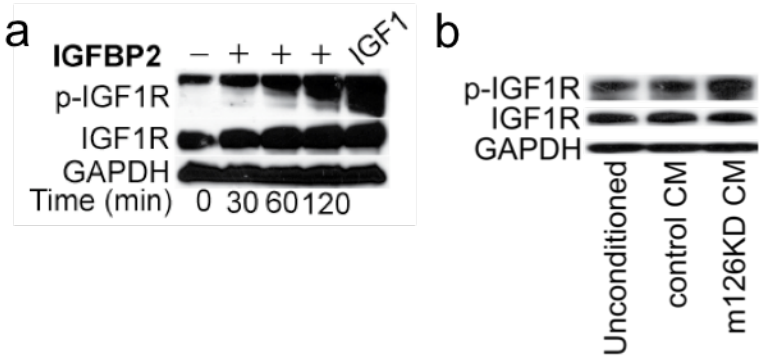

Figure 41| Endothelial IGF1R undergoes phosphorylation upon stimulation with IGFBP2. a, HUVEC cells were treated with 520ng/ml rhIGFBP2 or 50ng/ml rhIGF-1 and subjected to western blot analysis for p-IGF1R, IGF1R and GAPDH. **b,** Conditioned media was collected by incubating MDA cells expressing a control hairpin or a hairpin targeting miR-126 in HUVEC media for 24h. HUVEC cells were then treated with the conditioned media for 30min and subjected to western blot analysis for p-IGF1R, IGF1R and GAPDH.

Finally, I sought to determine if recombinant IGFBP2 was enough to induce endothelial recruitment in the absence of other factors derived from cancer cells. Recombinant IGFBP2, which was mixed with matrigel and allowed to solidify in the bottom of a Boyden chamber, strongly recruited HUVECs through a porous trans-well insert in a dose-dependent manner (Figure 42). This endothelial chemotaxis effect was dependent on IGF1R as antibody-mediated inhibition of IGF1R suppressed endothelial chemotaxis towards the recombinant IGFBP2 source (Figure 42). Consistent with this, pre-incubation of recombinant IGFBP2 protein was also sufficient, in a dose-dependent manner, to promote endothelial migration and this IGFBP2-induced migration was eradicated when IGF1R was inhibited with a blocking antibody (Figure 43). These findings suggest that the miR-126/IGFBP2/IGF1 pathway enhances endothelial migration towards metastatic cells through activation of IGF1R on endothelial cells.

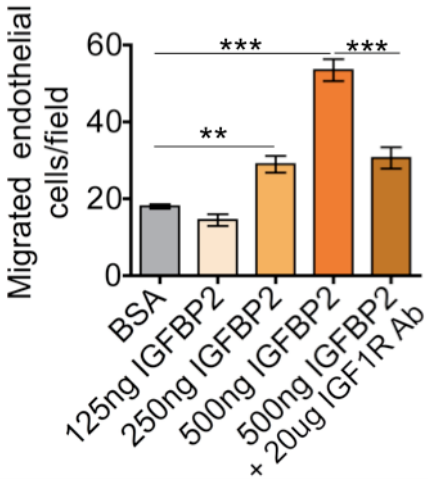

Figure 42| IGFBP2 enhances endothelial chemotaxis. IGFBP2 gradient was simulated by mixing the given amounts of recombinant IGFBP2 protein with matrigel (1:1) in the bottom of a well. Chemotaxis of 1.5 X 10^5 HUVEC cells along the IGFBP2 gradient was then assessed by counting the number of cells that had migrated to the basal side of trans-well inserts after 20h using ImageJ software. n=4; error bars represent s.e.m., p-values obtained using student's t-test. **P<0.001; ***P<0.0001.

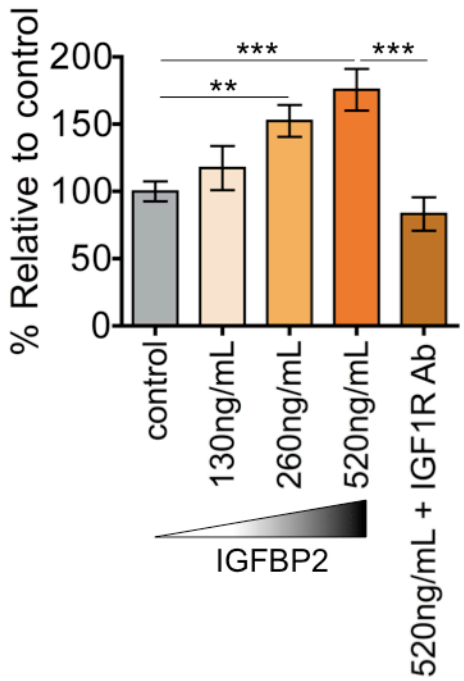

Figure 43| IGFBP2 increases endothelial migration. HUVEC cells were stimulated with the stated concentrations of recombinant human IGFBP2 protein and anti-IGF1R Ab (10μg/ml) for 40 min, trypsinized and 5 X 10^4 cells were seeded into a porous tranwell insert. The cells were allowed to migrate for 24 hours before the number of cells that had migrated across the membranes were quantified. n=6; error bars represent s.e.m.; p-values were obtained using a one-sided student's t-test. **P<0.001; ***P<0.0001.

PITPNC1 regulates IGFBP2-dependent Endothelial Recruitment

Given the identification of IGFBP2 as a secreted miR-126-dependent factor that mediates the endothelial recruitment phenotype, I wondered if either PITPNC1 or MERTK regulate the secretion of this factor from cancer cells. Knockdown of PITPNC1 using independent hairpins reduced IGFBP2 secretion from breast cancer cells, suggesting that PITPNC1 regulates endothelial recruitment at least partially through positively regulating the secretion of IGFBP2 (Figure 44).

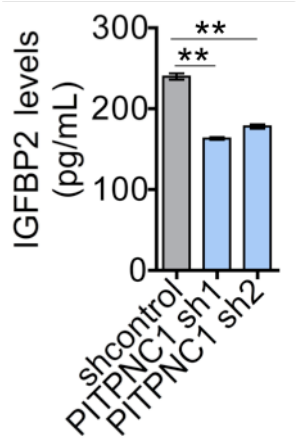

Figure 44| PITPNC1 regulates the secretion of IGFBP2 from breast cancer cells. IGFBP2 levels in conditioned media from Lm2 cells expressing control hairpin or two independent hairpins against PITPNC1 as determined by ELISA. n=4; error bars represent s.e.m.; p-values were obtained using a one-sided student's t-test. **P<0.001.

I next sought to determine whether IGFBP2 is epistatic to PITPNC1 with regards to endothelial recruitment. To this end, PITPNC1 was over-expressed in poorly metastatic MDA-231 cells and it was confirmed that over-expression of PITPNC1 was sufficient to promote endothelial recruitment. This enhancement in endothelial recruitment was occluded upon inhibition with IGFBP2 antibody neutralization, suggesting that IGFBP2 epistatically interacts with PITPNC1 in the setting of endothelial recruitment (Figure 45). These findings are consistent with PITPNC1 mediating endothelial recruitment by regulation of IGFBP2 secretion, which reveal that a single microRNA can regulate two separate genes that converges to a single pathway that is crucial to the key metastatic phenotype of endothelial recruitment.

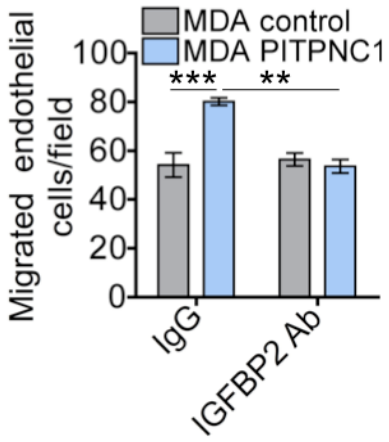

Figure 45| PITPNC1-driven endothelial recruitment is dependent on IGFBP2. 2.5 X 10^4 MDA cells over-expressing PITPNC1 or a control vector were seeded in quadruplicate. Trans-well migration of 5 X 10^4 HUVEC cells towards the cancer cells was then assessed in the presence of 50 ng/ml IGFBP2 Ab or 50 ng/ml control IgG Ab. n=6; error bars represent s.e.m., p-values obtained using a one-sided student's t-test. **P<0.001; ***P<0.0001.

MERTK mediates Endothelial Recruitment by antagonizing GAS6 signalling

I next investigated the mechanisms by which the other miR-126 target gene MERTK mediates endothelial recruitment. Unlike PITPNC1, knockdown of MERTK did not lead to decreased IGFBPP2 secretion, suggesting that MERTK mediates endothelial recruitment through an IGFBP2-independent mechanism. To elucidate the mechanism by which MERTK tyrosine kinase receptor mediates endothelial recruitment, the effect of its known soluble ligand Gas6 on cancer-mediated endothelial recruitment was examined. The addition of recombinant Gas6 at physiological concentrations similar to that found in human serum suppressed miR-126-dependent endothelial recruitment, revealing Gas6 to act as a potent inhibitor of endothelial recruitment (Figure 46).

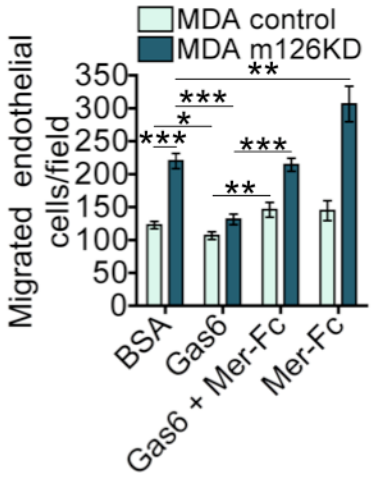

Figure 46| Gas6 inhibits miR-126 dependent endothelial recruitment. 2.5 X 10^4 MDA cells expressing a control hairpin or a hairpin targeting miR-126 were seeded in quadruplicate. Trans-well migration of 5 X 10^4 HUVEC cells towards the cancer cells in the presence of 1ng/ml GAS6 and/or 10µg/ml MerFc was then assessed by counting the number of cells that had migrated to the basal side of porous inserts in images obtained using ImageJ. n=4; error bars represent s.e.m., p-values were obtained using student's t-test. *P<0.05; **P<0.001; ***P<0.0001.

MERTK exists in both membrane bound and soluble forms, where the soluble form has been found to act as a decoy receptor to negatively regulate MERTK receptor activation on cells expressing it. To determine if MERTK ectodomain was indeed cleaved from breast cancer cells, the conditioned media from MDA-231 cells was analysed by western blotting for MERTK. Soluble MERTK was indeed detected in the conditioned media of MDA-231 cells (Figure 47a). ELISA analysis of conditioned media from MDA/miR-126KD and MDA/control cells was then performed to confirm that soluble MERTK levels significantly increased upon miR-126 inhibition, revealing soluble MERTK levels to be regulated by miR-126 in breast cancer cells (Figure 47b).

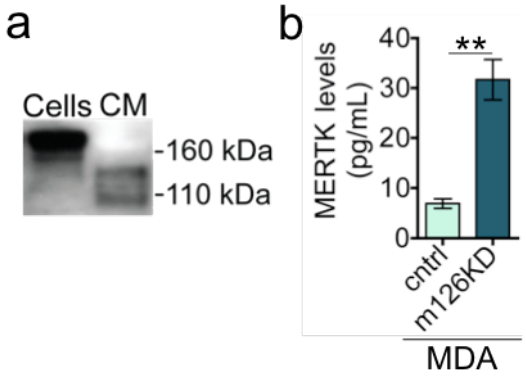

Figure 47| Ectodomain of MERTK is secreted by breast cancer cells. a, Western blot analysis of MERTK in MDA cellular lysate and conditioned media. **b,** Soluble MERTK levels in conditioned media from cancer cells was quantified by ELISA; n=4. Error bars represent s.e.m., p-values obtained using the one-sided student's t-test. **P<0.001.

I then hypothesized that soluble MERTK released from cancer cells may promote endothelial recruitment by acting as decoys to bind and inhibit Gas6. Consistent with this, the addition of recombinant soluble MERTK extracellular domain (MerFc) suppressed both exogenous and recombinant Gas6-mediated suppression of endothelial recruitment by cancer cells (Figure 46). This effect was miR-126 dependent, suggesting that secreted MERTK from metastatic cells inhibit Gas6 by acting as a decoy receptor, thus reducing the inhibitory effects of Gas6 on cancer cell-mediated endothelial recruitment.

To determine whether the recombinant forms of IGFBP2 and MERTK (expressed by metastatic cells) and Gas6 (present in human serum) are sufficient to regulate endothelial chemotaxis, trans-well chemotactic assays was performed by solidifying matrigel containing these factors at the bottom of the well and allowing endothelial cells to migrate towards these factors. Low, physiological doses of recombinant Gas6 suppressed endothelial chemotaxis that was induced by recombinant IGFBP2. However, the suppressive effect of Gas6 on endothelial chemotaxis was relieved upon the addition of recombinant soluble MERTK ectodomain (Figure 48). Interestingly, unlike recombinant IGFBP2, pre-incubation with Gas6 did not affect endothelial migration, suggesting that Gas6 specifically inhibits chemotactic migration (Figure 49). These findings suggest that while IGFBP2 mediates a positive migratory and chemotactic signal to endothelial cells, soluble MERTK receptor antagonizes an inhibitory chemotactic signal mediated by Gas6.

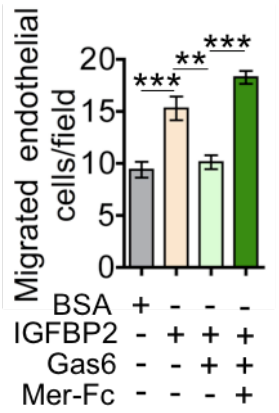

Figure 48| Ectodomain of MERTK rescues Gas6 inhibition of endothelial chemotaxis. Chemotaxis of HUVECs towards an IGFBP2 source was assessed in the presence of Gas6 (5ng/mL) and MerFc (10ug/mL) protein; n=4. Error bars represent s.e.m., p-values obtained using the one-sided student's t-test. **P<0.001; ***P<0.0001.

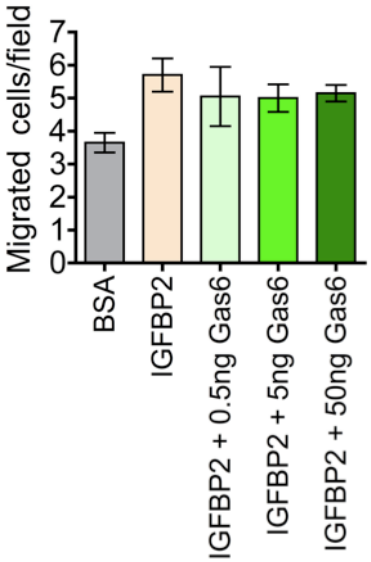

Figure 49| Ectodomain of MERTK does not inhibit IGFBP2-driven endothelial migration. HUVEC cells were stimulated with 520ng/ml recombinant human IGFBP2 protein and given concentrations of Gas6 for 40 min, trypsinized and 5 X 10^4 cells were seeded into a porous tranwell insert. The cells were allowed to migrate for 24 hours before the number of cells that had migrated across the membranes were quantified. n=6; error bars represent s.e.m.; p-values were obtained using a one-sided student's t-test.

GAS6 inhibits Endothelial Recruitment through activation of MERTK on endothelial cells

I next sought to identify the receptor on endothelial cells that mediate the suppressive effect of Gas6 on endothelial recruitment. Through pre-incubation with neutralizing antibodies, endothelial MERTK and AXL–two Gas6 receptors that are highly expressed on endothelial cells–were inhibited. Specifically, inhibition of MERTK rescued Gas6-induced suppression of endothelial recruitment, while inhibition of AXL had no effect (Figure 50). Consistent with this, siRNA-mediated knockdown of MERTK on HUVECs also occluded the suppressive effects of Gas6 on endothelial recruitment (Figure 51). These findings indicate that the miR-126/MERTK/Gas6 pathway mediates endothelial chemotaxis towards metastatic cells through activation of MERTK on endothelial cells. This is particularly interesting as it also shows that a single microRNA can regulate different genes that act in two divergent pathways, one activating and one inhibitory, which then eventually converge to mediate a single key metastatic phenotype.

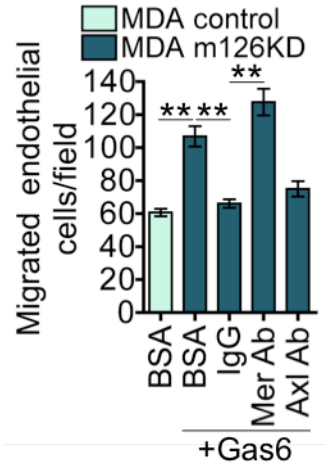

Figure 50| Antibody-mediated inhibition of endothelial MERTK suppresses miR-126 dependent endothelial recruitment. HUVEC cells were pre-treated with 10 μg/ml MERTK blocking Ab, 20 μg/ml AXL blocking Ab or 20 μg/ml IgG Ab for 1h before HUVEC recruitment capacity in the presence of 1ng/ml GAS6 was assessed; n=4; error bars represent s.e.m., p-values obtained using a one-sided student's t-test. **P<0.001.

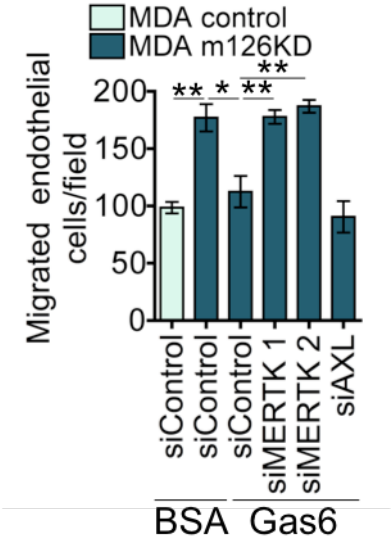

Figure 51| Gas6-mediated endothelial recruitment is dependent on endothelial MERTK. HUVEC cells were transfected with siRNAs targeting MERTK or AXL or a control siRNA. 72 hours after transfection, trans-well recruitment of HUVEC cells towards cancer cells in the presence of 1ng/ml GAS6 was assessed. n=4; error bars represent s.e.m., p-values obtained using a one-sided student's t-test. *P<0.05; **P<0.001.

IGFBP2 and MERTK are sufficient for in vivo Endothelial Recruitment

To ensure that the effects of recombinant IGFBP2 and MERTK seen *in vitro* were relevant in a physiological setting, I sought to determine if these recombinant proteins were sufficient to recruit endothelial cells *in vivo*. To this end, matrigel plugs containing BSA or recombinant IGFBP2 and soluble MERTK ectodomain were injected into the mammary fat pads of mice. Immunohistological staining of the derived plugs revealed recombinant IGFBP2 and MERTK to be sufficient to enhance *in vivo* recruitment of endothelial cells into matrigel plugs (Figure 52). These findings reveal IGFBP2 and soluble MERTK to be critical factors secreted by metastatic cells, which work together to promote endothelial recruitment that in turn enhances metastatic initiation and colonization.

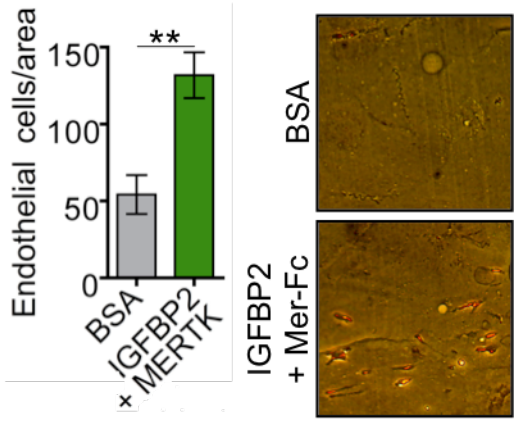

Figure 52| IGFBP2 and MERTK recruit endothelial cells *in vivo*. Endothelial recruitment to mammary fat pads was analysed in vivo using matrigel plugs containing either recombinant IGFBP2 (1ug/mL) and MERTK (10ug/mL) or BSA (11ug/mL). n=5. Error bars represent s.e.m. p-values obtained using the one-sided Mann-Whitney test. **P<0.001.

IGFBP2 as a Therapeutic Target for Metastasis Inhibition

Since my previous findings reveal IGFBP2 to be a potent mediator of the endothelial recruitment phenotype that is critical for successful metastatic efficiency, IGFBP2 is an attractive candidate for therapeutic inhibition with the potential for prevention of metastatic breast cancer. A hybridoma cell line that secretes a unique monoclonal antibody was generated from a mouse plasma cell line obtained upon immunization of a mouse with full length IGFBP2 as an antigen. In the initial screen, supernatant from the hybridoma cell line was able to significantly inhibit the ability of mir-126KD cells to recruit endothelial cells (Figure 53).

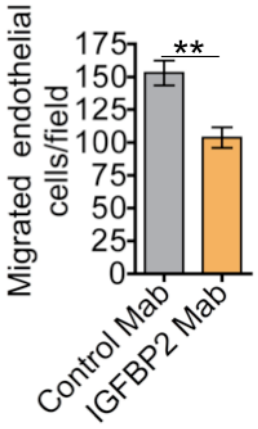

Figure 53| Hybridoma supernatant containing anti-IGFBP2 monoclonal antibodies inhibits endothelial recruitment. MDA cells expressing miR-126 or the control hairpin, were seeded in quadruplicate. Trans-well recruitment of 5 X 10^4 HUVEC cells in the presence monoclonal IGFBP2 antibodies (conditioned media from hybridoma at a concentration of 200 ng/ml) or control IgG Ab towards the cancer cells was then assessed. Images of the basal side of the trans-well inserts were obtained and the number of cells that had migrated was quantified using ImageJ. n=4; error bars represent s.e.m., p-values obtained using student's t-test. **P<0.001.

Individual clones were then isolated and expanded from the hybridoma cell line by limiting dilution. The monoclonal antibodies secreted by these individual clones were then tested for their ability to capture biotinylated IGFBP2 by ELISA (Table 12). A competitive binding assay was then performed by repeating the ELISA in the presence of recombinant IGF-1 (Table 12). Since endothelial recruitment is mediated by IGFBP2 binding to IGF-1, a therapeutic antibody should function by blocking binding of IGF-1 to IGFBP2.

Table 12: IGFBP2 Elisa screen for hybridoma clones

Clone	IGFBP2	+ IGF-1	Ratio
M1	2.53	1.82	1.39
M4	2.42	2.09	1.16
M5	0.10	0.38	0.28
M6	2.27	1.98	1.14
M9	2.43	2.14	1.14
M13	2.37	2.09	1.13
M14	2.39	1.12	1.13
M15	2.43	2.16	1.12
M16	2.36	2.11	1.12
M18	0.56	0.80	0.70
M20	2.42	2.22	1.09

Based on the ELISA, a total of eleven monoclonal antibodies (9 positive for inhibiting IGFBP2–IGF-1 binding + 2 negative for IGFBP2–IGF-1 binding) were selected for further testing in the endothelial recruitment assay. Consistent with ELISA results, the two monoclonal antibodies that were negative for IGFBP2 binding did not significantly affect HUVEC recruitment, while all the monoclonal antibodies that were positive for IGFBP2 binding significantly inhibited HUVEC recruitment at a concentration of 1μg/ml (Figure 54).

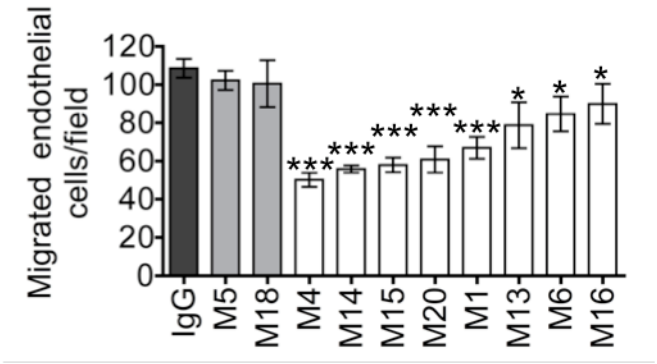

Figure 54| Monoclonal antibodies raised against IGFBP2 inhibit endothelial recruitment to varying degrees. MDA cells expressing miR-126 or the control hairpin, were subjected to the HUVEC recruitment assay in the presence of 1 μg/ml monoclonal IGFBP2 antibody obtained from individual hybridoma clones or control IgG Ab. n=4; error bars represent s.e.m., p-values obtained using student's t-test. *P<0.05; **P<0.001; ***P<0.0001.

I next wondered if the monoclonal antibodies targeting IGFBP2 were able to suppress endothelial recruitment at a lower concentration, which would give insight into the potency of the individual antibodies. To this end, the top four performing antibodies from the previous assay was tested was their ability to inhibit endothelial recruitment at a concentration of 200ng/ml (Figure 56). Interestingly, although all four antibodies still significantly suppressed endothelial recruitment, the order of efficacy of the four antibodies changed at 200ng/ml as compared to 1μg/ml. One particular clone was identified to be a promising candidate for therapeutic efficacy in metastasis suppression due to its potency and consistency in suppressing endothelial recruitment and further testing will be performed to determine its ability to inhibit *in vivo* metastasis.

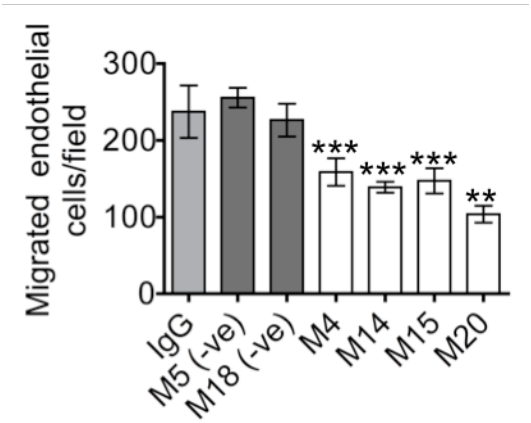

Figure 55| Monoclonal IGFBP2 antibodies suppress endothelial recruitment at a low concentration. MDA cells expressing miR-126 or the control hairpin, were subjected to the HUVEC recruitment assay in the presence of 200 ng/ml monoclonal IGFBP2 antibody obtained from individual hybridoma clones or control IgG Ab. n=4; error bars represent s.e.m., p-values obtained using student's t-test. **P<0.001; ***P<0.0001.

MERTK as a Therapeutic Target for Metastasis Inhibition

My earlier findings also identify cleaved MERTK ectodomain that is secreted by cancer cells to be an important positive mediator of metastatic initiation and colonization, suggesting that it can also be potentially targeted for therapeutic inhibition of metastasis. However, MERTK has two closely related family members that are both extremely similar in structure and respond to the Gas6 ligand as well. Thus, it is important to determine if these other family members, AXL and Tyro3, have any effect on endothelial recruitment since inhibitors of MERTK could potentially inhibit either of these due to the structural similarity between the three receptors.

I first sought to determine if Gas6 signalling in cancer cells had any effect on endothelial recruitment since previous studies focused on the effects of Gas6 signalling in endothelial cells. To this end, miR-126KD and control cells were pre-incubated with physiologically relevant concentrations of Gas6 or BSA before performing the endothelial recruitment assay. Gas6 incubation of cancer cells did not significantly impact endothelial recruitment, suggesting that Gas6 signalling in cancer cells did not mediate this important metastatic phenotype (Figure 56).

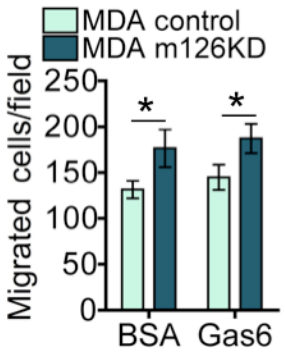

Figure 56| Gas6 suppresses endothelial recruitment independent of cancer cell signalling. Cancer cells were pre-treated with 1ng/ml GAS6 or BSA for 1h before HUVEC recruitment capacity was assessed; n=4; error bars represent s.e.m., p-values obtained using a one-sided student's t-test.

I next wondered if AXL inhibition in either cancer cells had any effect on endothelial recruitment since I had previously shown that AXL inhibition in endothelial cells had no effect on endothelial recruitment (Figure 50-51). To this end, I knocked down AXL using siRNAs and performed the endothelial recruitment assay. Interestingly, AXL inhibition in cancer cells significantly enhanced endothelial recruitment significantly (Figure 57). Since AXL and MERTK can potentially function in the same signalling network, I postulated that AXL inhibition might modulate MERTK expression as well. Interestingly, initial analysis indicates that MERTK expression increases upon AXL knockdown in cancer cells, suggesting that a negative feedback pathway exist whereby MERTK is upregulated upon inhibition of AXL expression. These findings reveal that AXL and MERTK may be co-regulated in cancer cells in order to maintain a balance in the overall activity of these receptors. Thus, it is imperative to further elucidate the exact relationship between AXL and MERTK before pursuing MERTK as a therapeutic target for metastasis intervention.

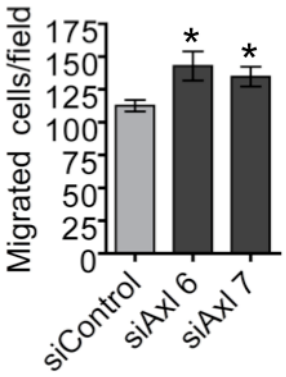

Figure 57| Knockdown of cancer-expressed AXL promotes endothelial recruitment. 2.5 X 10^4 MDA cells were transfected with siRNA targeting AXL or a control hairpin were seeded in quadruplicate. Trans-well migration of 5 X 10^4 HUVEC cells towards the cancer cells were then assessed. Images of cells that migrated through the trans-well inserts were obtained and analysed using ImageJ software. n=4; error bars represent s.e.m., p-values obtained using a student's t-test. *P<0.05.

Discussion

Here, I reveal that miR-126 co-ordinately regulates a novel set of angiogenesis and metastasis genes (IGFBP2, MERTK and PITPNC) that modulate two divergent pathways (IGF1 and Gas6 signalling), which then converge to mediate a single phenotype of endothelial recruitment that is crucial for metastatic initiation, leading to colonization. These findings underscore how critical the endothelial recruitment phenotype is to metastasis since they reveal cancer cells to regulate this phenotype through the modulation of multiple genes and pathways.

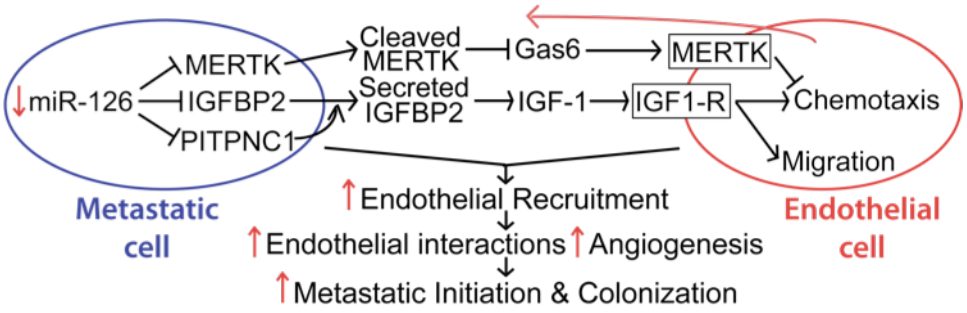

Figure 58| Overview of miR-126 regulation of endothelial recruitment.

The IGF1 signalling pathway, which is regulated by IGFBP2 secretion from cancer cells, was discovered to result in IGF1R phosphorylation and activation on endothelial cells. IGF1 acts as a trans-cellular mediator of endothelial recruitment by metastatic cells and miR-126 expressed by cancer cells modulates the IGF1 pathway by regulating its binding partner IGFBP2. Both IGF1 and IGF2 have well established roles in organismal and cellular growth and interest in these factors as therapeutic targets in cancer have been growing in recent years. However, these growth factors and their receptors are ubiquitously expressed in various tissues and the need for IGF signalling for normal physiology limits them as targets for therapeutic application.[87,88] My results indicate that IGFBP2 is a metastasis promoter that is typically over-expressed in metastatic human breast cancer cells. Furthermore, the robust effect of its antibody-mediated inhibition of endothelial recruitment by metastatic cancer cells provides a specific method through which the IGF pathway can be therapeutically targeted in breast cancer progression and angiogenesis. I have since begun development of monoclonal antibodies that target IGFBP2 and initial screens have identified a clone that has the potential to impair cancer progression *in vivo*.

Besides identifying IGFBP2 as a promoter of endothelial recruitment through its activation of a positive signalling pathway involved in this process, I have also discovered MERTK to be a promoter of endothelial recruitment through its inhibition of Gas6–a negative regulator of endothelial chemotaxis. Metastatic cancer cells secrete MERTK, which inhibit Gas6 signalling by acting as decoy receptors that competitively antagonize Gas6 binding to the MERTK receptor on endothelial cells. Thus, miR-126 controls the complex phenotype of metastatic initiation by modulating both positive and negative regulators of the endothelial recruitment phenomenon. Consistent with my findings for a role of MERTK in angiogenesis, a subset of patients with reinitis pigmentosa, a disorder that presents with reduced retinal angiogenesis, have been found to harbour somatic mutations in MERTK.[89]

In order to develop MERTK as a therapeutic target for metastatic inhibition, I have attempted to characterise the effects of AXL inhibition on endothelial recruitment since AXL responds to Gas6 and is structurally similar to MERTK. These findings revealed AXL inhibition in cancer cells to suppress endothelial recruitnment, which may be at least in part due to its effect on MERTK expression. Furthermore, Gas6-induced MERTK signalling on endothelial cells is also inhibitory to endothelial chemotaxis. Thus, when developing either monoclonal antibodies or small molecule inhibitors against MERTK for therapeutic intervention of metastasis, it will be crucial to ensure their specificity for only the cleaved MERTK ectodomain derived from cancer cells so that they do not target MERTK on endothelial cells.

** Experiments performed for Figure 35-53 were performed in collaboration with Nils Halberg, Ph.D.*

CHAPTER 5:
Regulation of Metastasis Suppressor microRNAs

Introduction

Metastasis suppressor microRNAs, including miR-335 and miR-126, have previously been determined to have expression levels that are inversely correlated with human breast cancer progression. In a previous study, miR-335 was determined to suppress metastasis by inhibiting cell migration and invasion through targeting SOX4 and Tenascin-C (TNC).[51] Meanwhile, in the previous chapters, I have revealed miR-126 to inhibit metastatic initiation by suppressing endothelial recruitment through targeting IGFBP2, MERTK and PITPNC. However, the upstream mechanisms that are employed by breast cancer cells to silence these two robust metastasis suppressor miRNA remain largely unresolved. Since both these miRNAs play key suppressive roles in metastasis, it is imperative to dissect and elucidate the underlying mechanism(s) that regulate them, potentially unveiling new therapeutic targets for metastasis suppression.

Interestingly, both miR-126 and miR-335 are intronic miRNAs–miRNAs that are encoded in the introns of either protein-coding or noncoding genes. In animals, the majority (~80%) of miRNAs are intronic and these intronic miRNAs are typically co-transcribed with the pre-mRNA that they reside in before the pre-mRNA is processed to generate pri/pre-miRNAs.[90,91] Several different methods for the processing of miRNAs from introns in pre-mRNAs have been described. The pri-miRNA transcript is released from introns that have been excised and linearized and this pri-miRNA is then processed to generate mature

miRNAs via the canonical miRNA biogenesis pathway. Alternatively, Drosha can generate pre-miRNAs directly through cleavage of excised lariats, linearized introns or unspliced pre-mRNAs.[92] Since intronic miRNAs are typically co-transcribed with the pre-mRNA they reside in, mechanisms that typically affect the generation of their host pre-mRNAs should affect the expression of these miRNAs as well. Mechanisms that could potentially be involved in regulation of pre-mRNA synthesis include genetic mutations, epigenetic regulation and transcriptional regulation.

Numerous mechanisms that can suppress the function of a gene have been described, one of the most commonly studied being genetic mutations. A common mutation that causes loss of gene expression is genetic deletion, whereby DNA sequences are lost from the genome. The copy number of a gene is typically tightly regulated to ensure that the functional product is generated at the correct level of expression. A deletion of one copy of an allele leads to a condition known as haploinsufficiency, which has been shown to promote oncogenesis when they affect tumour suppressor genes such as PTEN and p53.[93]

Another promising and expanding field focusing the regulation of gene expression is the field of epigenetics, which is the study of all mechanisms that regulate gene transcription and genome stability that are maintained throughout cell division, excluding changes in the DNA sequences. Epigenetic regulation of genes involves the control of chromatin structure through several mechanisms including DNA methylation and covalent histone modifications. In many human diseases including cancer, aberrant epigenetic regulation is often observed.[94]

DNA methylation results in silencing of genes and non-coding genomic region through methylation of the 5' position of the cytosine ring within CpG dinucleotides. CpG dinucleotides are typically concentrated in either regions of large repetitive sequences (e.g. centromeres and retrotransposon elements) or CpG islands, CpG-rich regions that are found in more than 50% of human gene promoters.[95] DNA methylation is highly important in determining cell and organismal fate and has been determined to be important in cellular processes such as long-term gene silencing leading to genomic imprinting, X chromosome inactivation and the suppression of transposable elements.

Transcriptional regulation has also been widely studied over the years and many transcription factor families have been identified. They typically bind to cis-regulatory sites that are upstream of genes and can either activate or repress transcription. In complex multicellular organisms, transcription factors act in complex networks where they cooperate and interact with each other. Transcription factors are also highly conserved and play important development roles. Many transcription factors have since been identified as oncogenes or tumour suppressors, revealing that changes in transcription factor-driven regulation of genes are often important drivers or suppressors of cancer.[96-98]

In addition to regulatory mechanisms that modulate the generation of host pre-mRNAs, the cleavage of miRNAs from host pre-mRNAs as well as the subsequent downstream processing into mature miRNAs could also potentially affect the expression of intronic miRNAs. Processing of pre-miRNAs into mature miRNAs post Drosha cleavage involves two major steps–exporting of pre-miRNAs from the nucleus into the cytoplasm, followed by cleavage of pre-miRNAs by Dicer into the mature miRNAs.[29,36] All these processing steps starting from the isolation of miRNA from pre-mRNAs to the final cleavage by Dicer thereby represent potential processes that could be deregulated in breast cancer cells to allow for the suppression of the expression of metastasis suppressor miRNAs.

Results

miR-335 locus is Genetically deleted in Metastatic Breast Cancer cells

To determine the mechanisms responsible for the silencing of metastasis suppressor miR-335, the MDA-231 breast cancer cell line and its various *in vivo* selected metastatic derivative sublines that show tropism to either the lungs (LM2) or bones (BoM2) were studied. All these metastatic sublines have previously been shown to display silencing of miR-335 through unknown mechanisms. To determine whether silencing of miR-335 occurred through genetic deletion of its locus, qPCR for the miR-335 locus was first performed on genomic DNA isolated from the various cell lines using two independent primer pairs that overlap across the genomic region encoding this miRNA.[99] All the metastatic derivatives of the parental MDA-231 line tested displayed a loss of copy number at the miR-335 locus relative to the parental MDA-231 line, while no copy number changes were noted at the control let-7e locus (Figure 59).

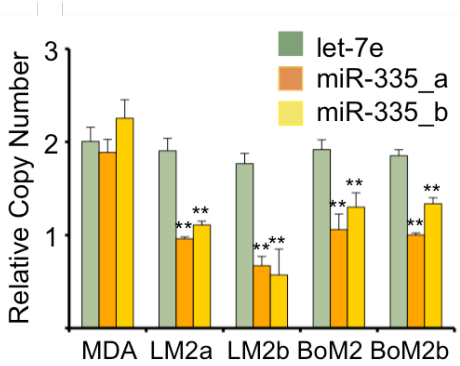

Figure 59| Genomic copy number analysis reveals deletion of the miR-335 locus in metastasis. Genomic qPCR was performed on DNA from the parental MDA-231 cancer cell line as well as its highly metastatic lung (LM2) and bone (BoM) derivatives using independent sets of primers. n=3; error bars represent s.e.m., p-values obtained using a student's t-test. **P<0.005.

To determine if this genetic deletion was specific to the MDA-231 breast cancer cell line, the CN34 cell population, which represents an independent primary malignant cell population, was also examined. Similar to the MDA-231 cell line, all *in vivo* selected lung, bone and brain metastatic derivatives of this CN34 population also displayed silencing of the miR-335 expression. Consistent with previous results, this inhibition of miR-335 expression was determined by qPCR to be due in part to copy number loss (Figure 60).

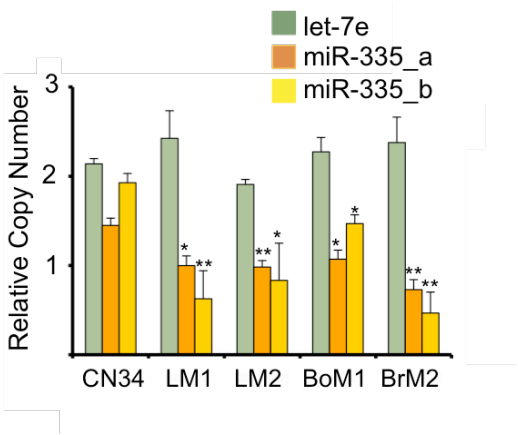

Figure 60| Genomic copy number analysis reveals deletion of the miR-335 locus in metastatic derivatives of a primary malignant population. Genomic qPCR was performed on DNA from the CN34 primary malignant cancer population as well as its highly lung metastatic (LM1a and LM2a), bone metastatic (BoM1), and brain metastatic (Br2a) derivatives. n=3; error bars represent s.e.m., p-values obtained using a student's t-test. *=$p<0.05$, **=$p<0.005$.

Array-comparative genomic hybridization (CGH) was next performed on the MDA-231 cell line, the CN34 population and their various metastatic derivatives using normal female genomic DNA as a reference control. The array-CGH results independently confirm that copy number loss is observed at the 7q32.2 locus (miR-335 locus) in all the metastatic derivatives relative to their respective parent lines (Figure 61). Chromosomal deletions that are common to all metastatic derivatives were extremely infrequent. Only one other region that displayed similar copy number loss in all derivatives from both breast cancer populations was identified–a region distal to Xp11.3. These findings reveal silencing of miR-335 expression in metastatic breast cancer cells to be at least partially due to genetic copy number loss at the miR-335 locus.

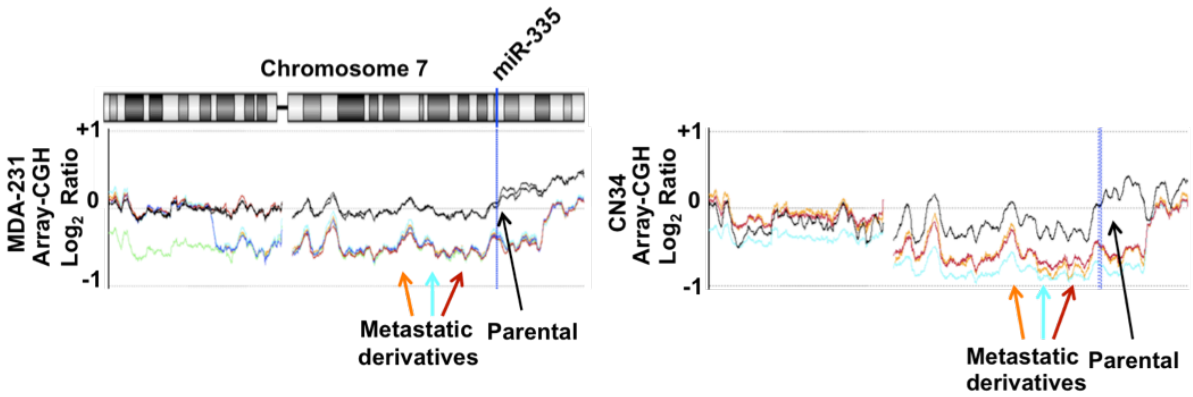

Figure 61| Array CGH analysis reveals deletion of the miR-335 locus metastasis. Array-Comparative Genomic Hybridization (CGH) plot reveals gross loss of copy number of chromosomal region on 7q encompassing miR-335 locus at 7q32.2 in MDA-231 and CN34 metastatic derivatives. Plot depicts Log_2 ratio of array-CGH signals from various lines relative to array-CGH signal from reference normal genomic DNA. The parental population is represented in black as biological replicates. Various metastatic derivatives are represented in color.

Epigenetic silencing of the miR-335 locus in Metastatic Breast Cancer cells

I wondered if there were any additional mechanisms through which miR-335 is silenced in metastatic breast cancer cells. miR-335 resides in the second intron of the mesoderm-specific transcript (Mest) gene (Figure 62), which is an imprinted gene that is expressed only from the paternally derived chromosome and is expressed highly in mesoderm tissues.[100,101] To determine if Mest and miR-335 are co-regulated, the expression levels of Mest and miR-335 across many breast cancer cell lines was first determined through qPCR and it was observed that there is a strong correlation (correlation coefficient $r^2 = 0.94$; $P < 0.0001$) between their expression levels (Figure 63). These findings suggest that the mechanisms that regulate the Mest transcript also modulate miR-335 expression, consistent with the model that the expression of intronic miR-335 is at least in part dependent on the expression level of Mest pre-mRNA.

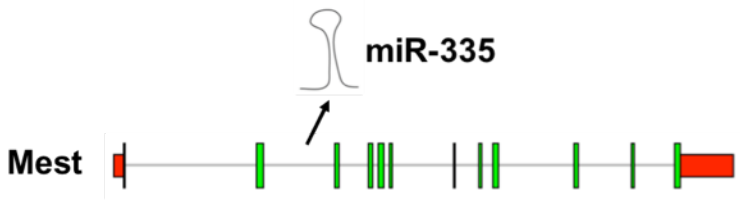

Figure 62| miR-335 resides in intron 2 of the Mest gene. Schematic of the Mest/miR-335 transcript reveals location of miR-335 in the second intron of Mest.

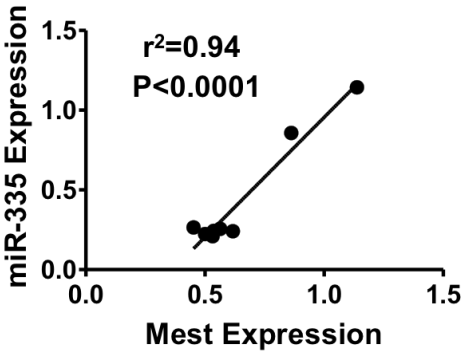

Figure 63| miR-335 expression is highly correlated to Mest expression. Quantitative relationship of mature miR-335 levels to Mest transcript levels in breast cancer cell lines (correlation coefficient r^2=0.94; P<0.0001).

The maternal allele of the Mest gene is imprinted developmentally. Examination of the Mest/miR-335 promoter revealed that there are three CpG islands upstream of the transcriptional start site (Figure 64). I next wondered if the Mest/miR-335 locus undergoes promoter hypermethylation in breast cancer cells and their metastatic derivatives. To this end, methylation-specific PCR (MSP) of these three CpG islands were performed in several cell lines. Consistent with imprinting of this locus, normal female genomic DNA contained both methylated and unmethylated copies of this locus at each of the CpG islands (Figure 65). Interestingly, both poorly and highly metastatic breast cancer cells (MDA-231 and its derivatives) and primary malignant metastatic populations (CN34 and its derivatives) display an increase in methylation at each of the three islands relative to normal female genomic DNA or the non-metastatic MCF breast cancer line (Figure 65). These findings are consistent with an increase in promoter hypermethylation at the Mest/miR-335 locus in metastatic breast cancer cells.

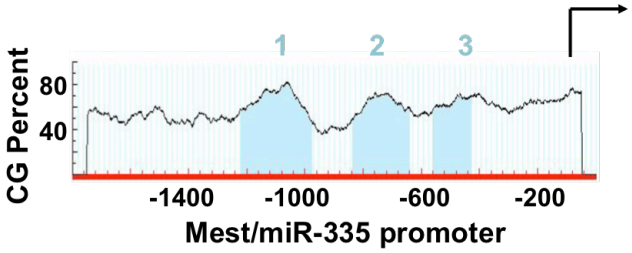

Figure 64| CpG islands in miR-335/Mest promoter. Quantification of CpG density reveals three CpG islands in the miR-335/Mest promoter.

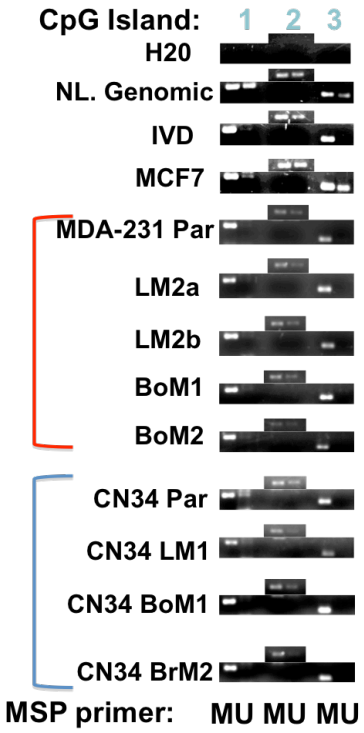

Figure 65| miR-335 locus is hypermethylated in metastatic breast cancer. Methylation specific PCR of 3 CpG islands in Mest/miR-335 promoter from bisulfite treated DNA of various lines. NL. genomic represents normal genomic DNA. IVD represents in vitro methylated DNA.

Pyrosequencing technology has been established in previous studies to be a useful next-generation sequencing platform for quantitative CpG methylation analysis. I next sought to identify the CpG islands(s) whose methylation status most strongly correlates with miR-335 expression through the use of pyrosequencing technology to better quantify DNA methylation.[56] I also wanted to determine whether highly metastatic cells undergo additional promoter methylation at the Mest/miR-335 locus relative to their parental lines. Pyrosequencing analysis of bisulfite-treated normal somatic DNA revealed the three Mest/miR-335 promoter islands to be 30-50% methylated–consistent with the imprinting of one Mest allele (Figure 66). Additionally, pyrosequencing of bisulfite-treated DNA from the MDA-231 (Figure 67) and CN34 (Figure 68) cancer cell populations and their metastatic derivatives validated the qualitative MSP findings of increased methylation of the Mest/miR-335 promoter region in metastatic breast cancer cells.

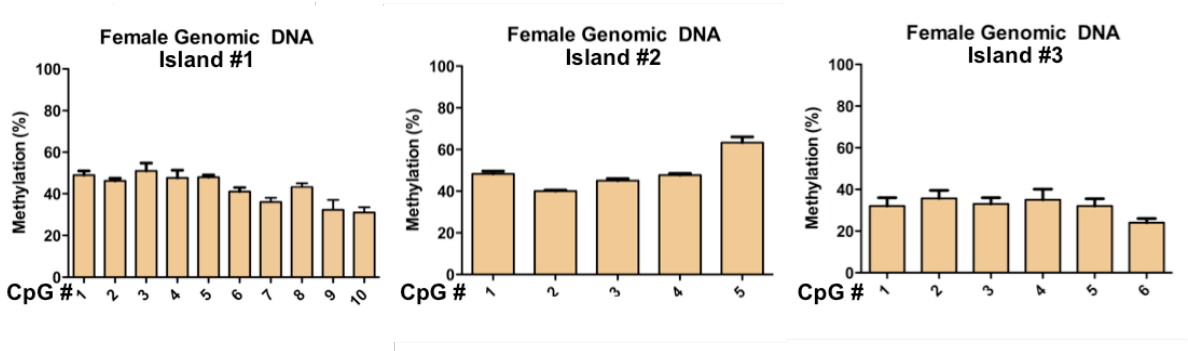

Figure 66| miR-335 locus to be 50% methylated in normal genomic DNA. Pyrosequencing reveals methylation status of three CpG island upstream of the miR-335 locus in female genomic DNA. All error bars represent s.e.m.

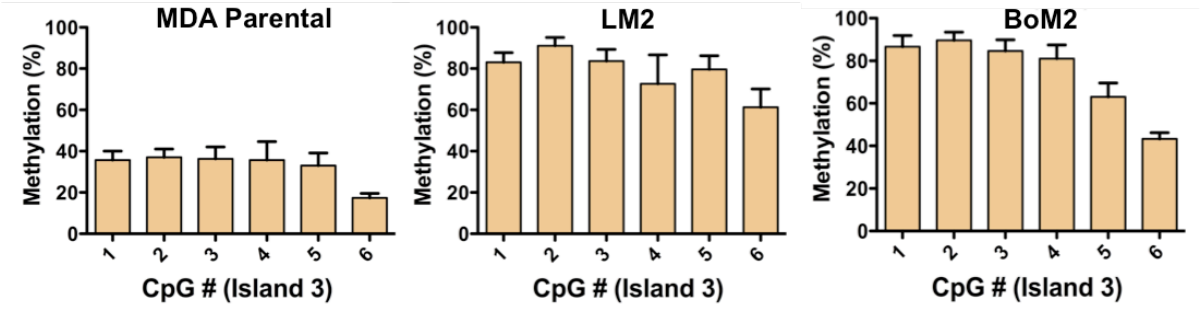

Figure 67| miR-335 locus is hypermethylated in metastatic derivatives of MDA-231. Pyrosequencing of bisulfite treated DNA reveals methylation percentage (y-axis) as a function of CpG dinucleotide position in island 3 of poorly metastatic MDA cells and their highly metastatic derivatives. All error bars represent s.e.m.

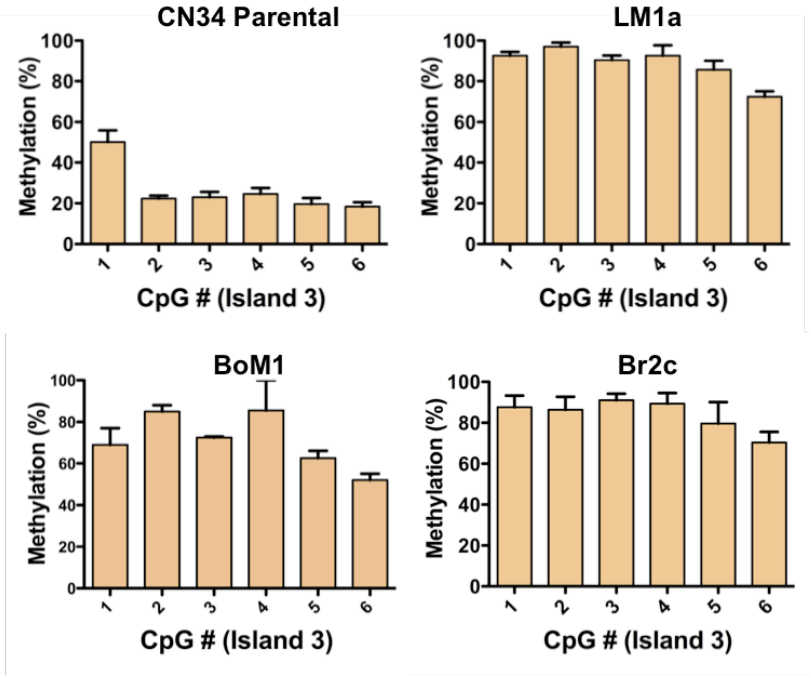

Figure 68| miR-335 locus is hypermethylated in metastatic derivatives of CN34 Par. Pyrosequencing of bisulfite treated DNA reveals methylation percentage (y-axis) as a function of CpG dinucleotide position in island 3 of CN34 Parental and their highly metastatic derivatives. All error bars represent s.e.m.

Importantly, the silencing of miR-335 was the most strongly correlated with the methylation status of island 3 (correlation coefficient r^2 = -0.81, P < 0.005; Figure 69) and the statistical significance of this correlation is maintained even across the methylation status of the individual dinucleotides throughout this island (Figure 70). Hypermethylation of island 3 was observed in all metastatic cancer derivatives obtained from distinct patients and quantification of methylation across the individual CpG dinucleotides in this island revealed a greater than twofold increase in highly metastatic derivatives relative to their parental cell lines (Figure 67-68). The metastatic LM2 and CN34 Lm1a populations displayed 78% and 88% aggregate methylation at island 3, while their respective parental MDA-231 and CN34 lines displayed 32% and 26% aggregate methylation. These findings reveal that there is enhanced promoter hypermethylation of the remaining Mest/miR-335 locus in the metastatic derivatives compared to the basal level observed in their respective parental cell lines.

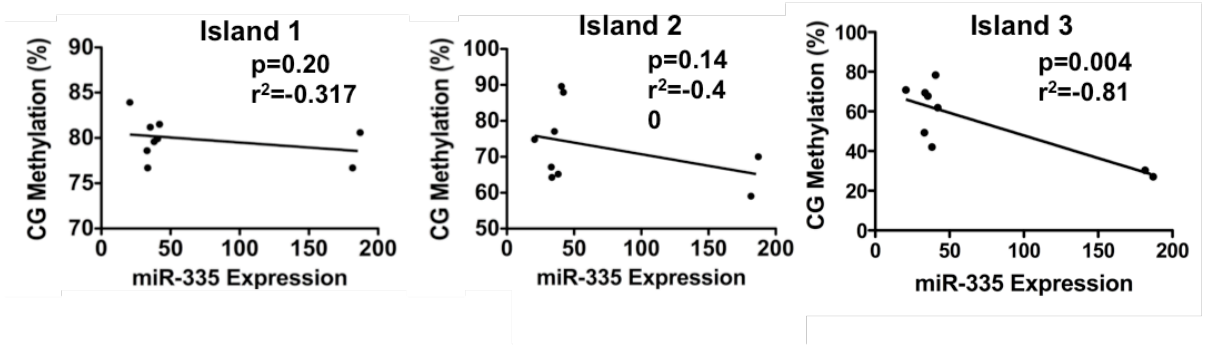

Figure 69| miR-335 expression is inversely correlated to CpG methylation. CpG methylation percentage as a function of miR-335 expression for each of the 3 islands in miR-335/Mest promoter.

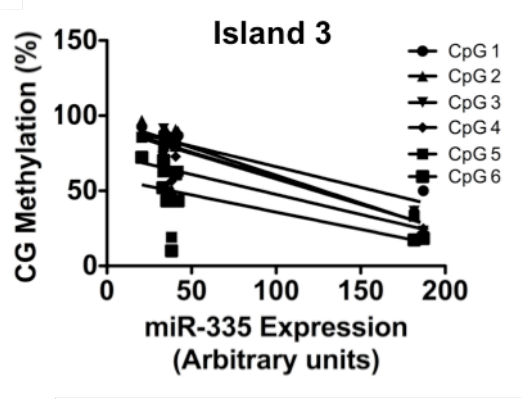

Figure 70| miR-335 expression is inversely correlated to methylation of individual CpG dinucleotide in island 3. CG methylation percentage for each CpG dinucleotide in island three as a function of miR-335 expression. CG methylation was quantified using pyrosequencing technology and represents average from triplicate reads.

I next sought to determine whether promoter hypermethylation is sufficient to silence mir-335 expression and specifically, if the promoter hypermethylation of the Mest/miR-335 locus and miR-335 expression are causally related. The poorly metastatic parental MDA-231 line and its lung metastatic derivative (LM2) were first treated with 5-Aza-deoxycytidine (5-Aza), which is an inhibitor of DNA methyltransferases that eventually leads to the inhibition of DNA methylation. Treatment with 5-Aza leads to significantly increased endogenous miR-335 expression by qPCR, revealing that promoter hypermethylation is sufficient to silence miR-335 expression (Figure 71). Similarly, treatment of CN34 primary malignant population and its metastatic derivatives with 5-Aza leads to enhanced miR-335 expression (Figure 71). Treatment with 5-Aza led to significantly increased Mest expression in both MDA-231 and CN34 parental lines and their metastatic derivatives (Figure 72), revealing that miR-335 is indeed co-regulated with its host Mest transcript and that the mechanism of regulation involves promoter methylation of this locus. Importantly, the absolute levels of

miR-335 and Mest expression after 5-Aza treatment were greater in the parental lines as compared to their metastatic derivatives, consistent with earlier findings that one copy of the miR-335 locus is deleted in metastatic cells. These findings reveal that besides modulation through genetic deletion, miR-335 is also epigenetically regulated during cancer progression through methylation of a specific CpG island (Island 3) in the Mest/miR-335 promoter.

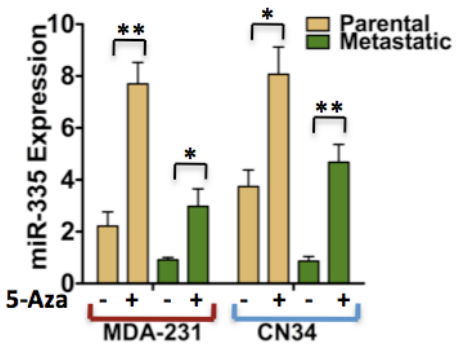

Figure 71| 5-Azacytidine restores expression of miR-335 in highly metastatic cells. qPCR of miR-335 expression in parental MDA-231 breast cancer line and its metastatic LM2 derivative and the CN34 primary malignant population and its metastatic derivative (CNLM1A) in the presence or absence of 5-Azacytidine (5uM treatment for 96 hours for MDA lines and 1uM for CN34 lines; metastatic lines n=6, parental lines n=3; error bars represent s.e.m., p-values obtained using a student's t-test. *P<0.05; **=p<0.005.

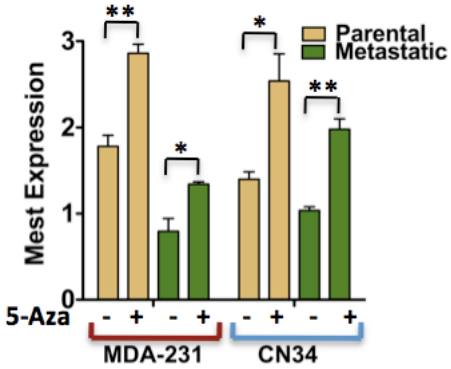

Figure 72| 5-Azacytidine restores expression of Mest in highly metastatic cells. qPCR of MEST expression in parental MDA-231 breast cancer line and metastatic LM2 derivative in the presence or absence of 5-Azacytidine. n=3; error bars represent s.e.m., p-values obtained using a student's t-test. *P<0.05; **P<0.005.

Tumour Initiation is etiologic basis of miR-335 silencing

Given that multiple mechanisms were discovered to be responsible for the silencing of miR-335 expression, I wondered what were the selective pressures that mediate miRNA silencing during cancer progression. Since miR-335 suppresses the key metastasis phenomenon of migration and invasion, its loss of expression during the metastatic cascade is expected. However, a previous study surprisingly revealed miR-335 expression to be lost in primary human breast tumours[51], bringing about an interesting paradox – what is the selective pressure for silencing of this miRNA during primary tumour formation when it does not have suppressive effects on proliferation or overall tumour growth?

I postulated that miR-335 plays a suppressive role early in tumour evolution such that its loss in a subset of aggressive breast tumours promotes early tumourigenesis, which is then retained throughout metastatic progression. To model early tumourigenesis, serial dilution experiments were performed with the highly metastatic LM2 breast cancer cell line, which displays silencing of miR-335, and a LM2 line that expresses highly level of retrovirally transduced miR-335. Implantation of 5 X 10^5 cancer cells into the mammary fat pads of immunodeficient NOD-SCID mice led to the formation of comparable number of tumours by either LM2 cells or miR-335 over-expressing LM2 cells (Figure 73a).

When the number of cancer cells implanted are decreased to 1 X 10^4 cells, the number of tumours formed by miR-335 over-expressing LM2 cells decreases relative to that formed by LM2 cells (Figure 73b). Strikingly, a further decrease in the number of cancer cells implanted to just 1000 cells resulted in an even more dramatic reduction in the number of tumours formed, where miR-335 over-expressing cells failed to form any tumours, as determined by either palpation by independent investigators or bioluminescence ($P < 0.0055$; Figure 73c, Figure 74).

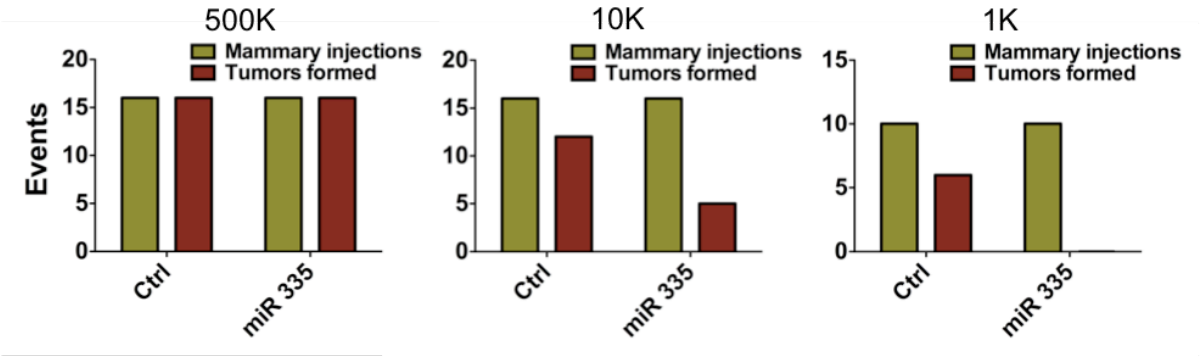

Figure 73| miR-335 inhibits tumours initiation. 5x10^5, 1x10^4 and 1000 LM2 breast cancer cells expressing a control hairpin or miR-335 were implanted into the mammary fat pads of nod-scid mice. Events represent mammary injections at onset (green) and tumour palpation at two weeks after implantation by two independent observers (cayenne). P <0.0003 for statistical significance of difference between control and low cell number cohorts (1K and 10K). P <0.006 for significance of difference between control and 1K cohort; p-values represent one-tailed Fisher's exact test values.

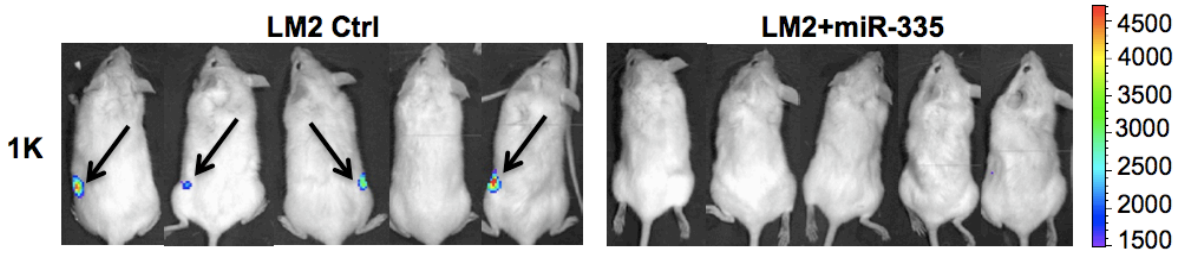

Figure 74| miR-335 suppresses mammary tumour formation. Bioluminescence images of mice two weeks after implantation of LM2 Control-hairpin expressing or miR-335 expressing cells.

Importantly, this effect on number of tumours formed is not due to altered tumour growth since miR-335 over-expression has been shown previously to not modulate proliferation of LM2 cells.[51] These findings reveal that miR-335 antagonises the ability of breast cancer cells to initiate tumours, thus playing an inhibitory role in the early stages of tumour formation, providing a handle for the selective pressure for miR-335 silencing in incipient breast tumours during initial tumorigenesis. Therefore, by reducing miR-335 through either genetic and/or epigenetic mechanisms, cancer cells gain a selective advantage in the primary tumour and during the course of metastatic progression. In a subset of such tumours with miR-335 loss, miR-335 expression is reduced to a level below the threshold needed to overcome the invasive and tumour reinitiating barriers, leading to successful end organ metastatic colonization.

Inactivation of miR-335 in Human Cancer

Having established that genetic and epigenetic mechanisms are responsible for the inactivation of miR-335 in metastatic cells and that this same inactivation of miR-335 is crucial for tumour initiation, I next sought mechanistic evidence for the inactivation of this locus in human breast cancer. Specifically, copy number alterations of the miR-335 locus were analysed in the representational oligonucleotide microarray analysis (ROMA) of 353 primary human invasive breast cancers resected from patients at the Memorial Sloan Kettering Cancer Center (MSKCC).[57] The analysis showed that copy number loss at the miR-335 locus on 7q32.2 occurred in 11.6% (n = 41/353) of human breast cancer tumours (Figure 75), suggesting that genetic inactivation of miR-335 in human breast cancer was a fairly common event. Interestingly, the subset of patients that developed distal metastatic spread displayed a greater rate of miR-335 genetic deletion (14.4%, n = 6/42) compared to those that did not develop distal metastatic relapse (11.2%, n = 35/311), revealing that the inactivation of this locus is more frequent in patients with higher rates of distal metastatic progression.

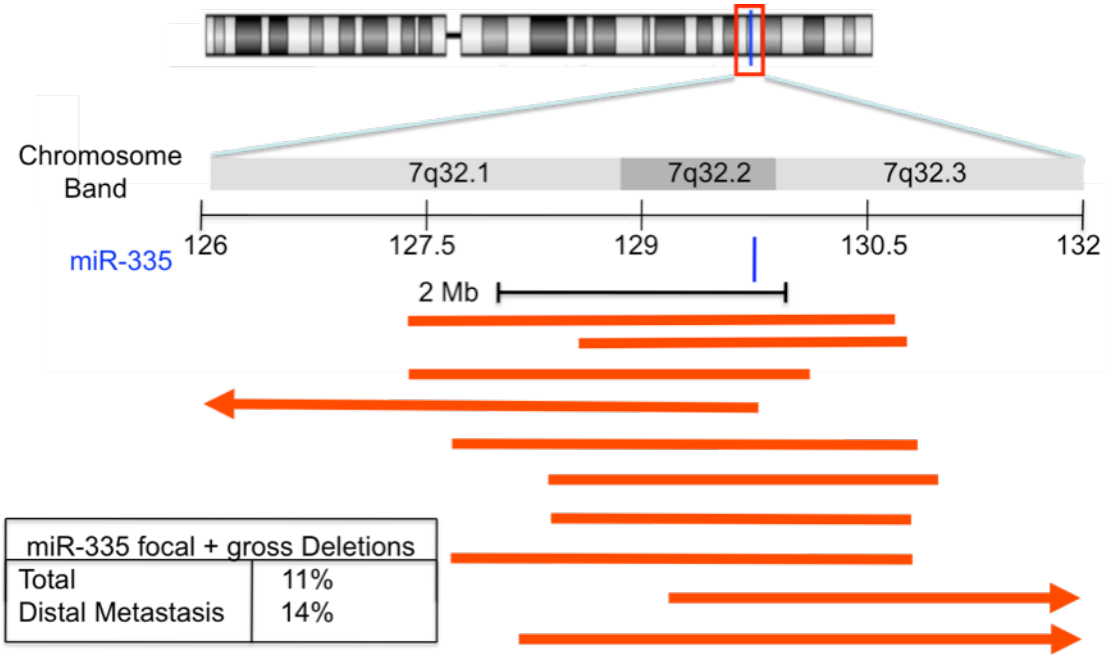

Figure 75| miR-335 locus is genetically inactivated in human breast cancer as a result of focal and gross deletions. Schematic representation of human chromosome 7 as well as a zoom schematic view of 7q32.2, the location of the human miR-335 locus. Red lines depict incidents of focal deletions in individual breast cancer tumours as defined by one arm of the deletion falling within 2 MB of the miR-335 locus. Arrows represent deletions spreading beyond the local region depicted. Inset summarizes frequencies of deletions (focal and gross) encompassing the miR-335 locus. The top percentage represents total incidence of deletions in the breast cancers of n=353 Patients while the bottom percentage represents the incidence of deletions in the subset that developed metastatic relapse.

To determine whether the genetic deletion of the miR-335 locus is enriched for during the course of metastatic progression, 11 primary breast cancers were obtained from patients who were diagnosed with metastatic breast cancer. Of these 11, 4 patients whose primary tumours displayed the highest expression levels for miR-335 were identified so that any subsequent comparisons with their respective metastases would be informative regarding miR-335 silencing. Metastases from these 4 patients were next obtained and analysed for miR-335 expression and copy number of the miR-335 locus by qPCR in matched

primary/metastasis samples. Each of the metastasis samples had decreased miR-335 expression relative to their respective primary samples (Figure 76) and this is at least in part due to a reduction in miR-335 copy number in the metastases as compared to their primary cancers (Figure 77). These findings are thus consistent with the enrichment of the silencing of miR-335 in cancer cells during metastatic progression, specifically through the deletion of this particular locus. Furthermore, these findings support a role for genetic inactivation of the miR-335 locus as a contributing factor for both breast cancer initiation and metastasis.

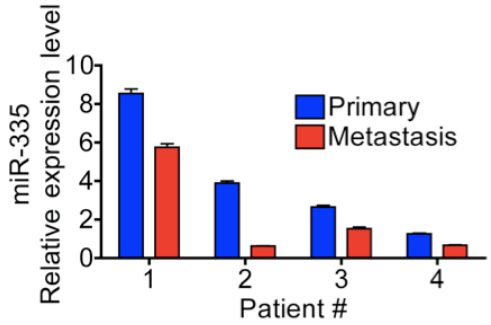

Figure 76| miR-335 expression in decreased in human breast metastases. qPCR of miR-335 expression in primary tumours and their respective metastases. n=3; error bars represent s.e.m.

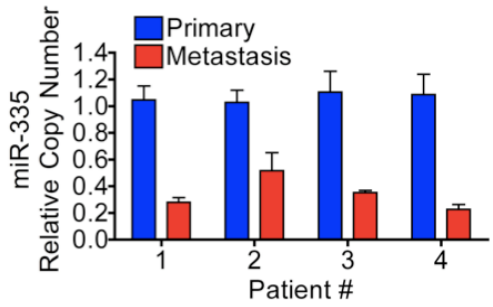

Figure 77| miR-335 locus is genetically inactivated in human breast metastases. qPCR for miR-335 copy number was performed on DNA from matched primary tumours and metastasis samples. n=3; error bars represent s.e.m.

I next wondered whether miR-335 expression correlates with the tumour-initiating capacity and invasiveness of breast carcinoma. Through analysis of the published copy number data, the frequency of miR-335 deletions in ductal carcinoma in situ (DCIS) samples[102]–neoplastic lesions that do not display the tumour initiation, invasion or metastasis phenotypes suppressed by miR-335–was determined. No deletion of the miR-335 locus (n = 0/50) was observed in DCIS samples as compared to invasive breast cancer samples (n = 41/353, $P < 0.0032$).

Finally, since miR-335 regulates the generic phenomenon of cancer initiation and invasion, I asked whether miR-335 deletion occurs in another type of malignancy, as well as whether this suppression of miR-335 expression is associated with cancer progression. Using the publicly available ovarian TCGA (The Cancer Genome Atlas) data set, I observed that focal deletion of the miR-335 locus occurred in 4.4% (n = 10/228) of ovarian cancers. Importantly, the deletion of this locus was significantly correlated with reduced recurrence-free survival (Figure 78), revealing that miR-335 expression level is highly predictive of ovarian cancer recurrence.

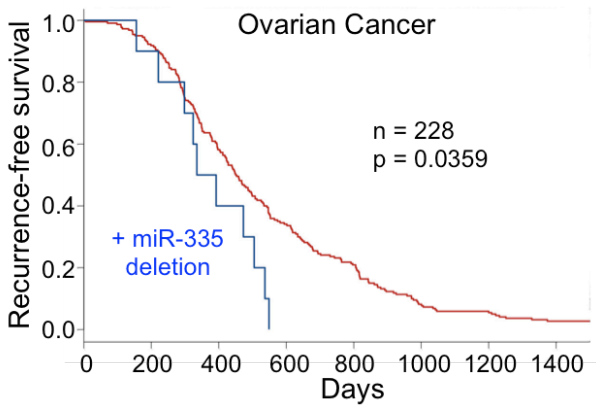

Figure 78| miR-335 expression predicts recurrence of human ovarian cancer. Kaplan-Meier curves for the ovarian cancer TCGA cohort depicting recurrence-free-survival of patients whose tumors displayed deletion of miR-335 (blue) and those that did not (red). n=228; P-value based on the log-rank test.

miR-126 is not inactivated by Genetic or Epigenetic mechanisms during Metastatic Progression

Given that metastasis suppressor miR-335 is inactivated through two separate mechanisms, genetic deletion and promoter hypermethylation, we wondered if the metastasis suppressor miR-126 is regulated through similar pathways. qPCR for miR-126 expression levels was first performed in genomic DNA isolated from the MDA-231 cell line and its metastatic derivatives, which have been previously shown to display miR-126 expression silencing, using two independent primer pairs that overlap across the genomic region encoding this miRNA. Unlike the miR-335 locus, no loss of copy number was observed at the miR-126 locus between the metastatic derivatives and their parental MDA-231 cell line, revealing that miR-126 is not inactivated via genetic deletion during metastatic progression (Figure 79). Consistent with this, there was also no deletion of the miR-126 locus observed in the CN34 metastatic derivatives relative to their parental malignant cell population (Figure 80).

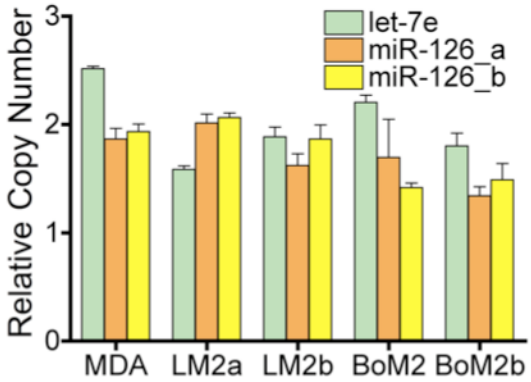

Figure 79| Genomic copy number analysis reveals no copy number loss of the miR-126 locus in metastasis. Genomic qPCR was performed on DNA from the parental MDA-231 poorly metastatic breast cancer cell line as well as its highly lung metastatic (LM2) and bone metastatic (BoM) derivatives. n=3; error bars represent s.e.m.

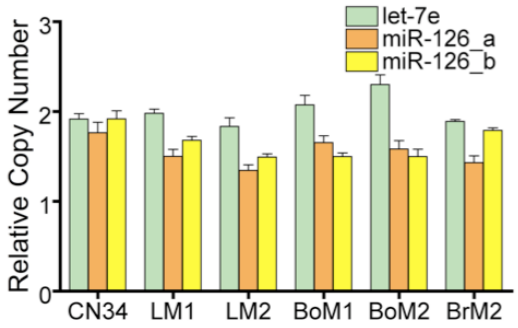

Figure 80| Genomic copy number analysis reveals no copy number loss of the miR-126 locus in metastatic derivatives of a primary malignant population. Genomic qPCR was performed on DNA from the CN34 primary malignant cancer population as well as its highly lung metastatic (LM1a and LM2a), bone metastatic (BoM1), and brain metastatic (Br2a) derivatives. n=3; error bars represent s.e.m.

I next wondered whether the miR-126 locus undergoes promoter hypermethylation in breast cancer cells and their metastatic derivatives. To this end, methylation-specific PCR (MSP) was performed for the only CpG island upstream of Egfl7 promoter, which is the transcript in which miR-126 resides in. Normal female genomic DNA contained both methylated and unmethylated copies of this locus (Figure 81). Similar to this, both poorly and highly metastatic breast cancer cells (MDA-231 and its derivatives) and primary malignant metastatic populations (CN34 and its derivatives) display both the methylated and unmethylated copies of this locus, with no consistent changes observed between the metastatic derivatives and their parental cell lines (Figure 81).

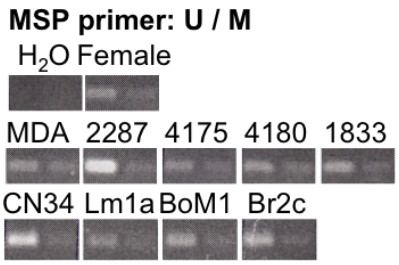

Figure 81| Methylation of miR-126/Egfl7 promoter locus does not regulate miR-126 expression in metastatic breast cancer. Methylation specific PCR of CpG island in miR-126/Egfl7 promoter from bisulfite treated DNA of various lines.

I next treated the poorly metastatic parental MDA-231 line and its highly metastatic LM2 derivative with 5-Aza to inhibit DNA methylation. Treatment with 5-Aza did not significantly increase endogenous miR-126 expression as assessed by qPCR, revealing that promoter hypermethylation is not regulating miR-126 silencing (Figure 82). Together, these findings suggest that miR-126 expression is not regulated by promoter hypermethylation in metastatic breast cancer cells.

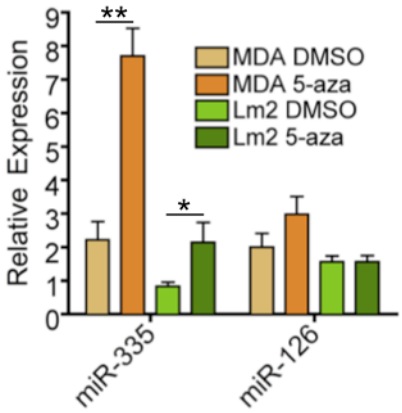

Figure 82| miR-126 expression remains constant after 5-Azacytidine treatment in highly metastatic cells. qPCR of miR-126 expression in parental MDA-231 breast cancer line and its metastatic LM2 derivative in the presence or absence of 5uM 5-Azacytidine (miR-335 expression shown as a positive control). n=3; error bars represent s.e.m., p-values obtained using a student's t-test. *P<0.05; **P<0.005.

miR-126 processing is defective in Breast Cancer Cells

Sanger sequencing of genomic DNA derived from the breast cancer cell line MDA-231 and its metastatic derivative LM2 revealed both cell lines to contain a SNP (SNP Rs4636297) on the pri-miR-126 transcript that is predicted to alter the secondary structure of miR-126. Specifically, both lines display a G in this position as opposed to an A (Table 13). Similarly, both the independent breast cancer population CN34 Par and its metastatic derivative CN34 LM1a also code for G at both alleles of miR-126 (Table 13). A previously study has shown this SNP to decrease the expression of miR-126 when it displays G as opposed to A.[103] These findings reveal that the genotype of this SNP is not responsible for the decrease of miR-126 expression between highly metastatic cells relative to their parental population. Although this SNP could contribute to the reduced levels of miR-126 in these cells, another mechanism must account for the decreased expression of miR-126 in highly metastatic cells relatively to poorly metastatic cells.

Table 13: Genotype at SNP Rs4636297

Cell Line	Genotype
MDA	GG
LM2	GG
CN34 Par	GG
CN34 LM1a	GG

I next wondered if there was any blockage in the various processing steps that are necessary for the biogenesis of miR-126. To determine the levels of the various precursors of miR-126, qPCR was performed on RNA derived from MDA-231 and its metastatic derivative LM2, as well as CN34 Par and its metastatic derivative CN34 LM1a, with primers specific for either pri-miR-126 or mature miR-126. Interestingly, the findings reveal that pri-miR-126 expression is higher in highly metastatic cells relative to their parental population (Figure 83a). This is in stark contrast to mature miR-126 levels, which are lower in highly metastatic cells relative to their parental population (Figure 83b), suggesting that miR-126 processing is hindered at one of the steps between generation of the pri-miR-126 transcript and the final cleavage of pre-miR-126 into its mature form.

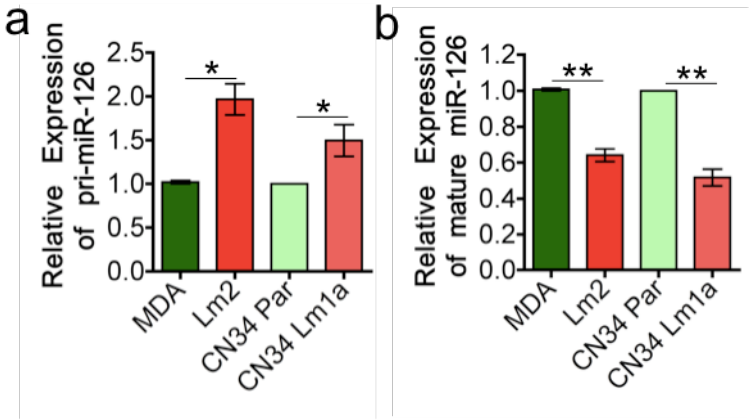

Figure 83| Expression levels of pri-miR-126 is enhanced in highly metastatic cells. qPCR of the (a) pri-miR-126 transcript and (b) mature miR-126 expression in parental MDA breast cancer line, its metastatic derivative LM2, CN34 primary malignant population and its metastatic derivative CN34 LM1a. n=3; error bars represent s.e.m., p-values obtained using a student's t-test. *P<0.05; **P<0.001.

To determine the exact step at which miR-126 processing is blocked, Northern blotting was performed with a probe that binds specifically to miR-126 in MDA-231 and its metastatic derivative LM2, as well as CN34 Par and its metastatic derivative CN34 LM1a. As a positive control, Human Umbilical Venous Endothelial Cells (HUVECs), which display high expression levels of mature miR-126, were used. Consistent with our qPCR results, the expression levels of pri-miR-126 are higher in LM2 and CN34 LM1a cells relative to MDA-231 and CN34 Par cells respectively (Figure 84). Meanwhile, the expression levels of pre-miR-126 are similar in MDA-231 and LM2 cells and higher in CN34 LM1a cells relative CN34 Par cells (Figure 84). Importantly, while levels of pri-miR-126 and pre-miR-126 in HUVEC cells are lower than that in the breast cancer cells, mature miR-126 is detectable in HUVEC cells but not in any of the breast cancer cell lines, consistent with qPCR results of reduced mature miR-126 expression in breast cancer and metastatic breast cancer (Figure 84). These findings suggest that the blockage in miR-126 processing occurs between synthesis of pre-miR-126 and mature miR-126, suggesting that the defect occurs either at the export of pre-miR-126 from the nucleus to the cytoplasm or the cleavage of pre-miR-126 into mature miR-126. Interestingly, another band was noted in northern blot of the HUVECs that was ~60 nt in length, suggesting that there might possibly be another non-canonical cleavage step between the synthesis of pre-miR-126 and mature miR-126 in endothelial cells.

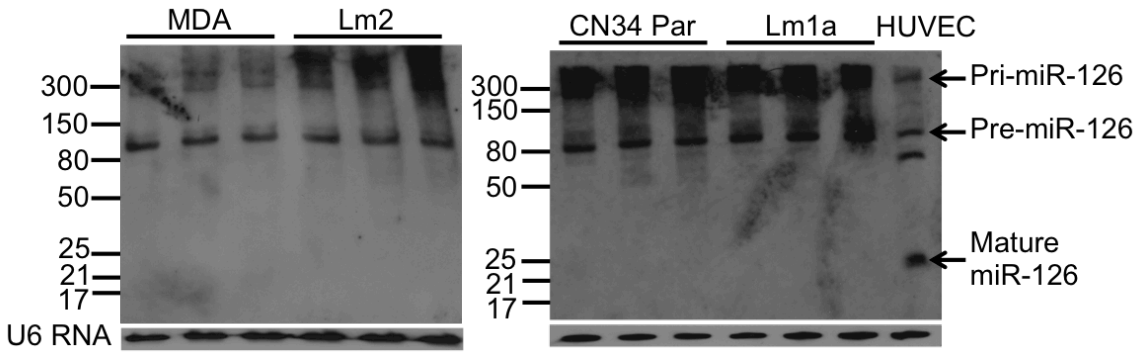

Figure 84| Processing defect in biogenesis of miR-126 in breast cancer cells. MDA-231 breast cancer line and its metastatic LM2 derivative, CN34 primary malignant population and its metastatic derivative (CNLM1A) and HUVEC cells were subjected to northern blot analysis for miR-126 and U6 spliceosomal RNA (control).

Discussion

These findings reveal the mechanisms through which miR-335, a robust and clinically validated metastasis suppressor, is silenced in human breast cancer. Since miRNAs are increasingly implicated in tumorigenesis and cancer progression, the various mechanisms that regulate the expression levels of these miRNAs are increasingly studied. The miR-335 locus undergoes both genetic and epigenetic silencing, leading to loss of heterozygosity (LOH) of the miR-335 function. The combined targeting of miR-335 by two independent mechanisms in all metastatic derivatives obtained from independent breast cancer populations underscores the importance of this molecule in the inhibition of metastatic progression of breast cancer. Additionally, the ability to target this locus with two separate mechanisms allows for the possibility that the suppression of miR-335 can be gradually increased as the metastatic cascades unfolds.

I further elucidated that miR-335 acts as an inhibitor of tumour initiation, causing it to be silenced in the primary tumour. This reveals that besides being a suppressor of invasion and metastatic colonization, miR-335 also acts as an inhibitor of tumour reinitiation during metastasis. Additionally, this miRNA is the second miRNA, after let-7, to be shown to have suppressive effects on tumour initiation in breast cancer. However, while let-7 suppresses proliferation and tumour growth, miR-335 inhibits tumour initiation without suppressing proliferation or tumour growth.[104]

The genetic deletion of the miR-335 locus during metastatic progression is likely to be biased towards the paternally inherited allele as that would result in a greater cancer progression advantage–the non-imprinted, paternal locus is deleted and the remaining imprinted, maternal locus is further silenced through promoter hypermethylation. Importantly, cancer cells utilise an underlying developmental mechanism of genomic imprinting to epigenetically silence the expression of miR-335 through hypermethylation, supporting the notion that conserved developmental regulatory networks can be reactivated during cancer progression to allow neoplastic cells to perform functions that are normally constrained to early development such as migration, invasion and self-renewal.

Interestingly, miR-126 appears to be regulated by completely distinct mechanisms from those that regulate miR-335, suggesting that metastasis suppressor microRNAs are not downregulated by common mechanisms. These findings reveal that miR-126 is not suppressed by genetic deletion or DNA methylation. However, there are other epigenetics mechanisms, such as post-translational modifications of histones that could regulate the expression of miR-126. In particular, histone deacetylation is known to regulate numerous proteins involved in cancer initiation and cancer progression.[105] Analysis of miR-126 expression levels, however, reveal that the pri-miRNA transcript is transcriptionally induced and not repressed in cells silenced for miR-126 expression. These findings suggest that epigenetic mechanisms cannot be responsible for miR-126 silencing, since epigenetic silencing would suppress the transcriptional induction of the pri-miR-126 transcript in cells that display miR-126 silencing.

These findings that highly metastatic cells have higher pri-miR-126 levels relative to their parental cell populations suggests that miR-126 suppression during metastasis is not mediated through transcriptional regulation, but rather, a processing step further downstream of that. Specifically, qPCR and Northern blotting analysis showed that there is a block in the processing of miR-126 from its pre-miRNA to mature form. Importantly, both pri-miR-126 and pre-miR-126 levels are either significantly higher or similar in highly metastatic cells relative to their poorly metastatic parental population, suggesting that the inhibition of the processing of pre-miR-126 into its mature form is the major mechanism responsible for the suppression of miR-126 in highly metastatic cells. Further studies will have to be performed to pinpoint the exact step whereby processing of miR-126 is blocked–the export of pre-miR-126 from the nucleus into the cytoplasm and the cleavage of pre-miR-126 by Dicer into its mature form. Upon identification of the exact processing step where miR-126 processing is inhibited, the exact mechanism through which miR-126 expression is suppressed in metastasis can then be elucidated. These findings thus reveal processing of pre-miRNAs as a novel mechanism through which cancer cells mediate microRNA expression levels.

CHAPTER 6:
General Discussion

The identification of metastasis suppressor microRNAs has shed light on new molecules and cellular biology underlying cancer progression. MiR-126 has been previously shown to play an integral role in the suppression of metastasis by breast cancer cells. In particular, I have shown that miR-126 inhibits endothelial recruitment by breast cancer cells through its suppression of target genes IGFBP2, MERTK, and PITPNC1. MiR-126 regulates two separate pathways to modulate a single process–endothelial recruitment. The first is an endothelial recruitment-promoting pathway whereby PITPNC1 regulates secretion of IGFBP2, which then binds to IGF1 and activates IGF1R signalling on endothelial cells. The second is an endothelial recruitment-suppressing pathway, where the cleaved ectodomain of MERTK acts as a decoy receptor that binds Gas6, which inhibits endothelial recruitment through its binding of the MERTK receptor on endothelial cells. Through the regulation of endothelial recruitment, miR-126 is able to modulate interactions between breast cancer cells and endothelial cells, which are crucial for metastatic initiation and metastatic angiogenesis, leading to metastatic colonization.

Besides the downstream mechanisms and effectors of metastasis suppressor microRNAs in metastasis, it is highly important to elucidate the upstream regulators of these microRNAs as they provide further insights into evolution of cancer during cancer progression. These results indicate that numerous mechanisms are used to govern the expression of metastasis suppressor microRNAs. MiR-335 is silenced in metastatic cells through two different mechanisms–one allele is genetically deleted while the other is epigenetically silenced through promoter hypermethylation. Additionally, miR-335 was uncovered to suppress tumour initiation, providing a selective pressure for the silencing of miR-335 expression in the primary tumour. In metastatic cells, miR-335 is regulated through genetic and epigenetic mechanisms while miR-126 is regulated post-transcriptionally during its biogenesis. Further studies will need to be performed to determine the exact mechanism through which miR-126 is inhibited in metastatic cells.

Role of Endothelia in Metastatic Initiation

During the study to elucidate the cellular determinants underlying metastasis, endothelial cells were identified to be key cellular components in the process of metastatic initiation. Importantly, a previously uncharacterized mechanism that promotes metastatic angiogenesis has been identified – endothelial cell recruitment by metastatic cells. Traditionally, studies of metastatic angiogenesis have revolved around the sprouting of new vessels from pre-existing vessels or the production of known angiogenic factors by cancer cells and/or the microenvironment.[106,107] A previous study has shown that VEGF induces the generic mobilisation of bone marrow-derived endothelial progenitor cells, leading to endothelial recruitment and increased tumour angiogenesis.[108] I have found IGFBP2 and MERTK to be both necessary and sufficient *in vitro* and *in vivo* for the recruitment of endothelial cells by metastatic cells and for the initiation of metastasis.

These findings also suggest that endothelial cells to play a role in metastatic initiation beyond angiogenesis. There has been increasing evidence for perfusion-independent activities of endothelial cells in other systems such as during developmental organogenesis and regeneration.[72] It is highly important to determine the nature of the exact interactions between cancer and endothelial cells that promote metastatic initiation, as it will allow greater insight into the process of metastatic initiation, while also potentially uncovering novel endothelial cell biology. Additionally, these interactions provide an additional handle for the therapeutic intervention of metastasis.

MicroRNA function

By studying the mechanisms by which miR-126 suppresses breast cancer metastasis, several interesting features of microRNAs have been uncovered. First, a microRNA was shown to have non-cell autonomous effects in cancer progression, allowing crosstalk between different cell types and regulating signalling in the microenvironment. Specifically, breast cancer cell expressed miR-126 regulates the expression of IGFBP2 and MERTK – two proteins that interact with proteins in the extracellular space, eventually activating the IGF1R receptor and inhibiting the MERTK receptor on endothelial cells. These findings highlight the capacity of microRNAs to regulate pathways extrinsic to the cells that express them, suggesting that the study of microRNAs needs to be expanded beyond the cells that express them in order to fully understand the functions of any particular microRNA in cancer progression.

Additionally, these findings reveal the ability of microRNAs to regulate a single phenomenon through the modulation of several genes and pathways. miR-126 suppresses three different genes, which participate in two divergent pathways that eventually converge to modulate the ability of cancer cells to recruit endothelial cells. These results reinforce the capability of microRNAs to act as master regulators of cellular functions. Through their ability to regulate several genes simultaneously, microRNAs can effectively regulate a specific phenomenon through the modulation of several different pathways that mediate the same phenomenon. Additionally, if mutations allow a single target to escape regulation by a specific microRNA, the microRNA retains the ability to mediate a particular phenomenon, as

it will still be able to modulate the expression of the remaining target genes that are involved in the same process.

These findings also revealed that microRNAs have the ability to select their target genes in a cell type specific manner. While previous studies have shown miR-126 to modulate SPRED1 and PIK3R2 expression in endothelial cells[66,68], these results reveal miR-126 to regulate IGFBP2, MERTK and PITPNC1 expression in breast cancer cells. The mechanism underlying this cell type specific regulation is unknown and its elucidation will give us further insights into how microRNAs establish target specificity.

Dysregulation of microRNAs in Cancer

Besides uncovering new features of microRNA function, these findings also reveal several interesting features regarding the dysregulation of microRNAs in cancer. Although microRNAs are generally downregulated in cancer and metastasis, additional layers of regulation were revealed to be involved in the silencing of microRNAs in breast cancer metastasis. Importantly, these findings indicate that two highly robust metastasis suppressor genes are regulated through two highly different sets of mechanisms. miR-335 is regulated through mechanisms that are commonly deregulated in modulation of oncogenes and tumour suppressors–genetic deletion and epigenetic regulation through DNA methylation. The regulation of miR-335 is particularly interesting as it highlights how cancer cells hijack conserved developmental pathways when presented with opportunity. Specifically, since miR-335 resides in the intron of a known imprinted gene, breast cancer cells leverage on the existing promoter methylation to further inhibit miR-335 expression. In contrast, miR-126 is regulated through mechanisms that are specific to microRNA biogenesis. These findings indicate that there is a block in processing from the pre-miRNA to the mature miRNA. Given its enhanced expression in highly metastatic cells, the host gene of miR-126, EGFL7, may have pro-metastatic effects on cancer progression. Thus, it may be necessary to regulate miR-126 independently of EGFL7, providing a selective pressure for a regulatory mechanism that is specific to microRNA expression. These findings reveal microRNAs to be tightly regulated by numerous mechanisms in breast cancer including both generic regulatory mechanisms and microRNA-specific regulatory mechanisms. This reinforces the importance of microRNAs as key regulators of cellular phenotypes while also highlighting the ability of cancer cells to evolve numerous pathways to regulate several microRNAs simultaneously.

REFERENCES

1 *U.S. Breast Cancer Statistics*, <http://www.breastcancer.org/symptoms/understand_bc/statistics.jsp> (2012).

2 *Types of Breast Cancer*, <http://www.nationalbreastcancer.org/About-Breast-Cancer/Types.aspx> (2012).

3 *Molecular Subtypes of Breast Cancer*, <http://ww5.komen.org/BreastCancer/SubtypesofBreastCancer.html> (2012).

4 *How is breast cancer staged?*, <http://www.cancer.org/Cancer/BreastCancer/DetailedGuide/breast-cancer-staging> (2012).

5 *Breast cancer survival rates by stage*, <http://www.cancer.org/Cancer/BreastCancer/DetailedGuide/breast-cancer-survival-by-stage> (2012).

6 *SEER Cancer Statistics Review 1975-2008*, <http://seer.cancer.gov/csr/1975_2008/index.html> (2011).

7 Hanahan, D. & Weinberg, R. A. The hallmarks of cancer. *Cell* **100**, 57-70 (2000).

8 Chiang, A. C. & Massague, J. Molecular basis of metastasis. *N Engl J Med* **359**, 2814-2823, doi:10.1056/NEJMra0805239 (2008).

9 Eccles, S. A. & Welch, D. R. Metastasis: recent discoveries and novel treatment strategies. *Lancet* **369**, 1742-1757, doi:10.1016/S0140-6736(07)60781-8 (2007).

10 Talmadge, J. E. & Fidler, I. J. AACR centennial series: the biology of cancer metastasis: historical perspective. *Cancer Res* **70**, 5649-5669, doi:10.1158/0008-5472.CAN-10-1040 (2010).

11 Hurst, D. R., Edmonds, M. D. & Welch, D. R. Metastamir: the field of metastasis-regulatory microRNA is spreading. *Cancer Res* **69**, 7495-7498, doi:10.1158/0008-5472.CAN-09-2111 (2009).

12 Sleeman, J. & Steeg, P. S. Cancer metastasis as a therapeutic target. *Eur J Cancer* **46**, 1177-1180, doi:10.1016/j.ejca.2010.02.039 (2010).

13 Fidler, I. J. The pathogenesis of cancer metastasis: the 'seed and soil' hypothesis revisited. *Nat Rev Cancer* **3**, 453-458, doi:10.1038/nrc1098 (2003).

14 Langley, R. R. & Fidler, I. J. The seed and soil hypothesis revisited--the role of tumor-stroma interactions in metastasis to different organs. *Int J Cancer* **128**, 2527-2535, doi:10.1002/ijc.26031 (2011).

15 Kang, Y. *et al.* A multigenic program mediating breast cancer metastasis to bone. *Cancer Cell* **3**, 537-549 (2003).

16 Minn, A. J. *et al.* Genes that mediate breast cancer metastasis to lung. *Nature* **436**, 518-524, doi:10.1038/nature03799 (2005).

17 Fidler, I. J. Selection of successive tumour lines for metastasis. *Nat New Biol* **242**, 148-149 (1973).

18 Bos, P. D. *et al.* Genes that mediate breast cancer metastasis to the brain. *Nature* **459**, 1005-1009, doi:10.1038/nature08021 (2009).

19 Fidler, I. J. Metastasis: quantitative analysis of distribution and fate of tumor embolilabeled with 125 I-5-iodo-2'-deoxyuridine. *J Natl Cancer Inst* **45**, 773-782 (1970).

20 Chambers, A. F. *et al.* Steps in tumor metastasis: new concepts from intravital videomicroscopy. *Cancer Metastasis Rev* **14**, 279-301 (1995).

21 Barkan, D., Green, J. E. & Chambers, A. F. Extracellular matrix: a gatekeeper in the transition from dormancy to metastatic growth. *Eur J Cancer* **46**, 1181-1188, doi:10.1016/j.ejca.2010.02.027 (2010).

22 Hedley, B. D. & Chambers, A. F. Tumor dormancy and metastasis. *Adv Cancer Res* **102**, 67-101, doi:10.1016/S0065-230X(09)02003-X (2009).

23 Paget, S. The distribution of secondary growths in cancer of the breast. 1889. *Cancer Metastasis Rev* **8**, 98-101 (1989).

24 Fidler, I. J. Critical determinants of metastasis. *Semin Cancer Biol* **12**, 89-96, doi:10.1006/scbi.2001.0416 (2002).

25 Hurwitz, H. *et al.* Bevacizumab plus irinotecan, fluorouracil, and leucovorin for metastatic colorectal cancer. *N Engl J Med* **350**, 2335-2342, doi:10.1056/NEJMoa032691 (2004).

26 Giantonio, B. J. *et al.* Bevacizumab in combination with oxaliplatin, fluorouracil, and leucovorin (FOLFOX4) for previously treated metastatic colorectal cancer: results from the Eastern Cooperative Oncology Group Study E3200. *J Clin Oncol* **25**, 1539-1544, doi:10.1200/JCO.2006.09.6305 (2007).

27 Sandler, A. *et al.* Paclitaxel-carboplatin alone or with bevacizumab for non-small-cell lung cancer. *N Engl J Med* **355**, 2542-2550, doi:10.1056/NEJMoa061884 (2006).

28 Barugel, M. E., Vargas, C. & Krygier Waltier, G. Metastatic colorectal cancer: recent advances in its clinical management. *Expert Rev Anticancer Ther* **9**, 1829-1847, doi:10.1586/era.09.143 (2009).

29 Bartel, D. P. MicroRNAs: genomics, biogenesis, mechanism, and function. *Cell* **116**, 281-297 (2004).

30 Bartel, D. P. MicroRNAs: target recognition and regulatory functions. *Cell* **136**, 215-233, doi:10.1016/j.cell.2009.01.002 (2009).

31 Lee, R. C., Feinbaum, R. L. & Ambros, V. The C. elegans heterochronic gene lin-4 encodes small RNAs with antisense complementarity to lin-14. *Cell* **75**, 843-854 (1993).

32 Friedman, R. C., Farh, K. K., Burge, C. B. & Bartel, D. P. Most mammalian mRNAs are conserved targets of microRNAs. *Genome Res* **19**, 92-105, doi:10.1101/gr.082701.108 (2009).

33 Carthew, R. W. Gene regulation by microRNAs. *Curr Opin Genet Dev* **16**, 203-208, doi:10.1016/j.gde.2006.02.012 (2006).

34 Schickel, R., Boyerinas, B., Park, S. M. & Peter, M. E. MicroRNAs: key players in the immune system, differentiation, tumorigenesis and cell death. *Oncogene* **27**, 5959-5974, doi:10.1038/onc.2008.274 (2008).

35 Ambros, V. The functions of animal microRNAs. *Nature* **431**, 350-355, doi:10.1038/nature02871 (2004).

36 Kim, V. N. MicroRNA biogenesis: coordinated cropping and dicing. *Nat Rev Mol Cell Biol* **6**, 376-385, doi:10.1038/nrm1644 (2005).

37 Shomron, N. & Levy, C. MicroRNA-biogenesis and Pre-mRNA splicing crosstalk. *J Biomed Biotechnol* **2009**, 594678, doi:10.1155/2009/594678 (2009).

38 Bushati, N. & Cohen, S. M. microRNA functions. *Annu Rev Cell Dev Biol* **23**, 175-205, doi:10.1146/annurev.cellbio.23.090506.123406 (2007).

39 Shomron, N., Golan, D. & Hornstein, E. An evolutionary perspective of animal microRNAs and their targets. *J Biomed Biotechnol* **2009**, 594738, doi:10.1155/2009/594738 (2009).

40 Lai, E. C. Micro RNAs are complementary to 3' UTR sequence motifs that mediate negative post-transcriptional regulation. *Nat Genet* **30**, 363-364, doi:10.1038/ng865 (2002).

41 Brennecke, J., Stark, A., Russell, R. B. & Cohen, S. M. Principles of microRNA-target recognition. *PLoS Biol* **3**, e85, doi:10.1371/journal.pbio.0030085 (2005).

42 Doench, J. G. & Sharp, P. A. Specificity of microRNA target selection in translational repression. *Genes Dev* **18**, 504-511, doi:10.1101/gad.1184404 (2004).

43 Ladomery, M. R., Maddocks, D. G. & Wilson, I. D. MicroRNAs: their discovery, biogenesis, function and potential use as biomarkers in non-invasive prenatal diagnostics. *Int J Mol Epidemiol Genet* **2**, 253-260 (2011).

44 Duursma, A. M., Kedde, M., Schrier, M., le Sage, C. & Agami, R. miR-148 targets human DNMT3b protein coding region. *Rna* **14**, 872-877, doi:10.1261/rna.972008 (2008).

45 Grimson, A. *et al.* MicroRNA targeting specificity in mammals: determinants beyond seed pairing. *Mol Cell* **27**, 91-105, doi:10.1016/j.molcel.2007.06.017 (2007).

46 Easow, G., Teleman, A. A. & Cohen, S. M. Isolation of microRNA targets by miRNP immunopurification. *Rna* **13**, 1198-1204, doi:10.1261/rna.563707 (2007).

47 Ota, A. *et al.* Identification and characterization of a novel gene, C13orf25, as a target for 13q31-q32 amplification in malignant lymphoma. *Cancer Res* **64**, 3087-3095 (2004).

48 He, L. *et al.* A microRNA polycistron as a potential human oncogene. *Nature* **435**, 828-833, doi:10.1038/nature03552 (2005).

49 Johnson, S. M. *et al.* RAS is regulated by the let-7 microRNA family. *Cell* **120**, 635-647, doi:10.1016/j.cell.2005.01.014 (2005).

50 Takamizawa, J. *et al.* Reduced expression of the let-7 microRNAs in human lung cancers in association with shortened postoperative survival. *Cancer Res* **64**, 3753-3756, doi:10.1158/0008-5472.CAN-04-0637 (2004).

51 Tavazoie, S. F. *et al.* Endogenous human microRNAs that suppress breast cancer metastasis. *Nature* **451**, 147-152, doi:10.1038/nature06487 (2008).

52 Yin, J. J. *et al.* TGF-beta signaling blockade inhibits PTHrP secretion by breast cancer cells and bone metastases development. *J Clin Invest* **103**, 197-206, doi:10.1172/JCI3523 (1999).

53 Chin, K. *et al.* Genomic and transcriptional aberrations linked to breast cancer pathophysiologies. *Cancer Cell* **10**, 529-541, doi:10.1016/j.ccr.2006.10.009 (2006).

54 Wang, Y. *et al.* Gene-expression profiles to predict distant metastasis of lymph-node-negative primary breast cancer. *Lancet* **365**, 671-679, doi:10.1016/S0140-6736(05)17947-1 (2005).

55 Arnold, S. A. *et al.* Lack of host SPARC enhances vascular function and tumor spread in an orthotopic murine model of pancreatic carcinoma. *Dis Model Mech* **3**, 57-72, doi:10.1242/dmm.003228 (2010).

56 Tost, J., El abdalaoui, H. & Gut, I. G. Serial pyrosequencing for quantitative DNA methylation analysis. *Biotechniques* **40**, 721-722, 724, 726 (2006).

57 Hicks, J. *et al.* Novel patterns of genome rearrangement and their association with survival in breast cancer. *Genome Res* **16**, 1465-1479, doi:10.1101/gr.5460106 (2006).

58 Wang, X. *et al.* Aberrant expression of oncogenic and tumor-suppressive microRNAs in cervical cancer is required for cancer cell growth. *PLoS One* **3**, e2557, doi:10.1371/journal.pone.0002557 (2008).

59 Li, X., Zhang, Y., Ding, J., Wu, K. & Fan, D. Survival prediction of gastric cancer by a seven-microRNA signature. *Gut* **59**, 579-585, doi:10.1136/gut.2008.175497 (2010).

60 Guo, C. *et al.* The noncoding RNA, miR-126, suppresses the growth of neoplastic cells by targeting phosphatidylinositol 3-kinase signaling and is frequently lost in colon cancers. *Genes Chromosomes Cancer* **47**, 939-946, doi:10.1002/gcc.20596 (2008).

61 Watahiki, A. *et al.* MicroRNAs associated with metastatic prostate cancer. *PLoS One* **6**, e24950, doi:10.1371/journal.pone.0024950 (2011).

62 Wong, Q. W. *et al.* MicroRNA-223 is commonly repressed in hepatocellular carcinoma and potentiates expression of Stathmin1. *Gastroenterology* **135**, 257-269, doi:10.1053/j.gastro.2008.04.003 (2008).

63 Gao, W., Shen, H., Liu, L., Xu, J. & Shu, Y. MiR-21 overexpression in human primary squamous cell lung carcinoma is associated with poor patient prognosis. *J Cancer Res Clin Oncol* **137**, 557-566, doi:10.1007/s00432-010-0918-4 (2011).

64 Olson, P. *et al.* MicroRNA dynamics in the stages of tumorigenesis correlate with hallmark capabilities of cancer. *Genes Dev* **23**, 2152-2165, doi:10.1101/gad.1820109 (2009).

65 Murchison, E. P. *et al.* The Tasmanian devil transcriptome reveals Schwann cell origins of a clonally transmissible cancer. *Science* **327**, 84-87, doi:10.1126/science.1180616 (2010).

66 Wang, S. *et al.* The endothelial-specific microRNA miR-126 governs vascular integrity and angiogenesis. *Dev Cell* **15**, 261-271, doi:10.1016/j.devcel.2008.07.002 (2008).

67 Nicoli, S. *et al.* MicroRNA-mediated integration of haemodynamics and Vegf signalling during angiogenesis. *Nature* **464**, 1196-1200, doi:10.1038/nature08889 (2010).

68 Fish, J. E. *et al.* miR-126 regulates angiogenic signaling and vascular integrity. *Dev Cell* **15**, 272-284, doi:10.1016/j.devcel.2008.07.008 (2008).

69 Filipowicz, W., Bhattacharyya, S. N. & Sonenberg, N. Mechanisms of post-transcriptional regulation by microRNAs: are the answers in sight? *Nat Rev Genet* **9**, 102-114, doi:10.1038/nrg2290 (2008).

70 Guo, H., Ingolia, N. T., Weissman, J. S. & Bartel, D. P. Mammalian microRNAs predominantly act to decrease target mRNA levels. *Nature* **466**, 835-840, doi:10.1038/nature09267 (2010).

71 van de Vijver, M. J. *et al.* A gene-expression signature as a predictor of survival in breast cancer. *N Engl J Med* **347**, 1999-2009, doi:10.1056/NEJMoa021967 (2002).

72 Butler, J. M., Kobayashi, H. & Rafii, S. Instructive role of the vascular niche in promoting tumour growth and tissue repair by angiocrine factors. *Nat Rev Cancer* **10**, 138-146, doi:10.1038/nrc2791 (2010).

73 Kim, K. J. *et al.* Inhibition of vascular endothelial growth factor-induced angiogenesis suppresses tumour growth in vivo. *Nature* **362**, 841-844, doi:10.1038/362841a0 (1993).

74 Paez-Ribes, M. *et al.* Antiangiogenic therapy elicits malignant progression of tumors to increased local invasion and distant metastasis. *Cancer Cell* **15**, 220-231, doi:10.1016/j.ccr.2009.01.027 (2009).

75 Ebos, J. M. *et al.* Accelerated metastasis after short-term treatment with a potent inhibitor of tumor angiogenesis. *Cancer Cell* **15**, 232-239, doi:10.1016/j.ccr.2009.01.021 (2009).

76 Schmid, C. Insulin-like growth factors. *Cell Biol Int* **19**, 445-457, doi:10.1006/cbir.1995.1088 (1995).

77 Hwa, V., Oh, Y. & Rosenfeld, R. G. The insulin-like growth factor-binding protein (IGFBP) superfamily. *Endocr Rev* **20**, 761-787 (1999).

78 Firth, S. M. & Baxter, R. C. Cellular actions of the insulin-like growth factor binding proteins. *Endocr Rev* **23**, 824-854 (2002).

79 Baxter, R. C. Insulin-like growth factor binding proteins in the human circulation: a review. *Horm Res* **42**, 140-144 (1994).

80 Jones, J. I. & Clemmons, D. R. Insulin-like growth factors and their binding proteins: biological actions. *Endocr Rev* **16**, 3-34 (1995).

81 Wang, G. K., Hu, L., Fuller, G. N. & Zhang, W. An interaction between insulin-like growth factor-binding protein 2 (IGFBP2) and integrin alpha5 is essential for IGFBP2-induced cell mobility. *J Biol Chem* **281**, 14085-14091, doi:10.1074/jbc.M513686200 (2006).

82 Wang, H. *et al.* Insulin-like growth factor binding protein 2 enhances glioblastoma invasion by activating invasion-enhancing genes. *Cancer Res* **63**, 4315-4321 (2003).

83 Trivedi, D. & Padinjat, R. RdgB proteins: functions in lipid homeostasis and signal transduction. *Biochim Biophys Acta* **1771**, 692-699, doi:10.1016/j.bbalip.2007.04.014 (2007).

84 Linger, R. M., Keating, A. K., Earp, H. S. & Graham, D. K. TAM receptor tyrosine kinases: biologic functions, signaling, and potential therapeutic targeting in human cancer. *Adv Cancer Res* **100**, 35-83, doi:10.1016/S0065-230X(08)00002-X (2008).

85 Thorp, E. *et al.* Shedding of the Mer tyrosine kinase receptor is mediated by ADAM17 protein through a pathway involving reactive oxygen species, protein kinase Cdelta, and p38 mitogen-activated protein kinase (MAPK). *J Biol Chem* **286**, 33335-33344, doi:10.1074/jbc.M111.263020 (2011).

86 Sather, S. *et al.* A soluble form of the Mer receptor tyrosine kinase inhibits macrophage clearance of apoptotic cells and platelet aggregation. *Blood* **109**, 1026-1033, doi:10.1182/blood-2006-05-021634 (2007).

87 Laviola, L., Natalicchio, A. & Giorgino, F. The IGF-I signaling pathway. *Curr Pharm Des* **13**, 663-669 (2007).

88 Varela-Nieto, I., Hartl, M., Gorospe, I. & Leon, Y. Anti-apoptotic actions of insulin-like growth factors: lessons from development and implications in neoplastic cell transformation. *Curr Pharm Des* **13**, 687-703 (2007).

89 Gal, A. *et al.* Mutations in MERTK, the human orthologue of the RCS rat retinal dystrophy gene, cause retinitis pigmentosa. *Nat Genet* **26**, 270-271, doi:10.1038/81555 (2000).

90 Rodriguez, A., Griffiths-Jones, S., Ashurst, J. L. & Bradley, A. Identification of mammalian microRNA host genes and transcription units. *Genome Res* **14**, 1902-1910, doi:10.1101/gr.2722704 (2004).

91 Baskerville, S. & Bartel, D. P. Microarray profiling of microRNAs reveals frequent coexpression with neighboring miRNAs and host genes. *Rna* **11**, 241-247, doi:10.1261/rna.7240905 (2005).

92 Brown, J. W., Marshall, D. F. & Echeverria, M. Intronic noncoding RNAs and splicing. *Trends Plant Sci* **13**, 335-342, doi:10.1016/j.tplants.2008.04.010 (2008).

93 Berger, A. H. & Pandolfi, P. P. Haplo-insufficiency: a driving force in cancer. *J Pathol* **223**, 137-146, doi:10.1002/path.2800 (2011).

94 Rodriguez-Paredes, M. & Esteller, M. Cancer epigenetics reaches mainstream oncology. *Nat Med* **17**, 330-339, doi:10.1038/nm.2305 (2011).

95 Robertson, K. D. DNA methylation and human disease. *Nat Rev Genet* **6**, 597-610, doi:10.1038/nrg1655 (2005).

96 Pratap, J., Lian, J. B. & Stein, G. S. Metastatic bone disease: role of transcription factors and future targets. *Bone* **48**, 30-36, doi:10.1016/j.bone.2010.05.035 (2011).

97 Yang, J. Y. & Hung, M. C. Deciphering the role of forkhead transcription factors in cancer therapy. *Curr Drug Targets* **12**, 1284-1290 (2011).

98 Briegel, K. J. Embryonic transcription factors in human breast cancer. *IUBMB Life* **58**, 123-132, doi:10.1080/15216540600686870 (2006).

99 Hoebeeck, J., Speleman, F. & Vandesompele, J. Real-time quantitative PCR as an alternative to Southern blot or fluorescence in situ hybridization for detection of gene copy number changes. *Methods Mol Biol* **353**, 205-226 (2007).

100 Nishita, Y., Yoshida, I., Sado, T. & Takagi, N. Genomic imprinting and chromosomal localization of the human MEST gene. *Genomics* **36**, 539-542, doi:10.1006/geno.1996.0502 (1996).

101 Li, T. *et al.* An imprinted PEG1/MEST antisense expressed predominantly in human testis and in mature spermatozoa. *J Biol Chem* **277**, 13518-13527, doi:10.1074/jbc.M200458200 (2002).

102 Balleine, R. L. *et al.* Molecular grading of ductal carcinoma in situ of the breast. *Clin Cancer Res* **14**, 8244-8252, doi:10.1158/1078-0432.CCR-08-0939 (2008).

103 Harnprasopwat, R. *et al.* Alteration of processing induced by a single nucleotide polymorphism in pri-miR-126. *Biochem Biophys Res Commun* **399**, 117-122, doi:10.1016/j.bbrc.2010.07.009 (2010).

104 Yu, F. *et al.* let-7 regulates self renewal and tumorigenicity of breast cancer cells. *Cell* **131**, 1109-1123, doi:10.1016/j.cell.2007.10.054 (2007).

105 Eberharter, A. & Becker, P. B. Histone acetylation: a switch between repressive and permissive chromatin. Second in review series on chromatin dynamics. *EMBO Rep* **3**, 224-229, doi:10.1093/embo-reports/kvf053 (2002).

106 Carmeliet, P. & Jain, R. K. Molecular mechanisms and clinical applications of angiogenesis. *Nature* **473**, 298-307, doi:10.1038/nature10144 (2011).

107 Weis, S. M. & Cheresh, D. A. Tumor angiogenesis: molecular pathways and therapeutic targets. *Nat Med* **17**, 1359-1370, doi:10.1038/nm.2537 (2011).

108 Lyden, D. *et al.* Impaired recruitment of bone-marrow-derived endothelial and hematopoietic precursor cells blocks tumor angiogenesis and growth. *Nat Med* **7**, 1194-1201, doi:10.1038/nm1101-1194 (2001).